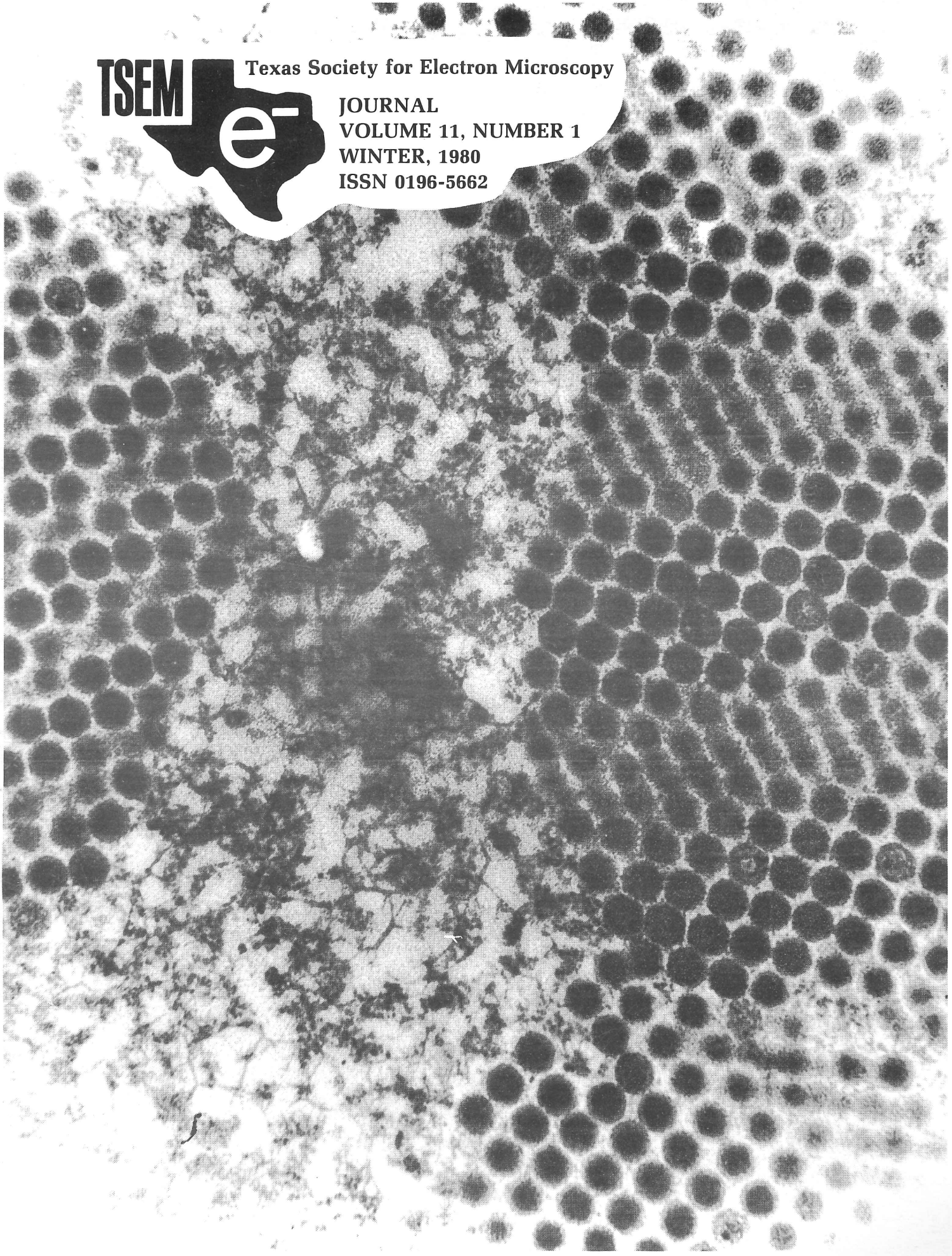

TSEM

Texas Society for Electron Microscopy

JOURNAL
VOLUME 11, NUMBER 1
WINTER, 1980
ISSN 0196-5662

100CX

Analytical Electron Microscope

The JEM-100C combines the very best in Transmission (TEM), Scanning (SEM) Scanning Transmission (STEM) & X-ray. The 100C offers the sophistication of four instruments in one plus superior performance in any single mode 2Å TEM, 30Å SEM, 15Å STEM, analysis of all elements from sodium on up from microareas of 200Å or less & selected area diffraction of a 200Å micro-area. Our side entry gonio-meter provides specimen tilt of ±60° for X axis & 360° rotation or ±45° for X & Y axis. Other accessories now available include a field emission gun, electron energy loss analyzer, and Lab6 gun.

JEOL

Specializing in
TEM – XRAY
SEM – AUGER
JEOL Application Laboratory, 477 Riverside Ave, Medford, Mass. 02155
617/391-7240

Contents

Volume 11, Number 1
Winter, 1980
ISSN 0196-5662

Texas Society for Electron Microscopy
"For the purpose of dissemination of research with the electron microscope"

ON THE COVER

Photograph courtesy of H. D. Mayor and L. E. Jordan, Department of Microbiology and Immunology, Baylor College of Medicine.

Electron micrograph of an ultra-thin section through a nucleus of African Green monkey kidney cells in tissue culture infected with simian adenovirus SV15. Arrays of virus particles often in honeycomb-like close-packed configurations are abundant. ×100,000.

What's the newest stage in SEM analytical automation?

This one.

This is our new Analytical Substage. A Philips "analytical + ". When you have one – and a SEM 501B – you have something special.

You have the means of loading four standard 1" metallurgical specimen mounts at a time. Outside the microscope. Without need of height adjustment. With no chance of error when inserting the carousel.

You have the option of mixing many combinations of samples and standards in one carousel, including "in-type" standards for light-element work. You can locate at least 16 pure-element standards in one mount. Compare a sample with up to 48 pre-mounted standards if you wish.

You have simple, highly accurate indexing of each analysis station by means of the stage rotation control. You can position repeat analysis points to within 2 µm. You can make Faraday cup measurements of the beam current.

Now the best part.

Add our new Stage Motor Drives. Now you can have a SEM with fully automated WEDAX! No other SEM has come this far in analytical automation. Because nobody else has a system center like Philips.

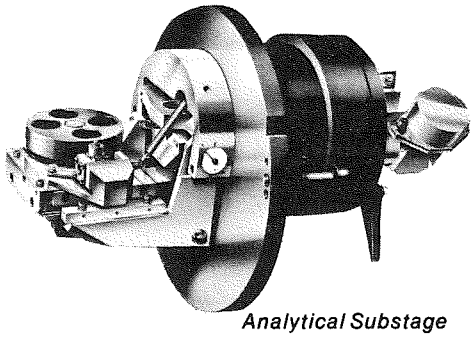

Analytical Substage with 4-sample carousel.

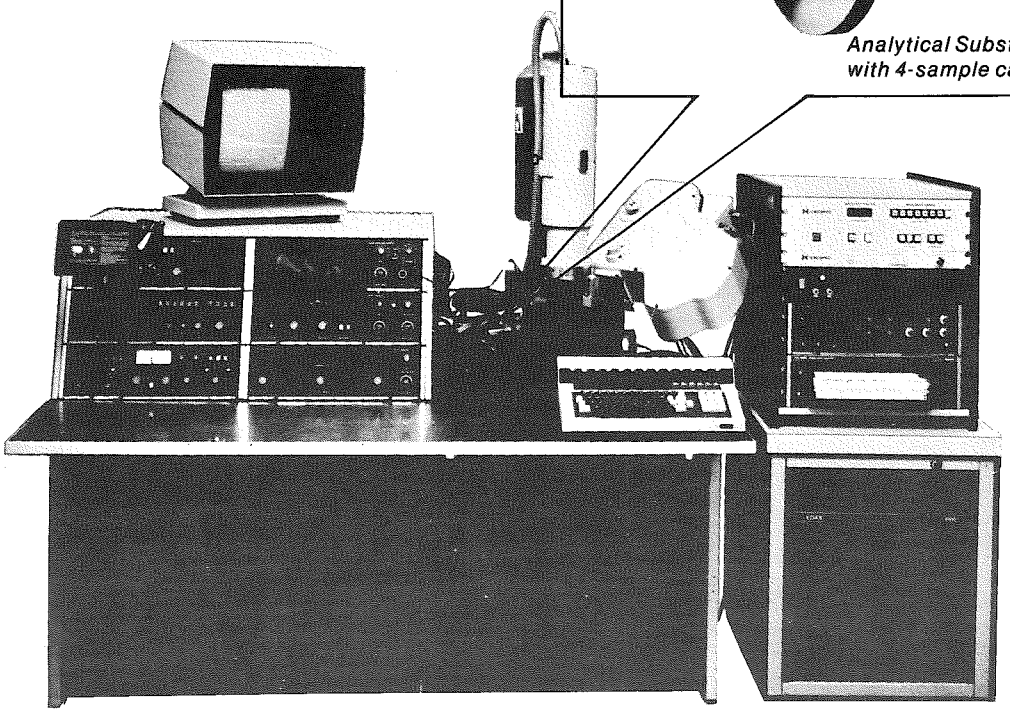

Philips' SEM gives you "analytical+"

PHILIPS

PHILIPS

For more information, contact:
Philips Electronic Instruments Inc.
85 McKee Drive, Mahwah
New Jersey 07430
Tel.: 201-529-3800

President's Message

It is the beginning of a new year and a new decade. In these past ten years, we have seen the Texas Society of Electron Microscopy grow from a small local group in the Houston area to the largest state Electron Microscopy Society in the United States. TSEM has gained national recognition through ventures such as the newsletter, gaining tax exempt status and participating in joint meetings with neighboring states. Such a venture as the joint meeting with LSEM has long been recognized as one of the most successful Electron Microscopy meetings in the nation. Each year since 1972 this meeting has been hosted in alternating years by the two societies. Both societies have grown and derived strength from this joint meeting.

Recently the TSEM Executive Council made the painful decision to abandon the TSEM/LSEM Meeting in favor of having a centrally located meeting once a year in Texas. This meeting would be open to all of our neighbors including Arkansas, Oklahoma, New Mexico and Louisiana, and will have regional flair.

There has been some concern expressed as to why this decision was made in light of the past success of this joint symposium. The TSEM Executive's Council first concern has always been our fellow TSEM members and their financial and professional needs. A primary concern was the cost to the individual for future meetings held in New Orleans. It was also felt that the lack of participation by the Texas members (especially students) at the last New Orleans meeting was a direct reflection of the distance and cost of travel in addition to the high hotel rates. There was no indication that expenses would be anything but greater at future New Orleans meetings. For these reasons the Executive Council voted unanimously to discontinue the joint LSEM/TSEM Meeting. We feel that the decision to hold a regional meeting in a centrally located city in Texas each year was for the best interest of the TSEM membership. We feel strongly that development of a regional meeting will be another step forward, and ask your support as well as the members of LSEM and our neighboring states in this endeavor.

As this new year begins I would ask that each TSEM member take the initiative to ask a non-member colleague to become a member of TSEM. Also, that each of you urge any old member who has let his membership drop to join TSEM again. The strength of the society is in its members. Only you as individual members can select and recruit interested scientists.

I wish each of you a successful and prosperous New Year.

Bill McCombs
President, TSEM

Editor's Comments

I am pleased to announce a new service available with this issue. You can now receive reprints of your articles in TSEMJ. Reprints should be ordered at the time of submission. The cost for 1980 will be $55.00 per 4-page section for the first 100 copies, and $15.00 per 4-page section for each additional 100 copies.

We enter the new year with a new name and consequently with a new ISSN number. Our new name reflects our growth as a scientific publication but the emphasis remains on Texas (regional news and matters close to home) and electron microscopy (ads for equipment and supplies, techniques, interesting pictures and new applications for electron microscopy as well as abstracts and full length articles). My continuing thanks to our corporate members who advertise and to our other advertisers for the TSEMJ, to our contributors and to our regional editors.

I received a nice newsletter from our friends in San Diego. The San Diego Society for Electron Microscopy was recently organized and has adopted our TSEM constitution and by-laws for its own. They are already quite active and will host the Spring Council Meeting of EMSA. Their San Diego Symposium on Electron Microscopy will be held Feb. 15-17, 1980 in La Jolla. In the newsletter they offered congratulations to Ivan Cameron and the TSEM for a great EMSA-MAS meeting in San Antonio. We appreciate their kind thoughts and hope to hear from them in the future.

I also received letters from TSEM members, Dr. Howard Arnott, Dean at University of Texas at Arlington and Dr. Lea Rudee, Provost at University of California at San Diego, containing words of appreciation for the fine quality of the TSEM Journal. I pass these along to all of you who have participated in this venture with me. Dr. Arnott writes " . . . It is really becoming a publication that Texas EM people can be proud of . . . Keep up the good work and congratulations!" Dr. Rudee writes "The article on the history of the TSEM brought back many memories. The quality of your newsletter is so far superior to even our most fanciful ideas that it does not bear comparison. In looking over this issue, I remember at least two speakers whose names did not get into Jerry Berlin's article. They are Bob Heidenreich and George Palade. I have no idea when they were there, but I am certain they did speak . . . ."

Our TSEM newsletter was enjoyed by many who came by the publications booth at the EMSA-MAS meeting in San Antonio. At the request of the EMSA council, I also mailed complimentary copies to the council members.

The decade of the 1970's has been one of phenomenal growth for our society. We are now the largest EMSA affiliate. Looking back over the history of TSEM as in our last issue, one can see the importance of joint TSEM-LSEM symposia to the growth of both societies. The first was held in 1972 in Fort Worth and by combining forces we were able to bring large corporate exhibits at a time when few national meetings were

held in this region. When we began rotating this winter meeting between New Orleans and San Antonio both societies were smaller and both cities were quite different. It is hard to imagine, but true, that in this past decade Houston has added to itself in population the equivalent of a city the size of New Orleans and San Antonio is now the 10th largest city. Viewed in this perspective it is exciting to look ahead into the 1980's. It is appropriate for TSEM to assume a major effort in planning regional meetings to include not only Louisiana and Mississippi but also Oklahoma, Arkansas, New Mexico and Colorado as well.

Part of our success as a society is our ability to reflect the needs and desires of a growing membership. The recent decision of the TSEM council for future meeting sites reflects a desire for flexibility. New approaches and different combinations are a necessity for our rapidly changing state. Travel costs are soaring; more national meetings are held in the Sun Belt; our favorite haunts-San Antonio and New Orleans and Houston **have been discovered.** We are now competing with large and rich organizations for convention space and time. We will continue to pursue the benefits obtained by active participation of our commercial exhibitors and provide regional meetings, particularly in years when major meetings are not held nearby. But we also want to retain some of the informality and friendly exchange in meetings at college campuses - like the recent successful meeting in Nacogdoches. We have a wonderful student membership in Texas and we want to make sure the benefits of our society are transferred to them and we in return receive their contributions. I think the decision for an altered format for regional meetings made by the TSEM council is a good one. The decision was not made in haste or by incorrect procedure. Our intent remains to foster new arrangements with Lousiana, since change and growth are inevitable when our goal is constant and our membership is expanding.

Our purpose remains "for the dissemination of research with the electron microscope." The next decade can be a good one for electron microscopy in Texas. Let us make it so.

Ann Goldstein
TSEM Journal Editor

TSEM CORPORATE MEMBERS

American Optical Corporation, L.B. Read, P.O. Box 1929, Dallas, Texas 75221. (214)747-8361.

Am Ray, Inc., Thomas Levesque, 5209 Kisar Dr., Lewisville, TX 75056.

Carl Zeiss, Inc., Dietrich Voss, 3233 Weslayan, Suite 191, Houston, TX 77027.

Collins Radio Goup - Rockwell Instruments, Donald L. Wilson, Mail Station 406-146, Richardson, TX 75080.

Cambridge-Imanco, Steve Miller, 9551 Williams Street, Rosemont Illinois 60018. (312)671-4270.

DuPont/Sorvall, Jim Gordon, Instrument Products, Quillen Bldg., Concord Plaza, Wilmington, Deleware 19898. Phone: 800-441-7493 or (302) 772-5678.

EG&G Ortec, Dick Neiman, 21718 Rotherham, Spring, TX 77379. Phone: (713) 353-0078 or 1-800-251-9732.

EDAX International Inc., Glen Gray, P.O. Box 135, Prairie View, Illinois 60069.

Electron Microscopy Sciences, M.J. Oulton, P.O. Box 251, Ft. Washington, Pennsylvania 17034.

Ernest F. Fullam, Inc., I.T. Stoneback, Advertising Mgr., P.O. Box 444, Schenectady, New York 12301.

ETEC Corporation, P.J. Breton, 3392 Investment Boulevard, Hayward, California 94545. Phone: (415) 783-9210.

International Scientific Instruments, Robert Ruscica, 3255 - 6C Scott Blvd., Santa Clara, Calif. 95050.

JEOL, USA, Inc., Paul Enos, 200 Walnut Way, Euless, TX 76039. Phone: (817) 267-6011.

Kevex, Alan Weckerling, 2909 Sherwood, Colleyville, TX 76034.

Ladd Research Industries, Inc., Mr. Ted Willmorth, 1209 Dogwood Drive, Kingston, Tennessee 37763. Phone: (615) 376-6358.

L.K.B. Instruments, Inc., Jack Kirten, 5300 Telephone Road, Houston, TX 77017.

Montedison USA, Inc., Richard A. Steenrod, Jr., P.O. Box Drawer L, Bridgeton, Missouri 63044.

Overall Engineering, Inc., Edsel E. Overall, 15755 Daleport, Dallas, TX 75248.

Perkin-Elmer Corporation, Mike Mullen, 11110 Los Alamitos Boulevard, Suite 202, Los Alamitos, California 90720. Phone: (213) 596-2512.

Philips Electronic Instruments, Bob Peterson, 7302 Harwin Drive, Suite 106, Houston, TX 77036. Phone: (713) 782-4845.

Physical Electronics Industries, Inc., Thomas J. Baum, 324 North Central Expressway, Suite 119, Richardson, TX 75080.

Polaron Instruments, Inc., Dermot Dinan, 1202 Bethlehem Pike Line, Lexington, Pennsylvania 18732. Phone: (215) 822-3364/5.

Princeton Gamma Tech., Rod Jensen, 8408 Bridgetown Dr., Austin, TX 78753.

Schares Instrument Corporation, Margot Martin, 2600 S. Gessner, Suite 315, Houston, TX 77063. Phone: (713) 468-4460.

Scimetrics, Inc., P.O. Box 42204, Houston, TX 77042.

SCR Laboratories, Inc., Surface Analysis Section, Robert R. Keith, 4800 West 34th, Suite A-12, Houston, TX 77092.

Spectrochemical Research Lab, D. Raymond Slovinsky, 4800 West 34th Street, Suite A-12, Houston, TX 77092.

Technic, Inc., Robert Barr, 5510 Vine Street, Alexandria, Virginia 22310. Phone: (703) 971-9200.

Technical Instrument Co., John Meny, 13612 Midway Road, Suite 333, Dallas, TX 75240. Phone: (214) 387-0606.

Ted Pella, Inc., Thomas P. Turnbull, P.O. Box 510, Tustin, California 92680. Phone: (714) 557-9434.

LETTER TO THE EDITOR

November 28, 1979

A Letter to the Editor:

As a member of TSEM for six years, it is with regret that I learned the TSEM/LSEM joint symposiums are to discontinued. I was quite disturbed to discover this unilateral TSEM executive coucil decision was made without consulting the general TSEM membership. It seems that such a drastic move should have been brought up for discussion during the TSEM general business meeting at EMSA or a poll of the membership could have been conducted by mail. I question the wisdom of discontinuing the joint meetings and would like to have the reasons for doing so outlined at the TSEM business meeting in Houston.

Sincerely yours,

Mary Lou Percy

FUTURE MEETINGS

Spring TSEM Meeting: May 1980, at Baylor University in Waco, Texas.

SEM/1980: April 21-25, 1980. McCormick Inn, Chicago, Illinois. Contact: Dr. Om Johari, Box 66507, AMF O'Hare, Illinois 60666.

EMSA/MAS: Aug. 2-9, 1980. San Francisco, California. Contact: Dr. G.T. McKinley, Xerox, Palo Alto, California 94304.

LET TECHNICS MAKE SPECIMEN PREPARATION EASIER FOR YOU

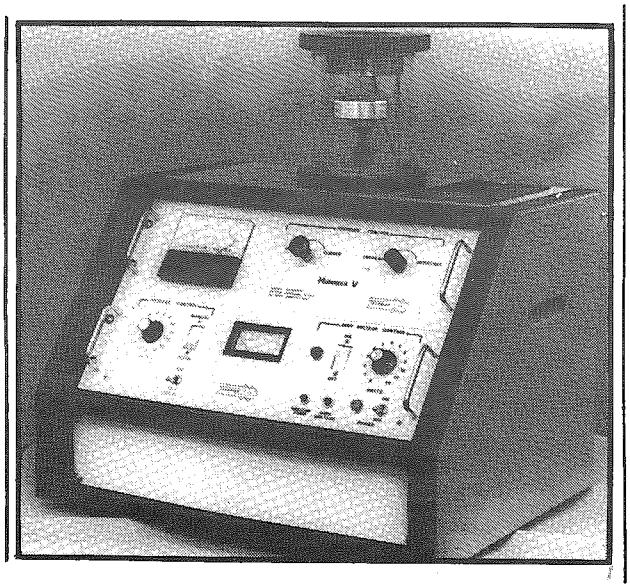

HUMMER V SPUTTER COATER

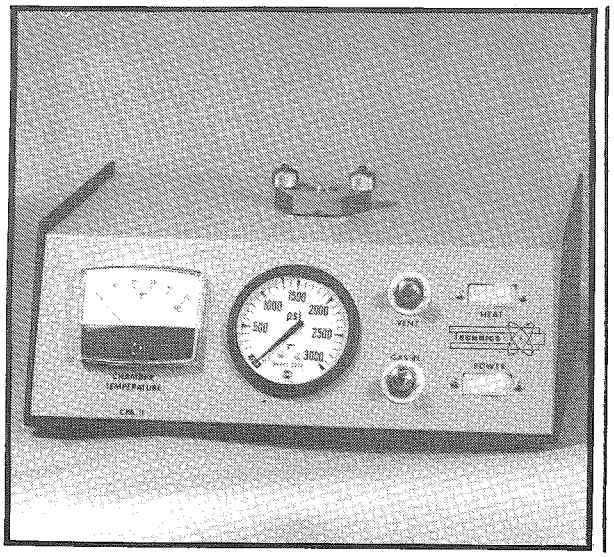

CPA II CRITICAL POINT DRYER

Technics Inc.
7950 Cluny Court
Springfield, VA 22153
(703) 569-7200
Telex 824445

Technics West Inc.
1754 Junction Avenue
San Jose, CA 95112
(408) 286-8700
Telex 357482

Technics GMBH Europa
Milbertshofener Str. 8
8000 München 40
Germany
(089) 35 23 75
Telex 05 29 334

The Molluscan Bivalve Hinge Ligament A Review

by
M. E. Marsh and **R. L. Sass**
Department of Biology
Rice University
Houston, Texas 77005

INTRODUCTION

The molluscan bivalve exoskeleton consists of two valves (shells) connected dorsally by an elastic ligament. The ligament serves the function of a hinge and causes the valves to gape on relaxation of the adductor muscle(s). The hinge ligament is nonliving and typically composed of calcium carbonate in a hydrated protein matrix; uncalcified ligaments have been observed only in the family Pectinidae (5,7). Although the form of the ligament varies among bivalve families, the ligament is always under strain when the valves are closed (12). Figure 1 is a drawing of the hinge region of the bivalve *Spisula solidissima* and is typical of bivalves with an internal ligament.

DISTRIBUTION OF CRYSTALS AND PRISMS

The hinge ligament is composed of long needle shaped aragonite ($CaCO_3$) crystals surrounded by an organic sheath and embedded in a protein matrix (2,8). The crystals, which are 100nm in width, are oriented perpendicular to the ligament growth lamellae and are rather widely spaced (Figs. 2,3,4, and 5).

A prism is a term used to describe a group of crystals which are associated in a discrete structural unit. In *Spisula solidissima* the crystals are distributed into two distinct types of prisms (8). One type of prism is located at the lateral surfaces of the ligament adjacent to the shell (see Fig. 1). These prisms are long roughly cylindrical rods oriented with their long axes normal to the growth lamellae (Fig. 2). The rods are composed of aragonite crystals in a protein matrix. The morphological long axes of the crystals are roughly parallel to the axis of the rod. These rods are called pseudo-prisms because they resemble the prisms in molluscan shells and vertebrate dental enamel. But unlike the prisms of shell and enamel, the crystals in the ligament are widely spaced and the pseudo-prisms are not delineated by an obvious noncalcified sheath. In electron micrographs, individual pseudo-prisms are discernible only by a slightly different orientation of the crystals in one prism with respect to those in another. When viewed in cross section (Fig. 3), very little space is seen between the prisms; the interprismatic space which exists is uncalcified.

The other type of prism is located in the central region of the ligament (see Fig. 1). Figure 4 is an electron micrograph of this area. Since the distribution of crystals appears the same in all planes sectioned normal to the cross-sectional plane, the basic structural unit is cylindrically symmetric. Figure 5 is an electron micrograph of a single prism in which the prism boundaries have been drawn in. The prisms are cylindrical but constricted at regular intervals. Because of the periodic constrictions, these structures are called noded prisms. The crystals are very closely packed at the nodes and widely spaced at the lobes. The noded prisms are arranged so that a node of one prism lies between lobes on adjacent prisms (Fig. 4). In this way the prisms fill space; thus there is no interprismatic space. The noded prisms have a diameter of about 4μm at the lobes, and like the pseudo-prisms, the long axis is perpendicular to the growth lamellae.

Although the pseudo-prisms are structurally very similar to shell and enamel prisms, the noded prisms are unique. In bivalves, when the shells close, the wedge-shaped ligament is extended ventrally. The lobes of the noded prisms are ellipsoidal and may lengthen in response to compression like an elliptical spring, a compression spring characterized by its great strength. The function of the rod shaped crystals is to give strength to the weak, but elastic protein matrix, enabling the ligament to force open the heavy valves against the weight of the animal's environment. The pseudo-prisms probably have a primarily structural function and contribute little to the elastic properties of the ligament.

CRYSTALLOGRAPHY

$CaCO_3$ occurs in three polymorphic (crystallographic) forms: calcite, aragonite, and vaterite. Calcite is the most thermodynamically stable at ordinary temperatures and pressures. Bivalve shell $CaCO_3$ is either calcite or more commonly aragonite; a vaterite shell has not been observed. The ligaments of about 30 species of bivalves have been analyzed by x-ray diffraction (5,13,15) and the $CaCO_3$ in all these ligaments is aragonite, even in species with a calcite shell.

Figure 6 is an electron micrograph at high magnifica-

Application/Nomination For Membership

I hereby apply/nominate for Regular ☐ Student ☐ Corporate ☐ membership in the Texas Society for Electron Microscopy.

Name of institution applicant or corporation nominee person _____

P. O. Address _____

_____

Information as to position, degrees, and qualifications for Membership: _____

_____

_____

_____

This nomination is accompanied by a statement of interest in and contributions to Electron Microscopy and associated fields of science.

One year's dues in the form of a check or money order should be sent with the application for Membership form. (Regular $10.00, Student $2.00, Corporate $75.00)

Signature of one Member making the nomination:

_____

Dated _____ 19 _____

This application to Membership in the Society, or this application for transfer from the grade of Student to Regular Member, signed by one Member should be sent to the Secretary to be presented at the next meeting of the Council or approval by a majority vote of the Council. Notice of approval will be mailed by the Executive Secretary.

_____

Presented to the Council at _____ meeting. Date _____

Action _____

Remarks _____

Send Application to: John Hansen
Univ. of Texas Health Science Center
Dept. of Anatomy
7703 Floyd Carl Drive
San Antonio, TX 78284

tion of a ligament cross section from *Mya arenaria*. The aragonite crystals are pseudo-hexagonal in cross section and have a thin band through the center. By electron diffraction of individual crystals it has been determined that these crystals are twinned about the (110) crystallographic plane (10). The two halfs of the crystals have the same orientation and the band is a thin lamella of the same composition but in twin orientation with respect to the parent crystal (i.e. the two halfs). Although inorganic sources of the mineral are commonly observed to be twinned, this is the only demonstration of twinning in biogenic aragonite. In the ligaments of all species analyzed, the crystals have a thin twin lamella through the center. In some species (notably *Spisula solidissima*) in addition to the central lamella, many of the crystals have multiple twin lamellae on both the (110) and $1\bar{1}0$) planes.

THE ORGANIC PHASE

Ultrastructurally two distinct organic phases can be identified in the ligament (2,8,9). One phase is the bulk elastomer in which the crystals are embedded. The other phase is a thin organic sheath approximately 10nm thick which surrounds each crystal. These phases can be distinguished in electron micrographs because the sheaths are more osmiophilic than the elastomer. Figures 7 and 8 are electron micrographs of the *Spisula* ligament which was decalcified in formic acid before fixation with OsO_4. In cross section osmiophilic sheaths are seen surrounding empty holes which were formerly occupied by the crystals (Fig. 9). The distribution of the sheaths is identical to the distribution of the crystals as can be seen by comparison of Figures 4 and 8, which are micrographs of the *Spisula* noded prism region. In Figure 4 the electron dense structures are the crystals; in Figure 10 they are decalcified sheaths.

Early studies on the composition of the ligament organic matrix did not make a distinction between the two phases. The matrix has been identified as protein with amounts of neutral sugars but no lipids (5,7). The amino acid composition of the total ligament protein is characterized by a high concentration of glycine and methionine residues (4,5,7,). In some ligaments the glycine concentration is as much as 66% of the residues and methionine 23% of the residues. A cross-linking agent, 3,3'-methylenebistyrosine, has been isolated from HCl hydrolysates of the ligaments from several species (1).

Recently the crystal sheaths have been isolated from the bulk organic phase by a papain digestion of the organic matrix (9). When the matrix protein is solublized by papain the sheaths remain bound to the aragonite crystals. Treatment of the sheathed crystals with dilute acid or EDTA, followed by dialysis to remove the inorganic components yields a preparation of the isolated sheaths which is soluble in salt solutions. Isolated sheaths can be visualized in the electron microscope by first fixing the sheathed crystals with glutaraldehyde, followed by EDTA to remove the crystals, OsO_4 fixation, and embedding (Fig. 9). The sheaths apparently remain intact and appear as hollow tubes. The isolated sheaths have a fluid appearance and their rigid adherence to the shape of the crystals is expectedly not preserved.

The ligament crystal sheaths have been characterized from the two species, *Spisula solidissima* and *Mercenaria mercenaria* (9). The concentrations of glycine and methionine residues is greatly reduced over their concentrations in the total ligament. There is a twofold increase in the concentration of acidic amino acids (including those residues which are actually amides) and basic amino acids in both sheath preparations. The carbohydrate component of the sheaths is small, less than 1% of the *Spisula* sheaths and about 5% of the *Mercenaria* sheaths.

NONCALCIFIED LIGAMENTS

In the family Pectinidae, the majority of the hinge ligament is uncalcified. This ligament has the wedge shaped structure shown in Fig. 1. Only the lateral margins of the ligament are calcified; the large central region comprising 90% of the volume is uncalcified.

Kelly and Rice (7) described the uncalcified region of ligaments from *Placopectin magellanicus* and *Aequipectin irradians* as a "homogenous amorphous substance of electron density." Their method of fixation was not given. However, when the ligaments from these same two species were studied in our laboratory, two distinct phases were observed in the electron microscope (11). When the tissue is fixed with potassium dichromate in OsO_4 at pH7.4 and sectioned longitudinally an extensive organized fiber network is observed within a homogeneous phase of lower electron density (Fig. 10). The fiber network is organized into long roughly cylindrical units and probably corresponds to the prismatic units observed in calcified hinge ligaments. When the ligaments are fixed for longer periods in OsO_4 at pH7.4 the major phase is extracted leaving only the fiber network. When the extracted material is observed in cross section, it can be seen that the fiber network is not composed of isolated fibers, but forms an extensive, perhaps continuous, sheet composed of many closed loops (see stereo pairs in Fig. 11). Undoubtedly this fiber network surrounds the elastic fibers and corresponds morphologically to the microfibrils associated with elastin in vertebrate tissues.

It is interesting that no fiber network has been found in calcified ligaments. It is possible that this network may be present in these ligaments but that the staining and fixation techniques used to date do not distinguish this phase. Studies are in progress in this laboratory on the calcified area on the Pecten ligaments. From studies of the calcified-noncalcified junction in this ligament, we hope to be able to distinguish the fiber network in the calcified region of the ligament and determine its relationship to the crystal sheaths. In pathological mineralization of arterial elastic fibers in humans, hydroxyapatite crystals have been found associated with the microfibrils (14).

ACKNOWLEDGEMENTS

Portions of the work reviewed were supported by Grants AM-18582 and DE-0078 from the National Institutes of Health, U. S. Public Health Service. Dr. Marsh is

the recipient of a Research Career Development Award of the National Institute of Health.

REFERENCES

1. Anderson, S. O. Isolation of a new type of cross link from the hinge ligament of molluscs. Nature (Lond.) **216**:1029-1030 (1967).

2. Bevelander, G. and Nakahara, H. An electron microscope study of the formation of the ligament of *Mytilus edulis* and *Pinctada radiata*. Calc. Tiss. Res. **4**:101-112 (1969).

3. Crenshaw, M. A. The soluble matrix from *Mercenaria mercenaria* shell. Biomineralization **6**:6-11 (1972).

4. Hare, P. E. Amino acids in the proteins from aragonite and calcite in the shell of *Mytilus californianus*. Science **139**:216-217 (1963).

5. Kahler, G. A., Fisher, F. M. and Sass, R. L. The chemical composition and mechanical properties of the hinge ligament in bivalve molluscs. Biol. Bull. **151**:161-181 (1976).

6. Kahler, G. A., Sass, R. L., and Fisher, F. M. The fine structure and crystallography of the hinge ligament of *Spisula solidissima*. J. Comp. Physiol. **109**:209-220 (1976).

7. Kelly, R. E. and Rice, R. V. Abductin: a rubber-like protein from the internal triangular hinge ligament of pecten. Science **155**:208-210 (1967).

8. March, M., Hopkins, G., Fisher, F., and Sass, R. Structure of the molluscan bivalve hinge ligament, a unique calcified elastic tissue. J. Ultrastruct. Res. **54**:455-450 (1976).

9. Marsh, M., Hamilton, G., and Sass, R. The crystal sheaths from bivalve hinge ligaments. Calcif. Tiss. Rev. **25**:45-51 (1978).

10. Marsh, M. E. and Sass, R. L. Aragonite twinning in the molluscan bivalve hinge ligament. Science, submitted.

11. Marsh, M. E., unpublished data.

12. Russell-Hunter, W. D. and Grant, D. C. Mechanics of the ligament in the bivalve *Spisula solidissima* in relation to mode of life. Biol. Bull. **122**:369-379 (1962).

13. Stenzel, H. B. Aragonite in the resilum of oysters. Science **136**:1121-1122 (1962).

14. Theman, T. E., Silver, M. D., Haust, M. D., McLoughlin, M. J., Wigle, E. D., and Williams, W. R. Morphological findings in idiopathic calcification of the ascending aorta and aortic valve affecting a young woman. Histopathol. **3**:181-190 (1979).

15. Wada, K. Crystal growth of molluscan shells. Bull. Natl. Pearl. Res. Lab. **7**:703-785 (1961).

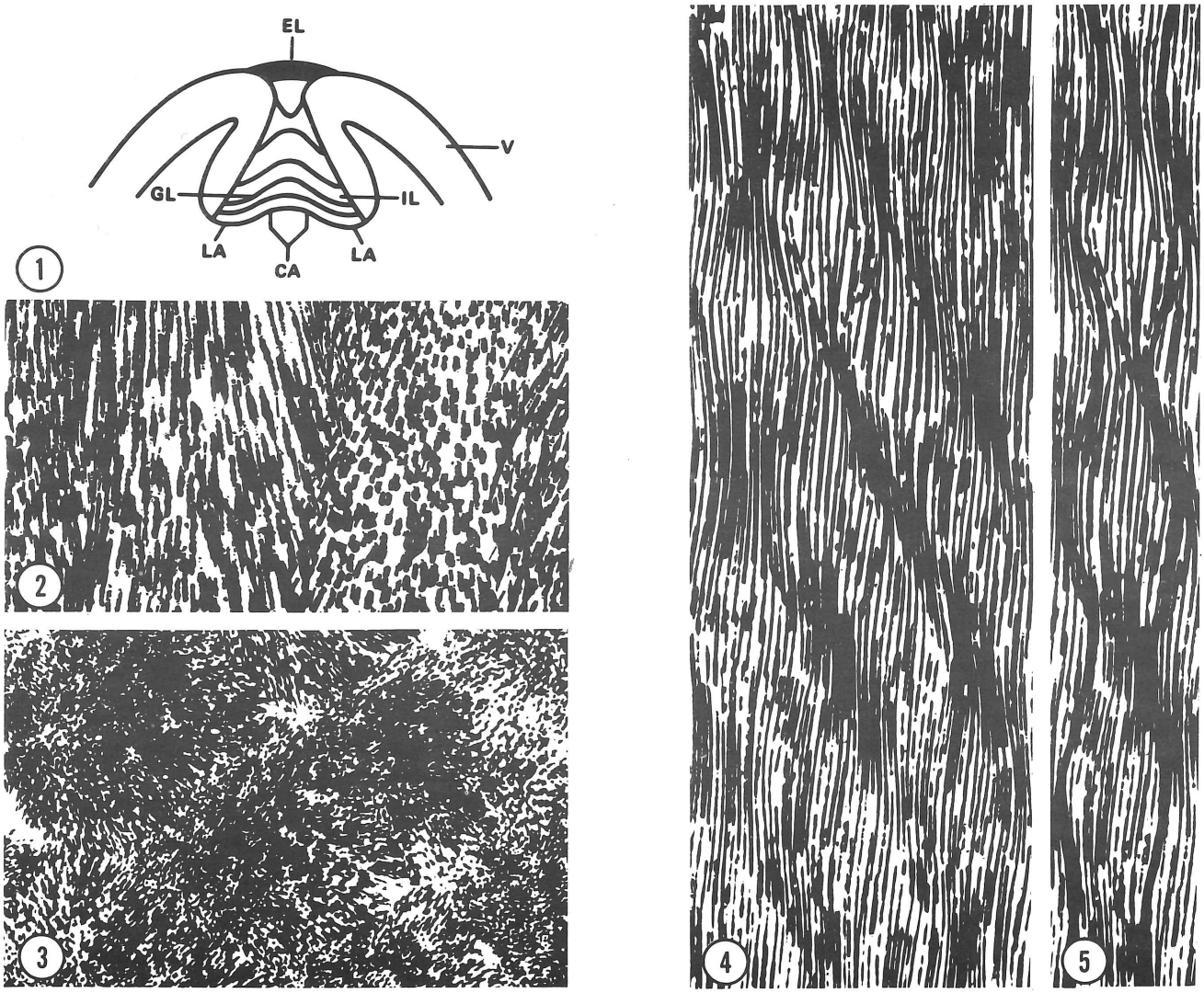

FIGURE 1: Drawing of a transverse section through the *Spisula* hinge region. EL, external ligament (uncalcified); IL, internal ligament, which is referred to as the hinge ligament and is calcified; GL, growth lamellae; LA, lateral area of ligament; CA, central area of ligament; V, valve (shell).
FIGURE 2: Transverse section from the lateral area of the *Spisula* ligament, showing the pseudo-prisms. Electron dense structures are the crystals. ×5500.
FIGURE 3: Cross section of the pseudo-prisms. Only a small amount of calcified interprismatic material is present. ×5600.
FIGURE 4: Transverse section from the central area of the *Spisula* ligament showing the noded prisms. Electron dense structures are the crystals. ×6000.
FIGURE 5: Same as Figure 4 showing one prism. The prism boundaries have been drawn in. ×6000.

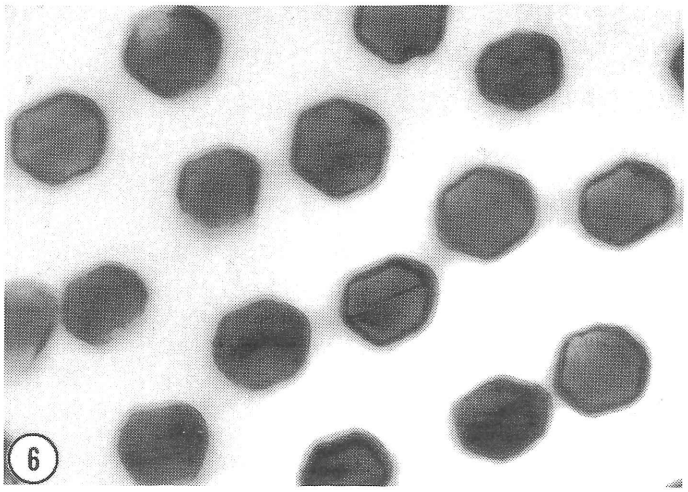

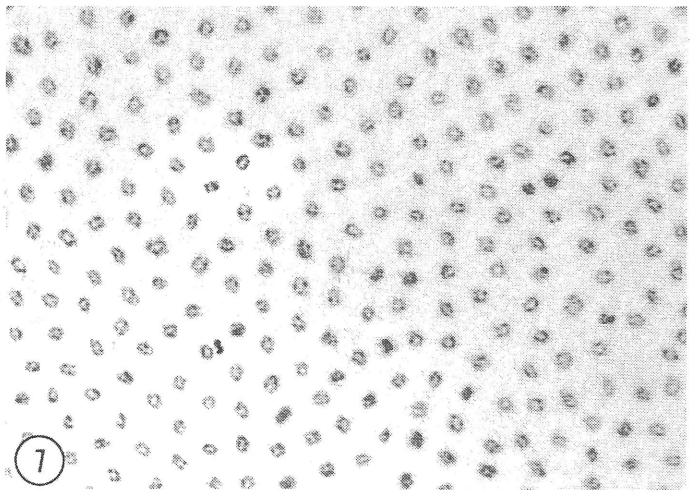

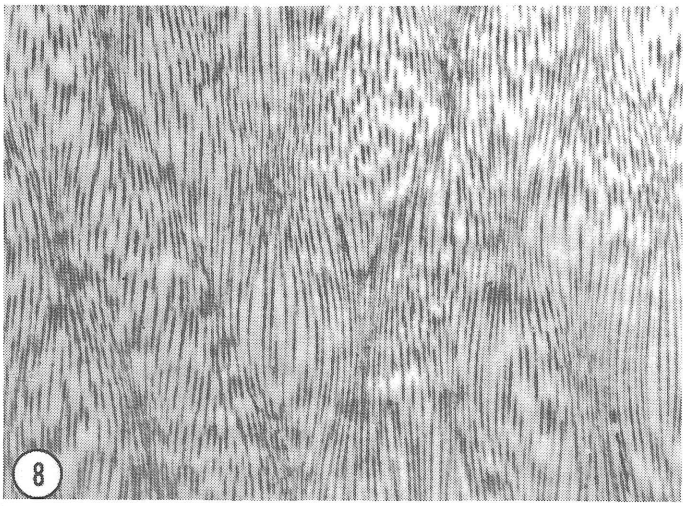

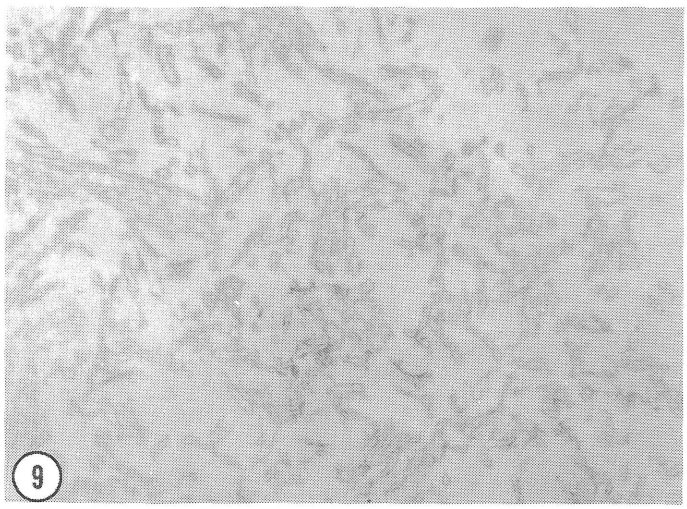

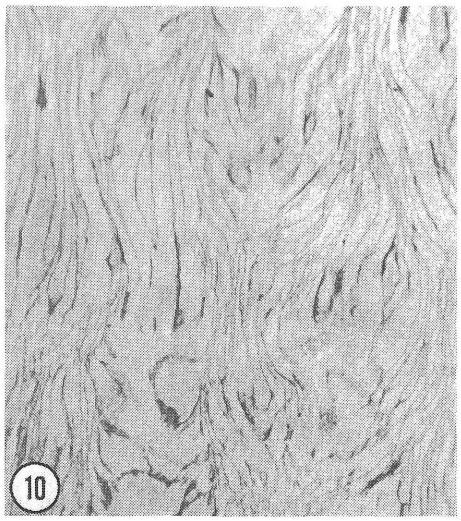

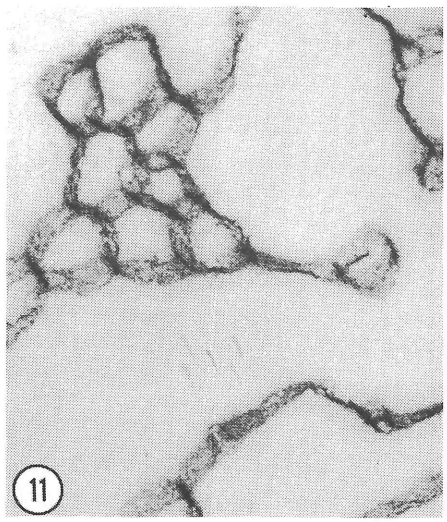

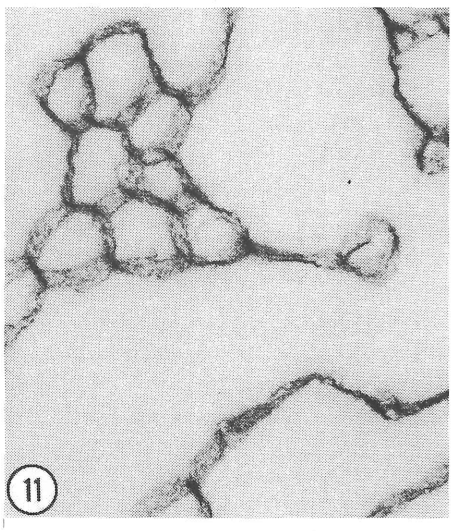

FIGURE 6: Section from the ligament of *Mya arenaria*, showing the pseudo-hexagonal cross sections of the aragonite crystals. The crystals have a thin twin lamella through the center. ×130,000.
FIGURE 7: Cross section through the decalcified *Spisula* hinge ligament. There are two distinct organic phases; the osmiophilic sheaths which surround empty holes once occupied by the crystals and the matrix of low electron density. ×40,000.
FIGURE 8: Transverse section from the decalcified *Spisula* ligament in the noded prism region. The electron dense structures are the crystal sheaths; the distribution of the sheaths is identical to that of the crystals (compare with Fig. 4). ×6000.
FIGURE 9: The isolated crystal sheaths from the *Spisula* hinge ligament. ×21,000.
FIGURE 10: Transverse section of the ligament from *Placopectin magellanicus*. There are two distinct phases; an electron dense extensive fiber network within a homogeneous phase of lower electron density. ×2900.
FIGURE 11: Stereo pair of a cross section from the *Aequipectin irradians* ligament. The major organic phase has been extracted leaving only the fiber network which forms an extensive sheet with many closed loop. ×38,000.

LONGKNIFEMAKER and VIBRATOME

aids for cytological sectioning

Medcast and Water Soluble Epoxy for EM & LM embedments

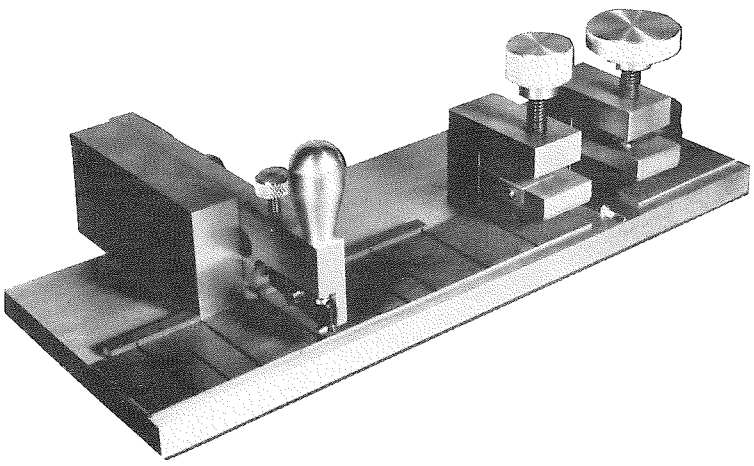

MI LONGKNIFE MAKER

produces glass knives for Light Microscopy
"Ralph" knives can replace metal knives

The Longknife Maker opens new horizons for sectioning large face histological size blocks in the semi-thin (1 - 4um) range using an ordinary rotary microtome. These knives cut glycol methacrylate plastic or paraffin embedded specimens. Knife edges are 25 - 38mm long.

8000 MI Longknife Maker

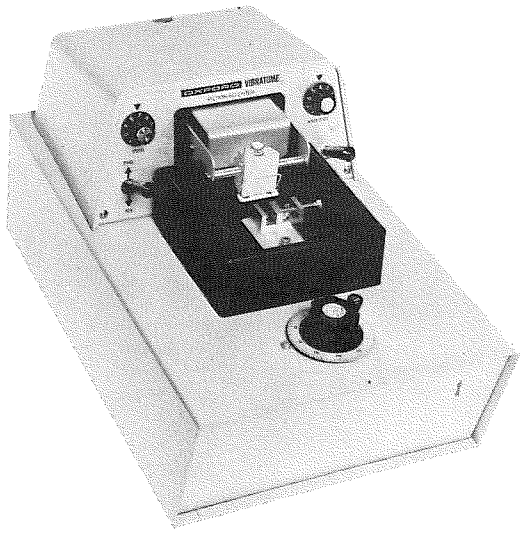

VIBRATOME

cuts fresh material or fixed, in liquid bath
re-embed thick sections for EM

The Vibratome uses a vibrating blade principle to section delicate, fresh tissue without distortion. Many interesting applications have been developed in the fields of tissue pathology, immunocytochemistry, tissue culture, botany, enzyme histochemistry and fluorescent antibody studies. As more work is reported, it is evident that Vibratome usefulness is increasing.

100 Vibratome

New **MEDCAST**

a clear color, low viscosity epoxy to replace Epon 812 for E M embeddings

18001	Pelco Medcast Kit	$23.00
18009	Pelco Medcast Resin	12.00 (500g)

New **WATER SOLUBLE KIT**

light colored, flexible water soluble plastic for Light Microscopy embedments - Quetol 523

18086	Quetol 523 Kit	$29.50

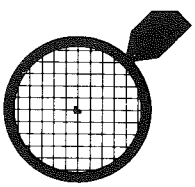

Ted Pella, Inc. *P. O. Box 510; Tustin, CA 92680 -- 714-557-9434 -- Telex 683454 Pelco Irin*

Application/Nomination For Membership

I hereby apply/nominate for Regular ☐ Student ☐ Corporate ☐ membership in the Texas Society for Electron Microscopy.

Name of institution applicant or corporation nominee person _____

P. O. Address _____

_____

Information as to position, degrees, and qualifications for Membership: _____

_____

_____

_____

This nomination is accompanied by a statement of interest in and contributions to Electron Microscopy and associated fields of science.

One year's dues in the form of a check or money order should be sent with the application for Membership form. (Regular $10.00, Student $2.00, Corporate $75.00)

Signature of one Member making the nomination:

_____

Dated _____ 19 _____

This application to Membership in the Society, or this application for transfer from the grade of Student to Regular Member, signed by one Member should be sent to the Secretary to be presented at the next meeting of the Council or approval by a majority vote of the Council. Notice of approval will be mailed by the Executive Secretary.

_____

Presented to the Council at _____ meeting. Date _____

Action _____

Remarks _____

Send Application to: John Hansen
Univ. of Texas Health Science Center
Dept. of Anatomy
7703 Floyd Carl Drive
San Antonio, TX 78284

Philips EM-400 Twin System
Imaging and analysis with no compromise

Electron Diffraction pattern of CdS from a single grain in a solar cell. Courtesy of Dr. J.W. Edington, Dept. of Aeronautical Engineering, Univ. of Del.

The EM-400 Electron Microscope with Twin Lens objective provides atomic level resolution combined with nano-PROBE capability for analysis of specimen areas as small as a billionth of a meter. For the first time, these capabilities are available to you in TEM, S(T)EM and SEM modes with no compromise in performance.

No compromise means TEM lattice resolution to 0.14 nanometres with ±60° of specimen tilt. Single switch operation to S(T)EM, SEM or micro-micro diffraction modes with probe sizes to 2.0 nanometres. X-ray detector collection angle of 0.13 sr — more than double currently available sensitivity.

No compromise in signal handling means providing six different signals. And the ability of mixing these in any sum or difference combination and display them as mono/dual, dual magnification and stereo images.

There's more. The EM-400 was specifically designed to provide an ultra-clean, high vacuum specimen environment to insure consistently successful microanalysis.

Don't compromise. Get complete details. Write to Philips Electronic Instruments, Electron Optics Group, 85 McKee Dr., Mahwah, NJ 07430.

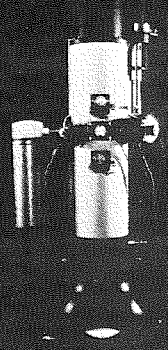

PHILIPS

Electronic Instruments

PHILIPS

Examining Virus Architecture With The Electron Microscope

by
Heather D. Mayor
Department of Microbiology and Immunology
Baylor College of Medicine

The revelation of the architecture of virus particles is a triumph for the transmission electron microscope. Until its advent, only the pox viruses were large enough to be seen, and then very imperfectly, by conventional light optics. Once the electron microscope was accepted as a standard biological tool it was obvious that the dimensions of most viruses (**15 - 150** nanometers (nm) in diameter - see Figure 1) rendered them ideal organisms for structural and architectural analysis with this instrument.

Most biological materials have very poor contrast in electron imagery because the scattering of the carbon atoms in the specimen support film is of the same order of magnitude as that produced by the carbon, nitrogen, oxygen, phosphorus, and sulfur atoms making up the specimen. Thus the first images produced by virus particles were singularly disappointing. Improvement in estimating the actual sizes and overall shapes of viruses was achieved by the technique of shadow casting first introduced in 1944 by Williams and Wyckoff (1). A thin film of a heavy metal such as gold or platinum was deposited under vacuum at an acute angle of incidence to the dried virus particles mounted on plastic films. Although virus particles could be detected confidently, the results were still disappointing as no internal structure was revealed and the granular nature of the deposited metal obfuscated any fine surface details. Often very small particles (e.g. poliovirus, approximately 20nm in diameter) were totally buried in the "shadow".

The introduction of the negative contrast technique by Brenner and Horne in 1959 (2,3) opened the way to a complete and systematic study of the architecture of virus particles and their subunits. The technique consists of essentially of embedding particles in an electrondense stain. The stain can penetrate the interstices of the particle revealing internal details as well as surface features. As a very thin film of an electron dense material such as phosphotungstic acid (PTA) can be used to enhance electron scattering and hence contrast, very fine structural details can be resolved. Thus as thick specimen areas are poorly penetrated by the stain and appear relatievly electron lucent, and thin areas are heavily stained and hence electron opaque, the technique is termed "negative" contrast. Negative contrast images of adenovirus and its associated virus and reovirus are shown in Fig. 2 and 3. As most negative stains have a limited pH range in which they are most effective the technique must be modified for different specimens and different methods of preparation before its yields optimal results.

Delineation of virus structure and architecture in the electron microscope through the technique of negative contrast led to the development of a new terminology for

ISI has just introduced the most powerful commercially available scanning electron microscope in the world. It is called the DS-130. It is pure genius.

Not everyone, however, needs that sort of capability. That's why ISI has the Alpha-9 and S-IIIA. They are...

THE TWO BEST SEM VALUES IN THE WORLD.

$16,400

The Alpha-9 is the world's lowest price SEM, but if you think low cost means low performance, think again. The Alpha-9 gives you 120Å guaranteed resolution, edge to edge micrograph sharpness and a host of outstanding features. Above all, it gives you micrographs you can be proud of.

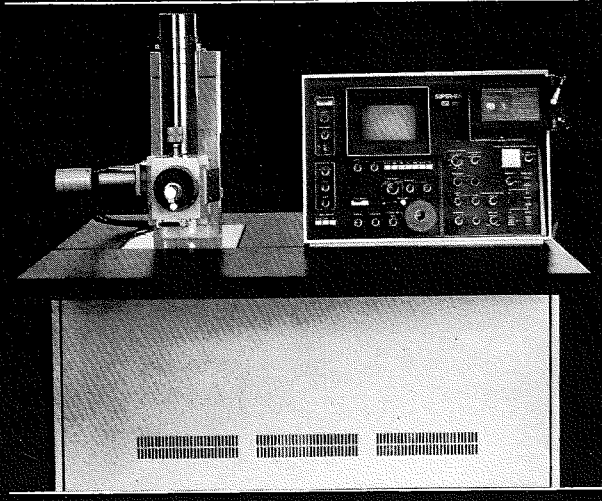

The S-IIIA. For the money, it offers more features and more performance capability than any other SEM—and it's expandable. That's why it's the #1 selling SEM in the world.

That's not all. **ISI has a number of reconditioned instruments at extremely affordable prices.** Ask about them. But hurry, they are on a first come-first served basis.

At these unbelievably low prices, anyone can have SEM power. Contact us for full specifications and/or a demonstration.

ISI International Scientific Instruments, Inc.

3255-6C Scott Boulevard • Santa Clara, CA 95050 • (408) 249-9840

the virus building blocks which were observed (4,5). The complete virus particle is known as the **virion**, a term denoting both intactness of structure and the property of infectiousness. All virions are composed of nucleic acid, either single- or double-stranded **RNA** or **DNA**, enclosed in a regularly arrayed protein coat, the **capsid.** The capsid is composed of subunits, either similar repeating protein molecules called structure units or of capsomers (aggregrates of structure units). Specificity and economy are important principles in the construction of virus particles. By specificity we mean that the viral subunits must fit together in a definite and reproduceable way. By economy we mean that large structures must of necessity be built from many copies of a few kinds of smaller subunits. These two principles lead irrevocably to an implicit particle symmetry and hence stability in the compiled structure. The capsids of the simplest viruses exhibit either helical or cubic symmetry of the icosahedral type (see Fig. 4). Icosahedral or 5:3:2 symmetry means that rotational axes of 5-fold, 3-fold, and 2-fold symmetry can be described which pass through the center of the particle. The structure composed of the nucleic acid surrounded by the capsid is the **nucleocapsid**. Some viruses are naked nucleocapsids, whereas others are enclosed in an envelope or **peplos** whose origin may be from cellular membranes. Some envelopes are covered with surface projections or **peplomers** of varying lengths spaced at regular intervals. These projections are presumably coded by the virus and are incorporated into the host cell membrane prior to virion maturation and release. All these details are readily resolved in the electron microscope subsequent to negative contrast staining. The shapes and relative sizes of seven well known animal viruses, 6 displaying icosahedral symmetry, 1 helical symmetry, are shown in Figure 4. Influenza virus (Fig. 5) has a nucleocapsid which displays helical symmetry. This symmetry is clearly seen in the purified nucleocapsid prepared from simian virus **SV5**, a virus very similar in structure and composition to influenza virus (Fig. 6). Adenoviruses display clear icosahedral symmetry and it is possible to determine the number of capsomers or morphological subunits seen in the electron microscope (Fig. 2) by simple mathematics. An icosadeltahedron is a polyhedron whose faces are all equilateral triangles and which has 5:3:2 icosahedral symmetry. Virus particle surface lattices can be expressed in terms of such an icosadeltahedron which has 20T equilateral triangles as faces where T is the triangulation number (6). The number of chemical structure units (polypeptides) in the capsid is 60T. If these are arranged in groups of 5's and 6's - pentamer-hexamer clusters (by far the most common arrangement in all icosahedral viruses studied to date) - we can determine the number of capsomers or morphological subunits (M) by the equation M = 10T+2. Thus for adenovirus (Fig. 2) T = 25 and there are 252 capsomers making up the capsid. For the nucleocapsid of herpes virus (Fig. 7) T = 16 and the capsomer count is 162. For reovirus (Fig. 3) T = 9 and M = 92. For wart virus (Fig. 8) T = 7 and M = 72. It is still difficult to determine the number of capsomers accurately for some of the very small viruses using the negative contrast technique. Thus for adeno-associated virus (Fig. 2) T numbers of 1 and 3 have been proposed. These differences should be resolved in the near future with current high resolution electron microscopes and biochemical analysis.

Not all protein subunits in icosahedral viruses are grouped into clusters of hexamers and pentamers. Dimers and trimers are possible solutions that do not violate the symmetry requirements e.g. two plant viruses, tomato bushy stunt virus and turnip crinkle virus have been found to have dimer clustering so that with a T number of 3 there is a capsid count of 90 (60T/2) rather than the 32 predicted in the pentamer-hexamer configuration (7).

The intriguing diversity in the end products of the replication processes of viruses is shown clearly following examination of negative contrast preparations in the electron microscope. Herpes viruses that are potentially non-infectious through loss of their surrounding envelopes are sharply resolved as T = 16 icosadeltahedra. However, potentially infectious particles encased in their surrounding images in the electron microscope. Particles which lack a nucleic acid core are easily detected by their electron dense centers (Fig. 7) evidence for complete penetration.

Mistakes in assembly of viral building blocks (Fig. 8) are common findings, particularly with viruses that yield many defective progeny or which grow poorly in the tissue culture environment which is the basis of most virus production in the laboratory. Additional problems in interpretation occur when a profusion of capsomers, and their aberrant distribution, lead us to infer that we are seeing an image representing not the "top" surface of the virus particle alone but a composite image of both "top" and "bottom" surfaces superimposed and often out of register. Many of these problems have been solved elegantly by Klug and his colleagues (8,9) using high resolution electron micrography and computergenerated superposition patterns.

Collections of small identical particles present ideal conditions for crystallization. These conditions are met in many small animal viruses both in intracellular aggregates and in purified preparations. From theoretical considerations only the small viruses should form true crystals. This is because the van der Waals forces operative at longer ranges are not sufficiently strong to hold large spherical particles (diameters around 100mμ or more) in a firm crystalline array. Thus crystals are formed with the smaller picornaviruses, such as poliovirus, but not with the larger virions such as herpes viruses and myxoviruses (influenza).

For true crystals, the strict requirements of regular replication of lattice points limits the allowable axes of rotational symmetry to 1-,2-,3-,4-, and 6-fold axes. The observation that virus particles with 5-fold axes do indeed form reasonable close-packed arrays may represent an efficient compromise. Nature may combine the need for structural economy in building the virus particle, with the advantage, as far as survival of the virus as an organism is

TWO INTO ONE WILL GO.

WORLD'S FIRST COMBINED LIGHT AND ELECTRON MICROSCOPE

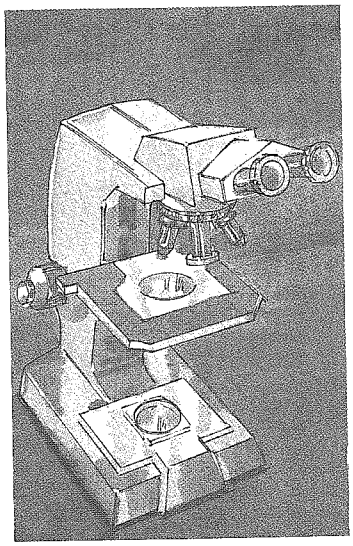

The ISI LEM-2000 combines a high resolution light microscope...

At last—undisputed direct light-electron image correlation of the same specimen area.

The flexibility is incredible. Section thickness may range from ultrathin-phase contrast to over one micron-polychromatic stain examinations.

The stage relocates any area selected by the operator and the microprocessor-controlled 6 lens, 100 kV EM is truly state-of-the-art.

Another key advantage of the LEM-2000 is its large grid size of 7 mm diameter to accommodate large tissue sections. An advanced electron optical design provides extremely wide flat fields at low magnifications. Result: distortion free brilliant images at all magnifications. Among many other standard features are EM Stereo and a fully automatic photography system.

Find out more about this revolutionary concept in diagnostic microscopy. Call or write ISI for details.

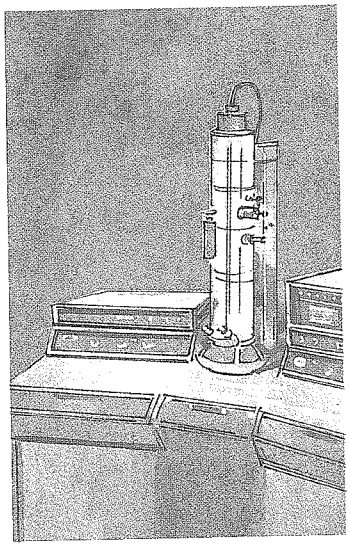

...with a 100 kV transmission electron microscope into one powerful instrument.

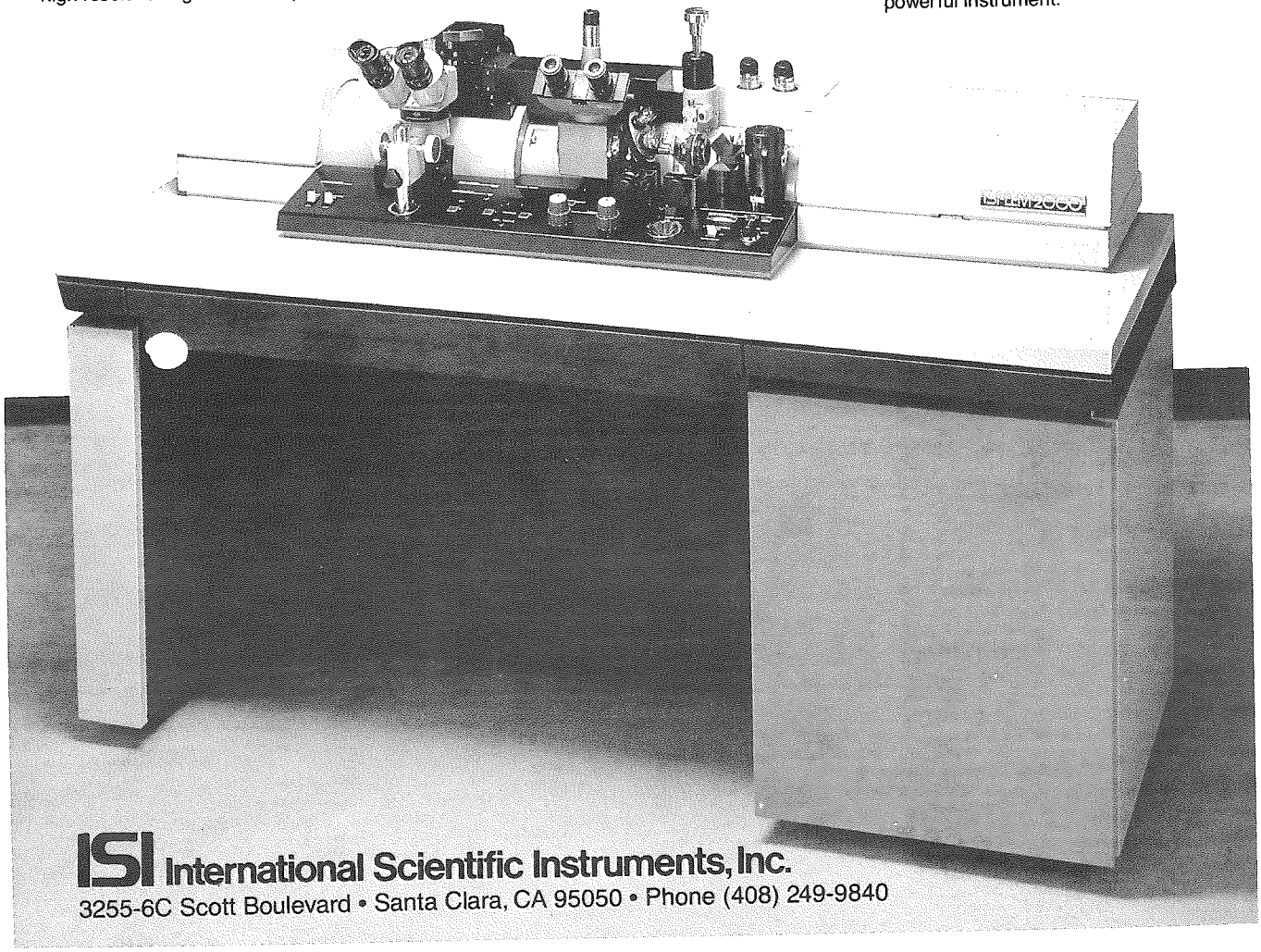

ISI International Scientific Instruments, Inc.

3255-6C Scott Boulevard • Santa Clara, CA 95050 • Phone (408) 249-9840

concerned, of being able to produce as many progeny as possible in a limited space. In fact for the some of the larger viruses (e.g. adenovivus in which the virus particle has the actual shape of an icosahedron) the icosahedron, by virtue of its hexagonal outline, is quite ideally fitted to a honeycomb-like packing in 3 dimensions (Fig. 9).

Identification of small animal viruses in ultra-thin sections of infected cells is often a difficult procedure as the particles, particularly when they occur singly, are usually indistinguishable in morphology and diameter from cell organelles such as ribosomes. One should identify confidently as viruses only those small particles which occur in definite arrays(Fig. 10).

For larger particles (~70nm or more in diameter) such as adenovirus or herpes virus, arrays are the preferred environment (Fig. 11) but single particles can certainly be identified as viral if they are present in sufficient quantity. Envelope viruses may be confirmed if they appear contiguous to or are continuous with cellular membranes through which they may be presumed to be released by a budding mechanism (Fig. 12).

Working with large scale models is an integral part of electron microscopic determinations of virus architecture. Useful models of viruses can be constructed from ping pong balls. A T = 1 model (the simplest virus structure) is shown in Fig. 13a. A more complex model representative of adenovirus can be assembled by building the basic icosahedron from 252 balls (Fig. 13b). Reovirus is more accurately represented by using hollow 5- and 6-sided cardboard prisms as capsomers (Fig. 13c). Models built from geodestix (a type of tinker toy) and plastic connecting units are often useful in simulating the types of images obtained when both sides of a virus are imaged at one time and superimposed on one another (Fig. 13d). Of course there are many other options depending only on ingenuity and an adequate budget.

An elegant wooden model (Fig. 14) of a T = 3 virus capsid was built in 1963 by Dr. Donald Caspar now at Brandeis University. This model, which was shown in Houston in 1974 during the Life Shapes Exhibition organized by the Department of Microbiology, Baylor College of Medicine in cooperation with the Contemporary Arts Museum, was designed so that the units could assemble in only one way to form a stable shell. The bonding pattern chosen led to hexamer-pentamer clustering and 32 clusters corresponding to the morphological units observed in a plant virus, the turnip yellow mosaic virus.

As an alternative to model building, computers are now being coupled with the electron microscope to investigate virus architecture. Electron microscope images, because of the large depth of focus inherent in the transmission mode, represent density information from different levels within the specimen. Methods have been developed from computing 3-dimensional electron density maps from transmission electron micrographs of virus particles using Fourier analysis (10,11,12). After processing data from different views of one particle (obtained by tilting the specimen) or from several particles, a reconstruction of the particle's 3-D structure can be obtained for comparison with the electron microscope images. This approach, although available only in a few specialized laboratories, is certainly the future direction, particularly for broaching the as yet virtually untouched problems of the location and architecture **in situ** of the nucleic acid core of the virus. An encouraging start has been made with crystals of polyoma virus whose particle diameter is sufficiently small to allow preparation of large single crystals for analysis. It is hoped that the structure of the DNA core can be determined by computer analysis of electron density maps (13).

Computer graphics is also providing a new and exciting approach to the study of close packing of virus particles both inside infected cells and in extracellular arrays. Using a CDC 6000 computer and a graphics program named "ICOSA" developed by Philip Hendren now in the Department of Architecture at the University of Texas, it is possible to generate facsimiles of icosahedral viruses, fit them into a closely packed environment, and examine them from different directions (Fig. 15). In this way models for cleavage patterns similar to those expected using ultra-thin sectioning techniques of virus infected cells (see cover micrograph) can be constructed and compared with the actual electron micrographs. The graphics approach could prove invaluable in simulating those environments that are most significant in virus stability and survival and possibly the assembly mechanisms that are most vulnerable to intervention. The electron microscopy will play a seminal role in these new frontiers.

ACKNOWLEDGEMENTS

The author would like to thank Liane Jordan for taking the majority of the electron micrographs, Dr. Donald Caspar for Figure 14, and Philip Hendren and Philip Mayor and the Department of Architecture, University of Texas at Austin for allowing use of Figure 15 prior to publication.

This report is supported by Grant CA 14618 from the National Cancer Institute.

REFERENCES

1. Williams, R. C. and Wyckoff, R. W. G. (1944) J. Appl. Phys. **15**:712.

2. Brenner S., Streisinger, G., Horne, R. W., Champe, S. P., Barnett, L., Benzer, S. and Rees, M. W. (1959) J. Molec. Biol. **1**:281.

3. Horne, R. W., Brenner, S., Waterson, A. P. and Wildy, P. (1959) J. Molec. Biol. **1**:84.

4. Caspar, D. C. D., Dulbecco, R., Klug, A., Lwoff, A., Stoker, M. P. G., Tournier, P. and Wildy P. (1962) Cold Spring Harbor Symp. Quant. Bio. **27**:51.

5. Lwoff, A., Horne, R. W. and Tournier, P. (1962) Cold Spring Harbor Symp. Quant. Biol. **27**:51.

6. Caspar, D. C. D. and Klug, A. (1962) Cold Spring Harbor Symp. Biol. **27**:1.

7. Finch, J. T., Klug, A. and Leiberman, R. (1967) J. Mol. Biol. **50**:215.

8. Finch, J. T. and Klug, A. (1968) J. Mol. Biol. **15**:344.

9. Finch, J. T. and Klug, A. (1967) J. Mol. Biol. **24**:289.

10. De Rosier, D. J. and Klug, A. (1968) Nature London **217**:130.

11. Crowther, R. A. (1971) Phil. Trans. Roy Soc. London **261**:221.

12. Finch, J. T. (1974) J. Gen. Virol. **24**:359.

13. Adolph, K. W., Caspar, D. L. D., Hollingshed, C. J., Lattman, E. E. and Phillips, W. C. (1979) Science **203**:1117.

14. Hendren, P., Mayor, P. H., Chalmers, J. H. and Mayor, H. D. (1979) Computers and Biomedical Research {submitted}.

30Å RESOLUTION

THE ISI DS-130—SHEER GENIUS!

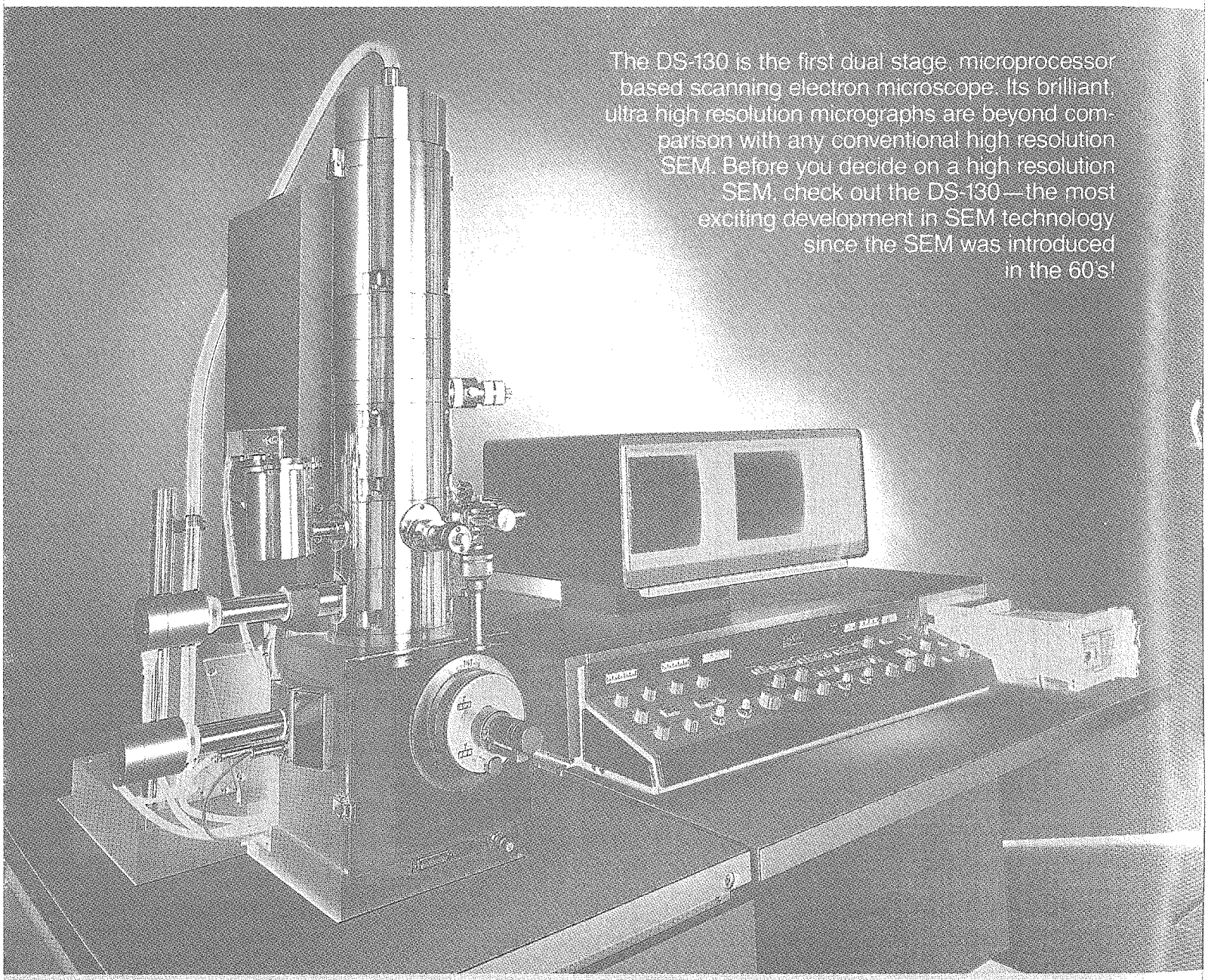

The DS-130 is the first dual stage, microprocessor based scanning electron microscope. Its brilliant, ultra high resolution micrographs are beyond comparison with any conventional high resolution SEM. Before you decide on a high resolution SEM, check out the DS-130—the most exciting development in SEM technology since the SEM was introduced in the 60's!

CALL COLLECT IF YOU WISH (408) 240-9840

For technical literature, circle the reader service number below.

ISI International Scientific Instruments, Inc.

1656 McCarthy Blvd., Milpitas, California 95035 (408) 240-9840

FIGURE 1

RELEVANT LENGTH UNITS FOR MEASUREMENT OF VIRUSES*

1 micron (μ) = 10^{-6} meter

1 Angstrom (Å) = 10^{-8} centimeter

1 millimicron (mμ) = 10^{-9} meter or 10^{-7} centimeter

1 mμ = 10Å

(Molecular dimension) ↑ ↑ (Atomic dimension)

nanometer (nm) = 10^{-9} meter

1 mμ = 1nm

*The modern transmission electron microscope with resolution limit below 5A can give clear images of most virus subunits.

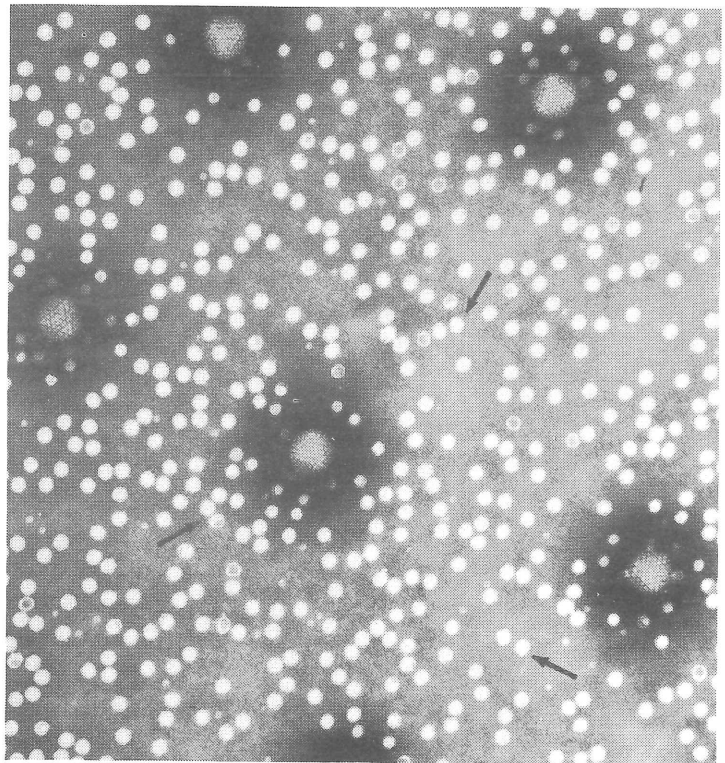

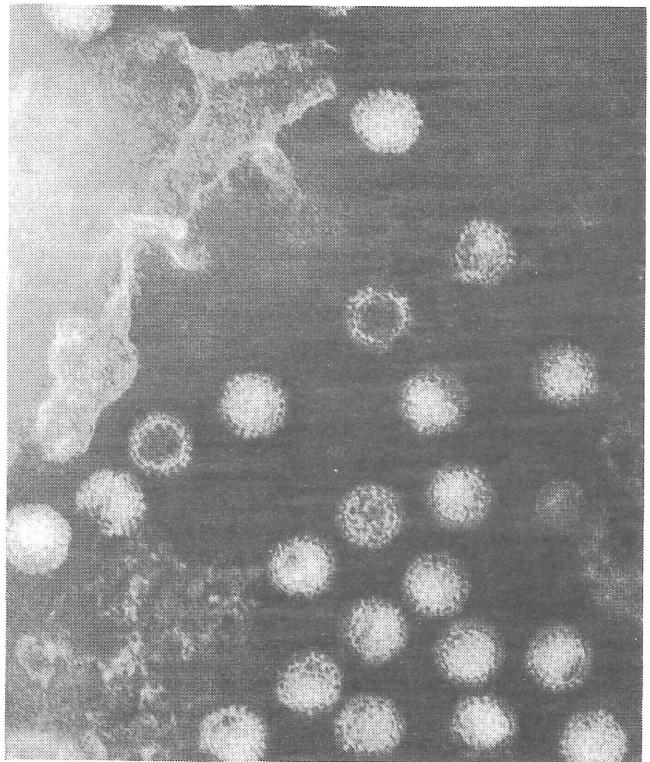

FIGURE 2: Electron micrograph of adenovirus (large particles) and its satellite, the adeno-associated virus (small particle, black arrows). Negative contrast preparation ×80,000.

FIGURE 3: Electron micrograph of reovirus particles. Negative contrast preparation. ×120,000.

WE'VE GOT YOU COVERED!

Here are 6 reasons why ISI has more scanning electron microscopes operating throughout the world than any other manufacturer:

1 DS-130
The Ultimate

The years ahead DS-130 is the world's first dual stage computerized SEM with a resolution of 30 Angstroms guaranteed. It does everything!

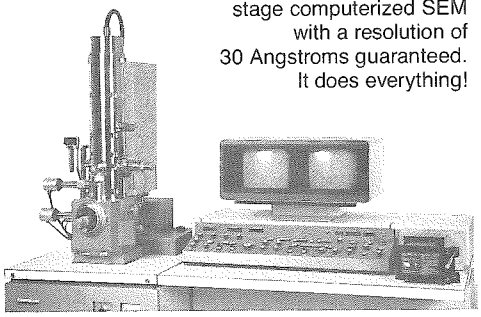

2 SYSTEM 100B
State-of-the-art

The System 100B is a superb research quality SEM featuring ISI's exclusive Automatic Beam System and many other advanced features.

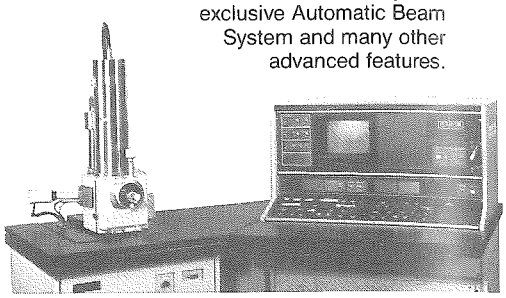

3 ISI 60A
Research quality

The popular ISI 60A offers a vast array of standard features. Guaranteed resolution 60 Angstroms.

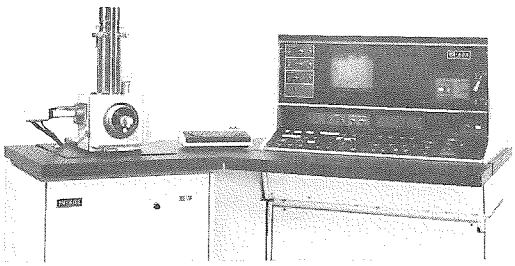

4 ISI-40
Flexibility

A fine research SEM, the ISI-40 offers the user extraordinary flexibility. Guaranteed resolution 60 Angstroms.

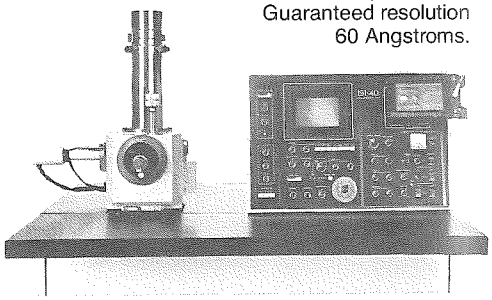

5 SUPER IIIA
The workhorse

Reliability and high performance are the outstanding characteristics of the Super IIIA. Resolution 70 Angstroms.

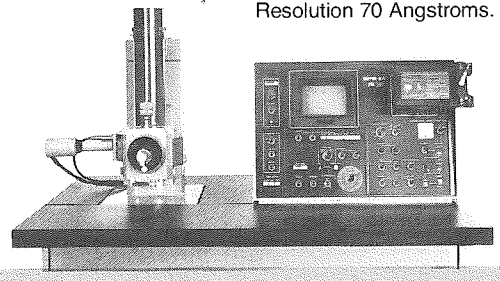

6 ALPHA-9
Simplicity

The Alpha-9 is an excellent performer for quality assurance, teaching and many other uses. 100 Angstroms resolution.

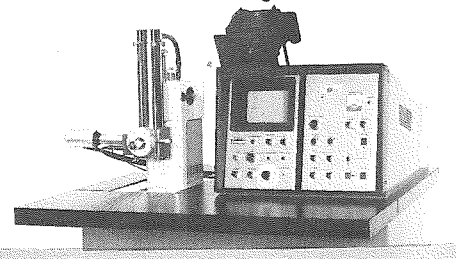

ISI has a SEM to meet your needs! That's why in the world of electron optics, it pays to see ISI first. Because ISI is first in product depth, first in sales, first in service, and first in versatility. We've got you covered! Get in touch.

ISI International Scientific Instruments, Inc.

3255-6C Scott Boulevard • Santa Clara, CA 95050 • (408) 249-9840

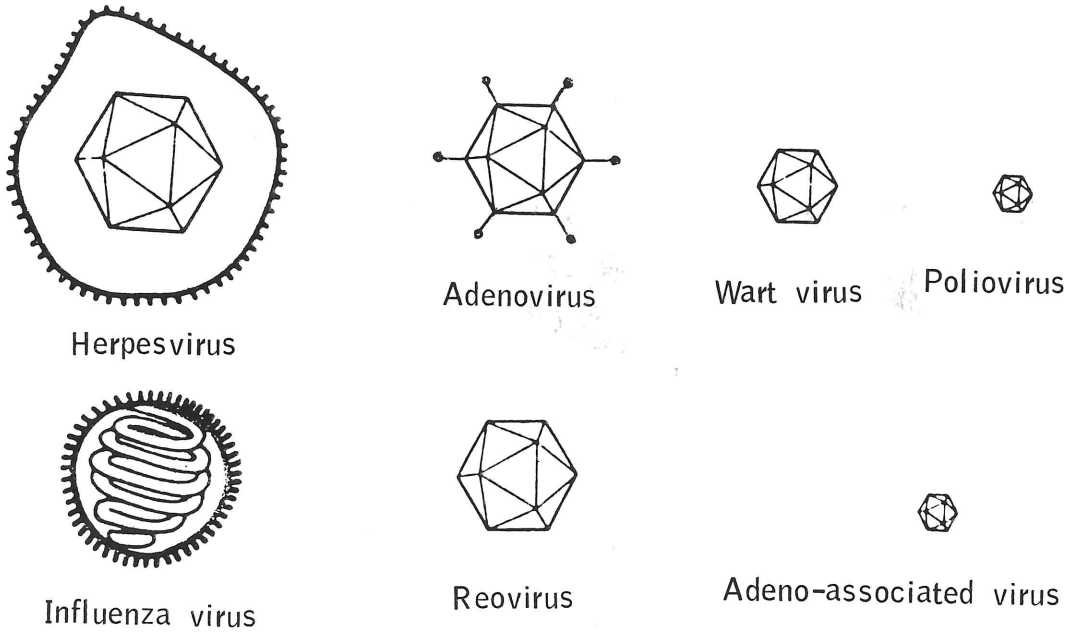

FIGURE 4: Basic shapes of 7 well known viruses-All except influenza (helical) exhibit icosahedral symmetry. Herpes and influenza are enveloped.

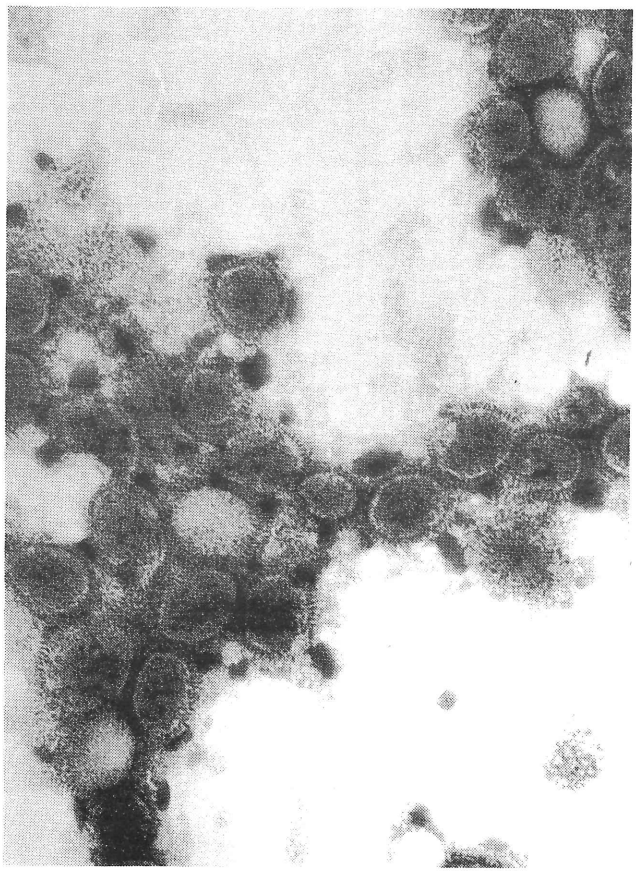

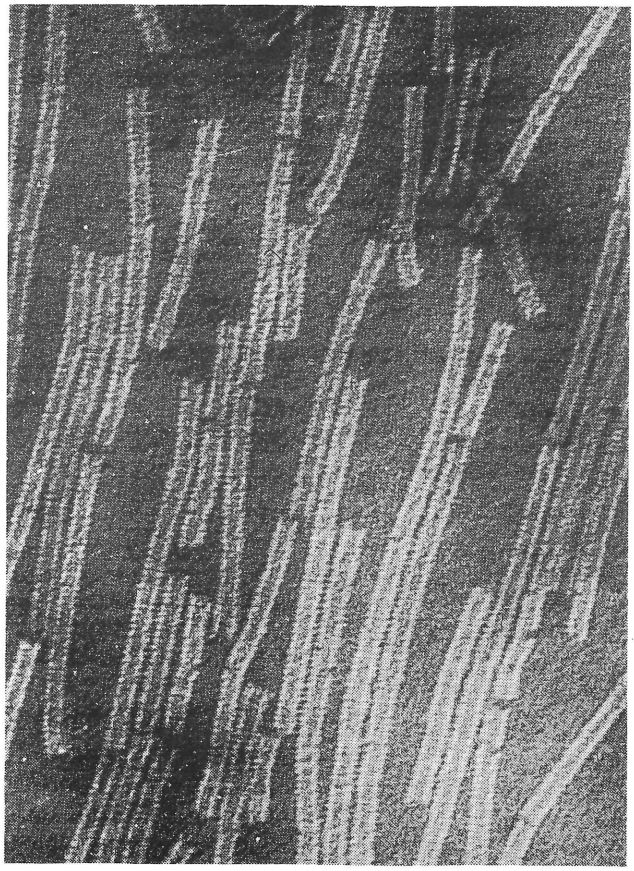

FIGURE 5: Electron micrograph of influenza virus. Negative contrast preparation. ×81,200.
FIGURE 6: Electron micrograph of the nucleocapsid of simian virus SV5. Negative contrast preparation. Helical structure is clear. ×220,000.

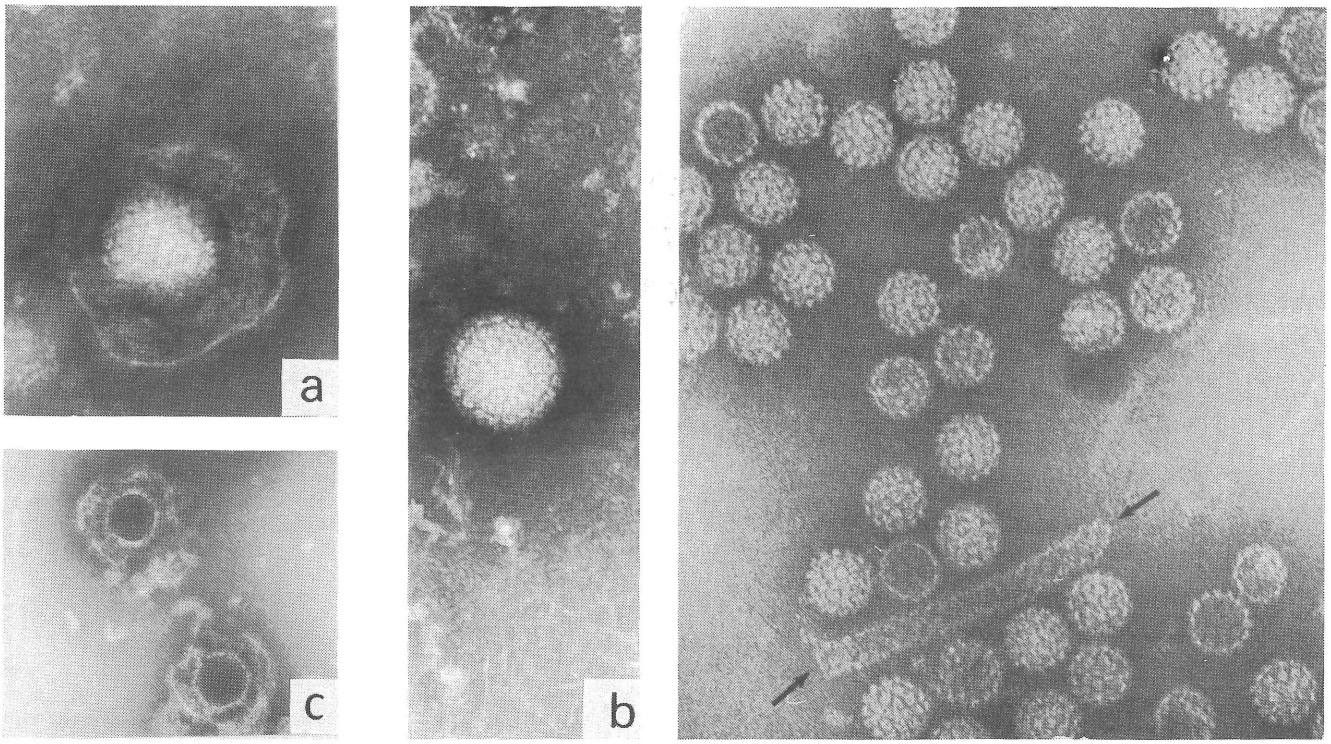

FIGURE 7: Electron micrographs of herpes virus. Negative contrast preparations. **a)** envelope is broken allowing good penetration of stain resulting in clear capsomer detail. ×150,000. **b)** naked icosahedral nucleocapsid. ×150,000. **c)** particles are deeply penetrated by the stain indicating absence of nucleic acid core. ×75,000.

FIGURE 8: Electron micrograph of papilloma (wart) virus. Negative contrast preparation. The tubular structure (arrow) indicates a mistake in virion assembly. ×160,000.

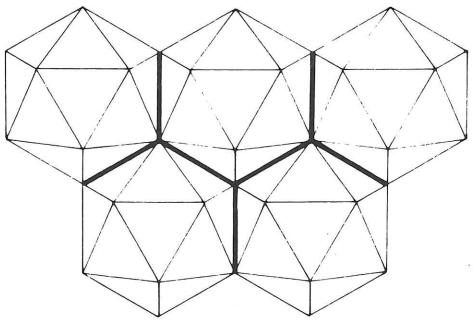

FIGURE 9: Diagram illustrating how icosahedral symmetry may be suited for packing virus particles "economically" in infected cells. Viewed along a 3-fold axis of rotational symmetry the 5 icosahedra form a plane tessellation or tiled pattern.

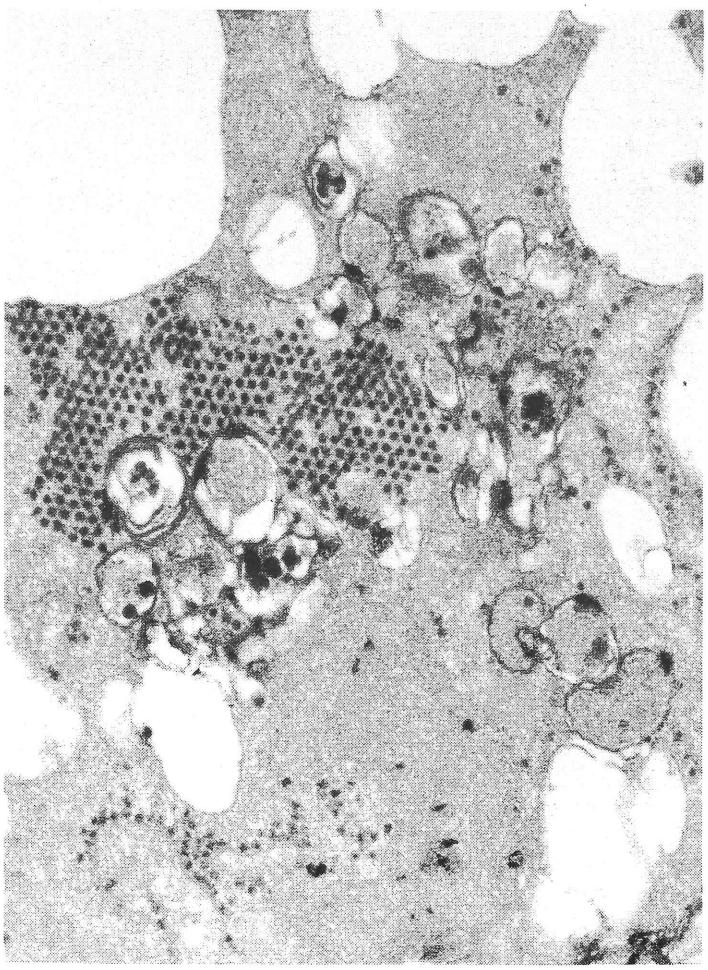

FIGURE 10: Electron micrograph of an ultra-thin section through a cell infected with adeno-associated virus. It is easy to discriminate the array of virus particles from the cellular ribosomes. ×60,000.

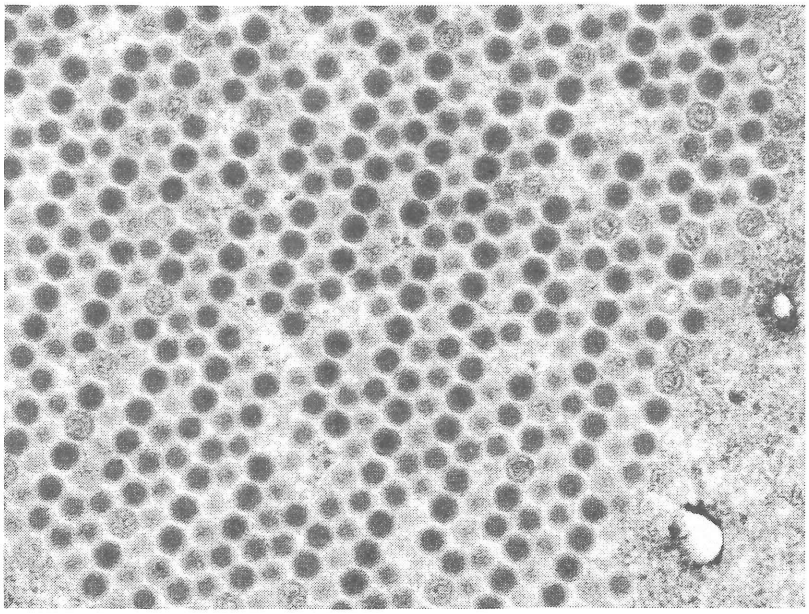

FIGURE 11: Electron micrograph of an ultra-thin section of a nucleus of a cell infected with adenovirus. Particles appear in a large crystalline array. ×80.000.

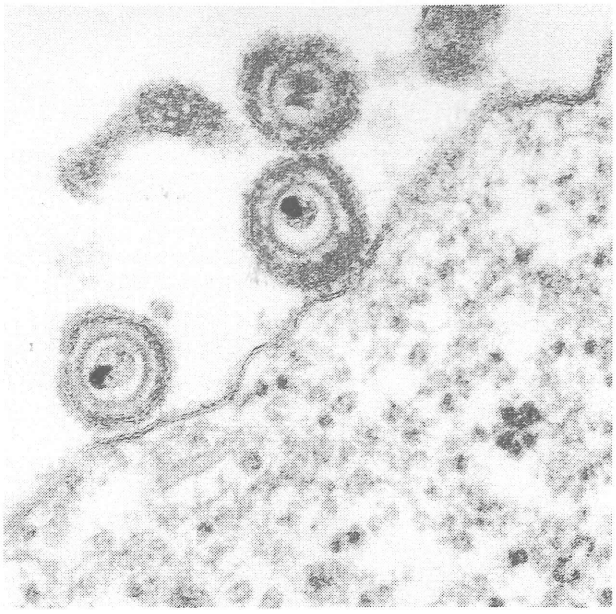

FIGURE 12: Electron micrograph of an ultra-thin section of a cell infected with herpes virus. Enveloped particles have budded through the adjacent plasma membrane. ×140.000.

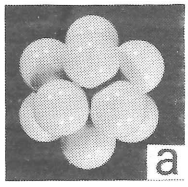

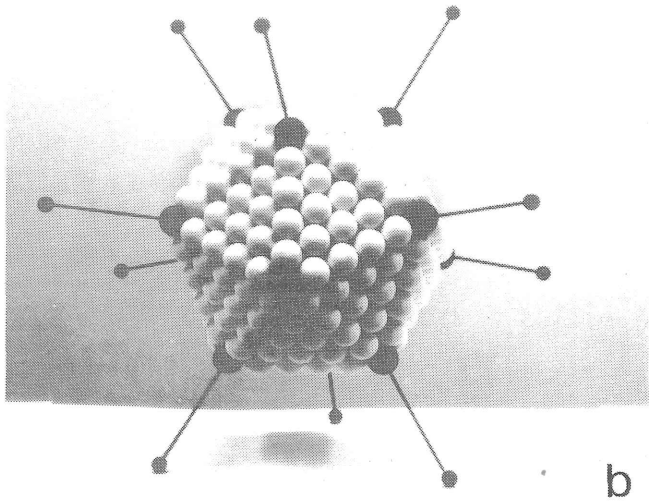

FIGURE 13: a) Icosahedron constructed from 12 ping pong balls. Viewed along a 3 fold axis of symmetry. T=1. **b)** Model for adenovirus. Icosahedron constructed from 252 ping pong balls and 12 rigid rods. Viewed along a 2 fold axis of symmetry. T=25. **c)** Model for reovirus. Ping pong balls in basic icosahedron have been replaced with 8 hexagonal and 12 pentagonal prisms. T=9 capsomers = 92. **d)** shadowgraph produced by a geodestix model representing a T=4 icosadeltahedron. Viewed along a 5-fold axis of symmetry.

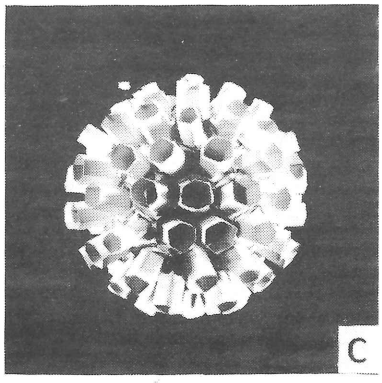

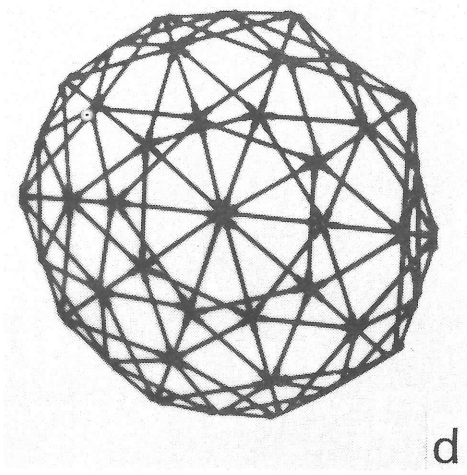

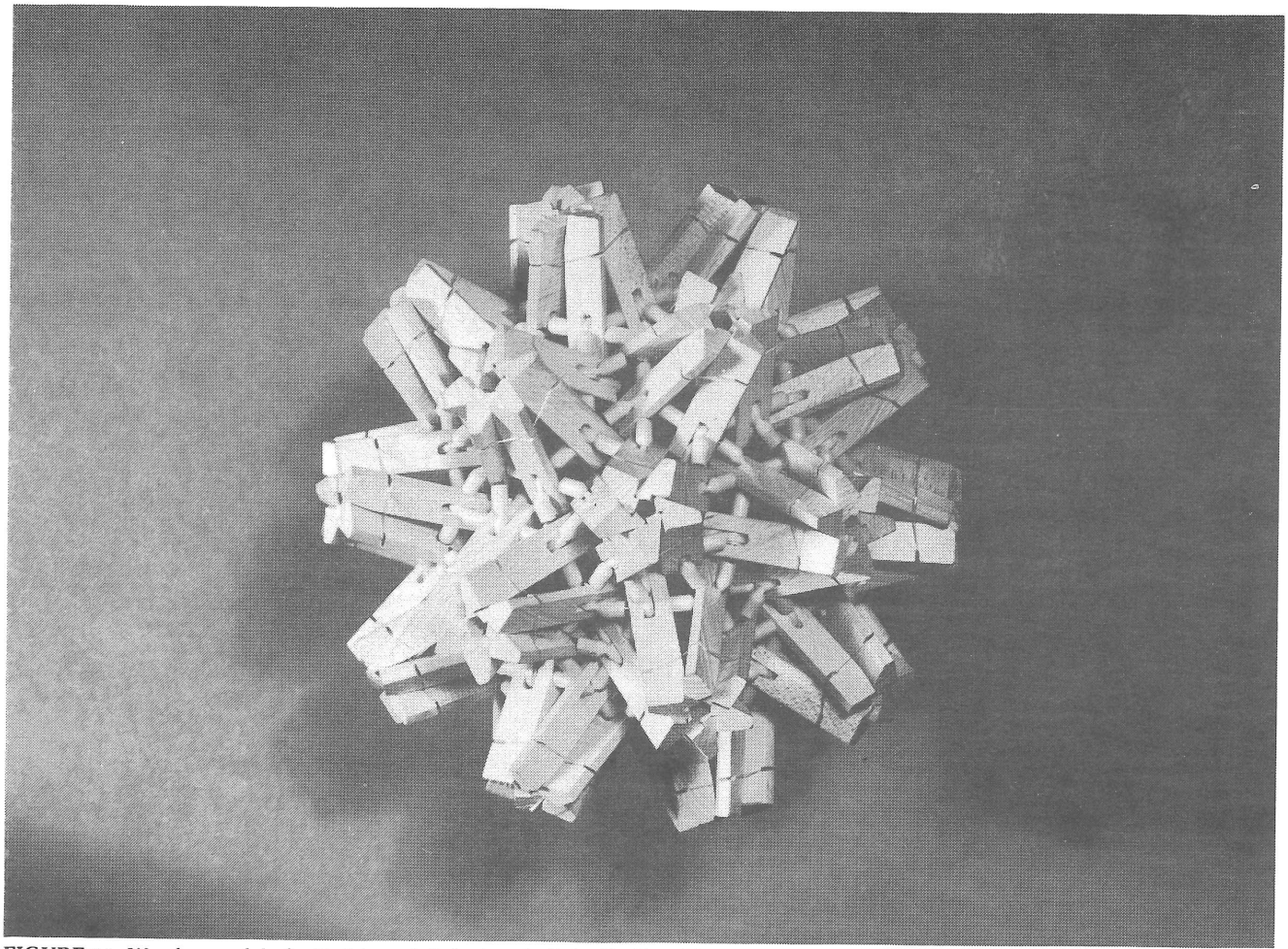

FIGURE 14: Wooden model of a T=3 icosadeltahedron built by Dr. Donald Caspar, Brandis University. Subunits can only fit together in one way to form a stable structure. Viewed along a 5 fold axis of symmetry.

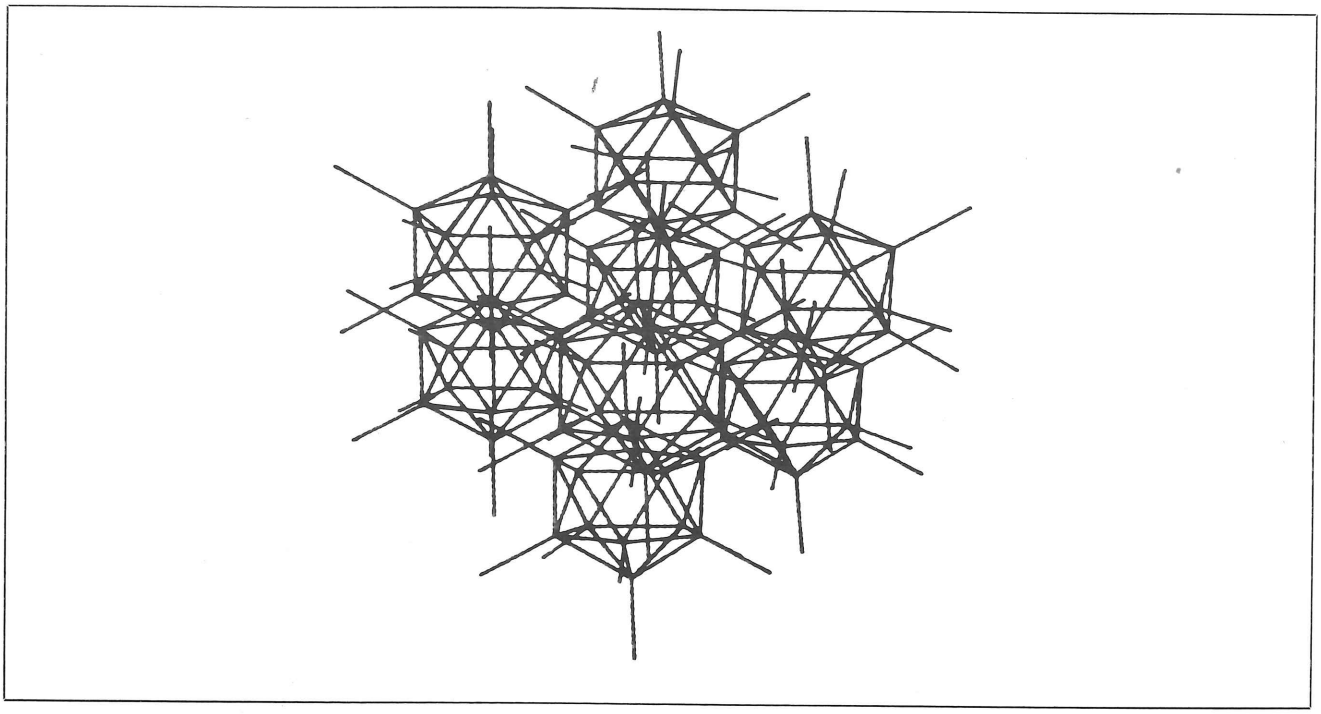

FIGURE 15: Computer graphics display using ICOSA program to simulate adenovirus particles with their attached fibers.

The Zeiss KF 2

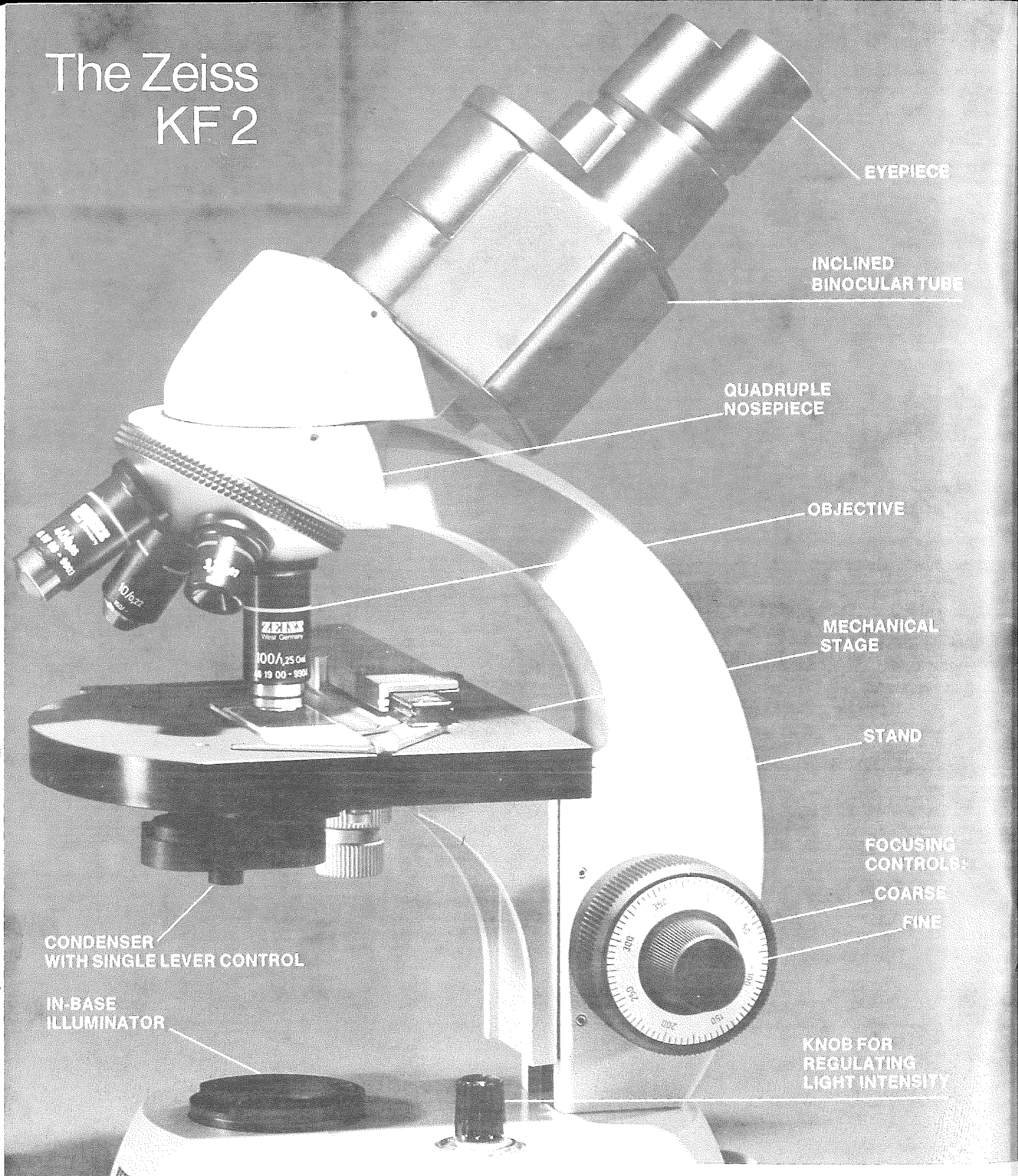

THE X-RAY ANALYZER YOU'VE BEEN ASKING FOR IS HERE...

The new PGT SYSTEM III fits your needs because your needs created it. It's the X-ray analyzer you've been asking for.

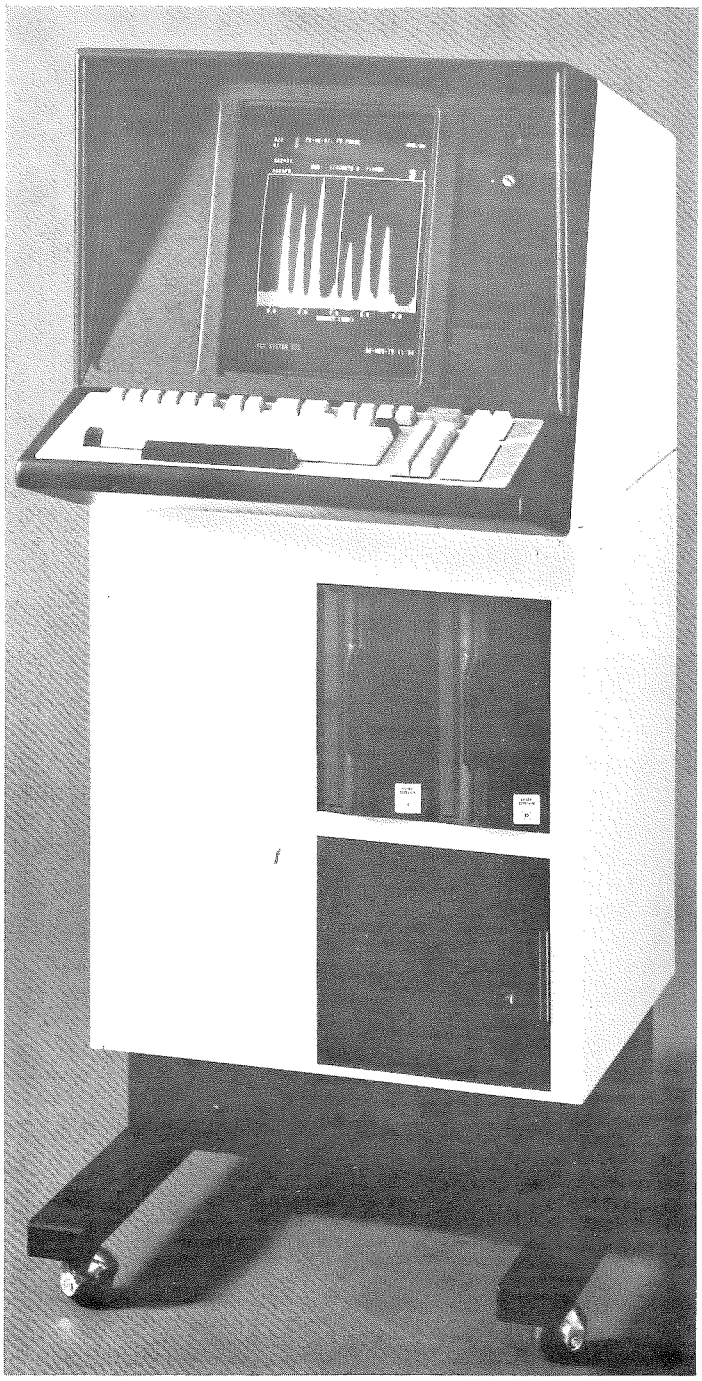

No other system gives you all the advantages of color with none of the drawbacks. Because the color display is truly flicker-free, you get a sharper image with less eye strain. But because of the unique color scheme, you also get high-quality black-and-white photos.

No other system remembers more. A double-sided, dual-density floppy disk is standard *in the qualitative system.* This means that 100 spectra can be stored and retrieved automatically. You start where most systems stop--with virtually unlimited data storage.

No other system grows up faster. Because of the unique hardware design, you can update from a qualitative or semiquantitative system to full quantitative capability *at your own facility.* It's a system that grows as fast as your needs.

No other keyboard is so easy to learn or use. You talk to it in English, and most qualitative and semiquantitative routines are single-key functions. It talks back in English too, with prompts from the video screen for all multiple-step routines.

No other system gives you 96 predefined windows. You get color-coded, predefined element windows, with automatic integrals.

To find out more about the **PGT System III,** make arrangements today for your own demonstration. After all, you asked for it.

PGT
PRINCETON GAMMA-TECH

X-ray Microanalysis Systems for SEMs, TEMs, and Probes

Box 641 Princeton, NJ 08540
(609)924-7310 Cable PRINGAMTEC Telex 843486

Analytical Research Services

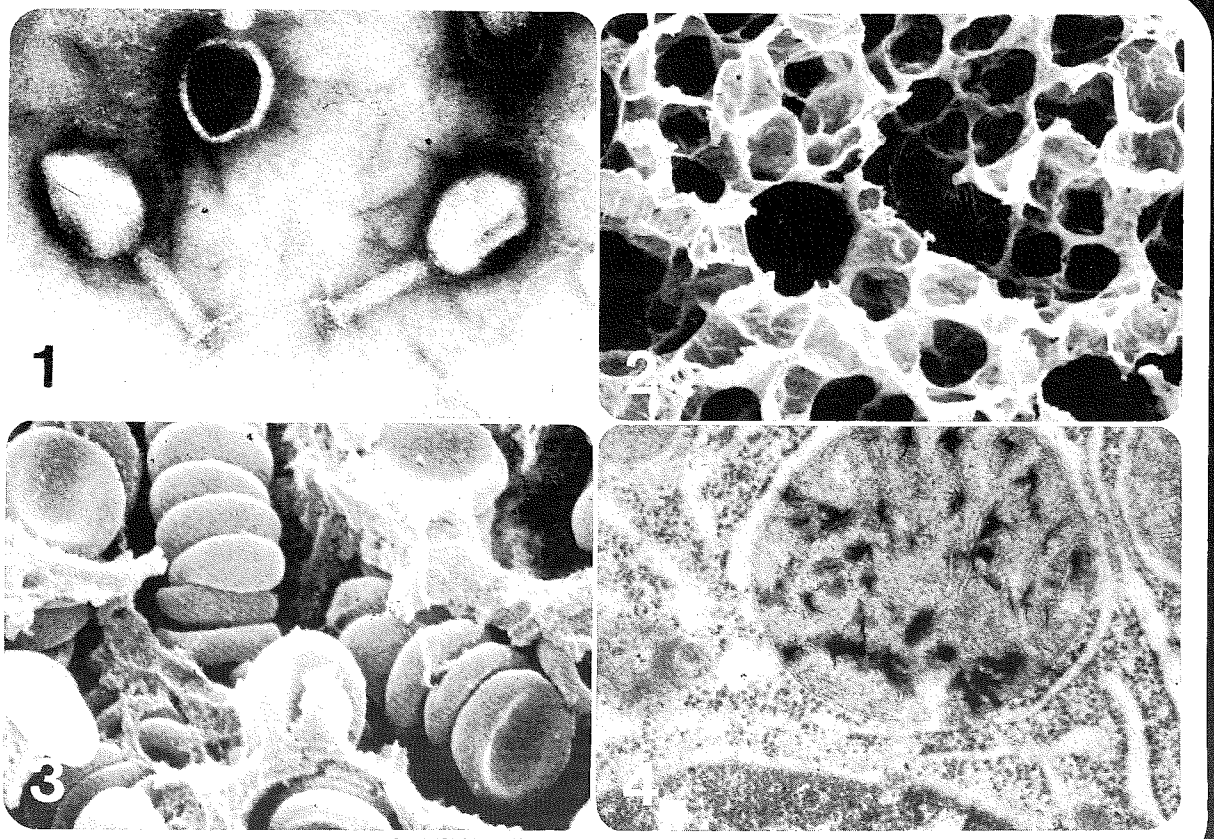

1. T-4 Phage, TEM (PTA) 97,500X 2. Rat Lung, SEM (CPD) 100X 3. RBC's In Situ , SEM (CPD) 3000X 4. Mitochondrial Inclusions Diseased Human Lung, TEM 19,000X

Scanning Electron Microscopy
Two High Resolution SEM's with Television Scan, Video Tape Recorder, Tensile Stage, High Temperature (to 1600°C) Heating Stage, Rotating Monofilament Stage and other accessories. Critical Point Drying (CPD) for biological specimens.

Electron Probe Microanalysis
Energy and Wavelength Dispersive

Transmission Electron Microscopy
Diamond Knife Thin Sectioning with "Cryo" capability of Biological, Polymer, Ceramic and Metallurgical Samples; Replication and Shadowing; Freeze Fracturing and Etching; Stereopairs and negative staining.

Quantitative Image Analysis
"Quantimet" Image Analyzing Computer with Automatic Detector and Shape Discrimination Modules (data taken either from your samples or micrographs)

Auger/ESCA
Complete System Including Ion Gun for Sputter-Etching and Depth Profiling Into the Sample

X-Ray Diffraction
Wide and Small Angle

Optical Microscopy • Thermal Analysis (DTA, TGA, TMA) • Infra-Red Spectroscopy • Particle Size Analysis • Small Particle Identification • Failure Analyses

For Further Information, call Dr. John Stasny, Head, Biological Division.
Expert Consulting—Prompt Results • All services available on short or long term basis
Write or call today for our brochure

STRUCTURE PROBE, INC.

SPECIALISTS IN MATERIALS RESEARCH

Philadelphia
535 East Gay Street, West Chester, PA 19380
(215) 436-5400

New York Area
230 Forrest Street, Metuchen, NJ 08840
(201) 549-9350

New England Area
1100 Main Street, Suite 306, Bridgeport, CT 06604
(203)-333-5400

Abstracts

THE ULTRASTRUCTURAL RELATIONSHIP OF PLASMA CELLS TO THE CELLULAR CONSTITUENTS OF OVINE HAEMAL LYMPH NODES. Dr. F. Al-Bagdadi, Department of Veterinary Anatomy and Fine Structure and Dr. C. Seger, Department of Veterinary Science, Louisiana State University, Baton Rouge, Louisiana 70803.

Haemal lymph nodes were collected from different regions near the internal organs of five Louisiana native sheep. These sheep were given phenobarbitol I. V. Small sliced pieces were fixed in 3% glutaraldehyde in phosphate buffer (PH 7.4), and postfixed in 1% osmium tetroxide and embedded in epon. Ultra-thin sections were examined with a Zeiss 10 electron microscope. It has been reported that plasma cells have contact with macrophages in the lymph nodes and the spleen of rodents and in cases of multiple myeloma in humans. The plasma cells, in their contact with macrophages, are believed to carry out immunospecific functions at their contacts. These cellular contacts between plasma cells and macrophages have been reported in pathological conditions. The plasma cells in ovine haemal lymph nodes have similar contacts with cells other than macrophages such as lymphocytes, leukocytes, and mast cells. Some of these plasma cells demonstrated cytoplasmic processes reaching similar cytoplasmic processes of other cells in the ovine haemal lymph nodes. A similar functional relationship as that between plasma cells and macrophages could be suggested between the plasma cells in our specimen and that of the cells named above. This remains to be confirmed.

HEPATIC COPPER CONCENTRATION AND DISTRIBUTION IN PRIMARY BILIARY CIRRHOSIS. S.S. Barham, R.H. Wiesner, and E.R. Dickson, Departments of Cell Biology and Gastroenterology, Mayo Clinic, Rochester, Minnesota 55901.

Primary biliary cirrhosis is a chronic, ultimately fatal disease characterized by progressive intrahepatic cholestasis. Hepatic copper concentration increases with progression of the liver disease. The relationship between increased hepatic copper and liver injury remains speculative. Therefore we investigated the relationship between hepatic copper concentration, distribution of copper, and progression of disease. Fourteen patients representing the histologic spectrum of the disease were examined by light microscopic histologic staining, atomic absorption spectraphotometry, transmission electron microscopy (TEM) and x-ray energy spectroscopy (XES). Light microscopic examination revealed numerous cytoplasmic granules which stained positively with rhodanine. The intensity of rhodanine staining correlated with copper values determined by atomic absorption spectraphotometry. Electron-dense organelles with perinuclear distribution, presumably lysosomes, were visualized by TEM and appeared to increase with histologic progression of the disease. XES of liver tissue revealed that copper was distributed throughout hepatocytes but appeared to increase in lysosomes with progression of the disease. These results indicate that hepatic copper concentration increases progressively with advancing histologic stage. Copper distribution is both cytological and lysosomal but predominately lysosomal late in the disease, a pattern similar to that seen in Wilson's disease and in Bedlington terriers.

WOUND HEALING: THE EFFECTS OF COLCEMID AND CYTOCHALASIN B, G.F. Barratt and P.S. Baur, Dept. of Cell Biol. UTMB, Shriners Burns Inst., Galveston, Texas.

Contraction is the primary mechanism of wound closure in open skin wounds. The force of this phenomenon is thought to be effected by myofibroblasts, specialized fibroblasts containing bundles of microfilaments. These cells also contain microtubule arrangements. Microtubules have also been implicated in the wound healing process. The exact role of these two cellular components in wound healing contraction has not been resolved. In this study, cytochalasin B (CB) which disrupts microfilaments and colcemid which disrupts microtubules were applied daily to open skin wounds on the dorsum of hairless mice. No significant differences were found between control and CB-treated wounds. However, colcemid-treated wounds differed significantly from the control and CB-treated wounds on day 3 through day 10. At 10 days the wounds of control and CB-treated animals were 98% and 93% closed, respectively, while the wounds of colcemid-treated animals were 79% closed. Control and CB-treated wounds closed 43% and 31% respectively between day 4 and day 5. It is during this time that fibroblast proliferation and migration into the wound area occurs. Ultrastructurally, myofibroblasts comprise 80-90% of the invading fibroblast population at this time. In contrast, colcemid-treated wounds closed only 18% by days 4-5. Fibroblasts proliferation was not seen in these wounds until days 8-9 when a 40% closure occurred. The myofibroblast population here was similar in morphology, fine structure, and quantity to those in the control and CB-treated wounds. Thus, CB failed to alter the rate of wound contraction while colcemid was able to suppress the onset of contraction for 5 days.

NEGATIVE IMAGING FOR SEM IMAGE RECORDING. J. Bast and W.A. Shannon, Jr. Veterans Administration Medical Center and Department of Cell Biology, University of Texas Health Science Center at Dallas, Texas 75235.

In an effort to simplify SEM photography and reduce costs, we have substituted automatic process paper in place of polaroid film for image recording. This has been accomplished with the positive/negative image option on an ISI-40 SEM. Other SEMs have the capability for modification for negative imaging.

The standard Polaroid film backing on the ISI-40 is replaced by a 5 X 7 inch Pelco negative carrier. AGFA-Gevaert rapid print paper is substituted for the Polaroid film. The 8 x 10 inch sheets are conveniently cut into four 4 x 5 inch sheets and loaded into the negative carrier. A negative image is selected to project directly on the paper. Varying the contrast and brightness setting provides for a micrograph of comparable quality to the previously used method. The use of automatic contrast/brightness allows for a great degree of success in setting correct exposure parameters. The exposed paper is fed directly into a Kodak Ektamatic processor to obtain the print.

This method allows for greater control over contrast in allowing the use of various contrast-graded paper and in developing through tray processing if desired. Reduced costs also enables a more thorough morphological study of structures, e.g., montages. A high quality negative or 35 mm slide can readily be produced from the print. Although not required, fixing and ferryotyping the micrograph gives a permanent print of publication quality. (Supported by the Veterans Adminstration.)

MICROANATOMY OF HYPOPHYSECTOMIZED DOG PANCREATIC ISLETS. S.B. Bates and W.A. Shannon, Jr., Veterans Administration Medical Center and Department of Cell Biology, University of Texas Health Science Center at Dallas, Texas 75235.

Hypophysectomy results in the alteration of cell structure at locations distant to the pituitary. The endocrine pancreas contains cells, i.e., D-cells, morphologically and immunocytochemically equivalent to those of the hypothalamus. The hypothalamus secretes SRIF (somatostatin, somatotropin release inhibiting factor). It is, therefore, of interest to determine the extent of any effect on the D-cells and islet cells.

There appeared to be fewer D-cells by both immunocytochemical and TEM analyses. A few of the D-cells observed exhibited a number of exocytotic events which indicated hypersecretion. Others appeared normal. The B-cells (insulin producing) appeared in many instances to be deteriorated. Mitochondria appeared swollen and secretory granules exhibited smaller and less dense cores. Fibrous-like crystalline material was often seen within the granules. Some B-cells were almost depleted of secretory granules. Some of the A-cells (glucagon-producing) appeared rather normal while others did not. The anomalous cells were especially apparent in duct epithelium. Glucagon immunofluorescense characterized these cells as being A-cells. The nuclei lost their charac-

teristic pleomorphic shape and the secretory granules had lost some of the density of the core. The normally clear peripheral halo appeared to contain some moderately dense material. Most were hypersecretory. Both A and D-cells were seen isolated among exocrine cells, with cell junctions evident.

Somatostatin has been proposed to exert a paracrine function and to inhibit both A and B-cell secretion. Hypersecretion of A and B-cells may reflect the apparent decrease in D-cell presence and overall lack of secretion.

SCANNING AND TRANSMISSION ELECTRON MICROSCOPY OF PNEUMOCYSTIS CARINII. Carlos W.M. Bedrossian, M.D., Richard H. Conklin, M.D., Ph.D., and Patrick T. Conner, MS II, Department of Pathology and Laboratory Medicine, University of Texas Medical School, Houston, Texas.

A 28 year old renal allograft recipient developed fever and hypoxemia while immunosuppressed. Her chest x-ray showed bilateral pulmonary infiltrates and an open lung biopsy was performed. The GMS-stained imprints revealed occasional pneumocystis Carinii organisms approximately 4-6μ in diameter. Light microscopy showed diffuse alveolar damage and foamy exudate. Numerous conglomerates of pneumocystis organisms were identified in GMS-stained sections from the biopsy and also noted in toluidine blue-stained thick sections.

By transmission electron microscopy (T.E.M.) the conglomerates were held together by slender foot-like processes growing from concave and convex surfaces of the organisms without the participation of fibrin. Voids were formed by the justaposition of uneven parasitic contours and the intertwined foot processes. The interior of the parasites varied from lamellated in well preserved cysts to a disperse fluffy matrix in apparently degenerating ones.

By scanning electron microscopy (S.E.M.) clam-shell shaped organisms with beaded borders corresponded to the crescents and cysts noted by T.E.M. The slender processes were noted in rough surfaces of the organisms whereas smooth surfaces displayed occasional budding. Filopodia with complex branching at their fimbriated ends connected with foot processes to further interlock the parasitic conglomerate and explain the foamy light microscopic appearance of the parasites.

SCHWANN CELL SARCOMAS, Louis R. Begin and Bruce Mackay, University of Texas System Cancer Center, Houston.

There have been very few reports on the ultrastructure of malignant tumors derived from cells of the peripheral nerve sheath. One reason for this is undoubtedly the difficulty that exists in recognizing these neoplasms by light microscopy. Many suspected cases are wrongly diagnosed because of the presence of a palisading arrangement of the cells, a suggestive but nonspecific feature; or a neurogenic identity may be assumed when the tumor is contiguous with a peripheral nerve, or where there is clinical evidence of neurofibromatosis. In a study of 150 soft tissue tumors which had been labelled neurosarcomas, we accepted 40 as authentic examples. The range of their ultrastructure will be described and compared and contrasted with that of benign peripheral nerve sheath tumors. The Schwann cell sarcomas show considerable morphologic diversity at the ultrastructural level, but dominant features are the presence of cytoplasmic extensions, longitudinally aligned microtubules, cell junctions which are often primitive, and a tendency to form mesaxons. There is, however, a wide range of fine structure among these neoplasms, ranging from cases with obvious differentiation to some that have primitive mesenchymal features.

FIBROBLAST ADHESION TO COLLAGEN SUBSTRATA: EFFECT OF PLASMA FIBRONECTIN (PFN). Marylyn Bennett and Frederick Grinnell, Dept. Cell Biology, University of Texas Health Science Center, Dallas, Texas 75235.

The adhesion of baby hamster kidney (BHK) cells (which secrete low levels of pFN) and human foreskin fibroblasts (HFF) (which secrete high levels of pFN) was studied by TEM and SEM on two dimensional and three dimensional collagen gels. Substrata were prepared on glass coverslips for SEM and in tissue culture dishes for TEM. Adhesion was carried out in serum free medium. Cells on tissue culture dishes were either embedded in the dishes or the cell layer was removed from the dishes with propylene oxide and embedded in pellet form. On 2-D gels, BHK cells required pFN for adhesion and were triangular in shape with many lamellipodial regions of attachment. On 3-D gels, BHK cells attached in the absence of added pFN and some cells spread in bipolar forms with filipodia extending into the collagen matrix. Microvilli and filipodia appeared to associate with individual collagen fibrils. In the presence of pFN, BHK spreading was increased and some lamellipodial regions of attachment were observed, but these stayed on top of the matrix. HFF cells did not require pFN for attachment to 2-D gels and were spread with lamellipodia. Regions of cell-collagen fusion were observed. On 3-D gels, HFF cells attached and spread with multiple filipodia regardless of whether pFN was present or absent in the incubations. The filipodia often appeared to be continuous with the collagen fibrils. The results indicate that cell morphology depends upon the structure of the extracellular matrix and the event to which cells penetrate a 3-D matrix may be controlled by the presence or absence of pFN. (Supported by a grant from the NIH, CA. 14609).

APERTURE DEVELOPMENT IN SPORES OF A MOSS, DITRICHUM PALLIDUM. Roy Curtiss Brown and Betty E. Lemmon, Department of Biology, University of Southwestern Louisiana, Lafayette, Louisiana 70504.

The spore walls of many mosses exhibit a localized aperture where the protonema emerges during germination. This paper describes the development of the aperture located on the proximal surface of spores of **Ditrichum pallidum** (Hedw.) Hampe. The sites of spore wall and aperture initiation are related to the arrangement of spores in the tetrad. Following meiosis each spore contains a single plastid which is appressed to the distal face with the nucleus in close proximity. Wall formation is initiated on the distal surface and spreads to the proximal surface. Prior to aperture formation both plastid and nucleus occupy a more central position in the developing spore. The first indication of aperture development is the appearance of cortical microtubules beneath the proximal wall in the vicinity of nucleus and plastid. A dynamic system of microtubules is evident throughout aperture development. At maturity the aperture consists of a pore containing fibrillar material surrounded by a thin annulus. The aperture is a complex modification of a spore wall involving exine, separating layer and intine.

MEMBRANE FUSION DURING EXOCYTOSIS IN THE VAS DEFERENS OF ASCARIS. Robert C. Burghardt, Department of Biology, Texas A & M University, College Station, Texas.

The structural organization of membranes of vas deferens cells in **Ascaris** were examined using conventional freeze-fracture and lanthanum impregnation techniques. Reorganization of cortical cytoplasm leading to exocytosis was observed in vas deferens cells from male worms recovered **in copula.** Prior to the secretory stimulus, secretory granule and apical plasma membranes were separated by a minimum distance of 50 nm. Stimulated cells initially exhibit adherence of the secretory granule to the inner aspect of the apical plasma membrane. Characteristic of the presumptive fusion site is the focal absence of microvilli above the interacting membranes. Although rosette-like structures are associated with secretory events occurring in the spermatozoa of **Ascaris** (Burghardt and Foor, J. Ultrastruct. Res. 62:190-202, 1978), membrane fusion in the vas deferens of the same experimental animal does not appear to involve these membrane specializations. Fusion of interacting membranes is followed by the formation of an aqueous channel which connects the interior of the granule to the lumenal space. Contact and fusion of adjacent secretion granules following the onset of granule fusion with the plasma membrane (compound exocytosis) was not detected.

IMPROVED METHODS FOR SEMI-THIN SECTIONING WITH RALPH-BENNETT KNIVES. James K. Butler, Ultrastructure Research Laboratory, Department of Biology, The University of Texas at Arlington, Arlington, Texas 76019.

Two devices, a retractor that converts a standard rotary microtome into a retracting microtome and a device for collecting and mounting semi-thin (1-4μm thick) plastic or paraffin sections are discussed. The attachable retractor improves the quality of sections obtained with a standard rotary microtome by eliminating return stroke scrubbing of the block against the knife edge. It also makes it feasible to use a fluid trough

on these microtomes since specimen retraction prevents the block wetting and fluid carry-over that occurs without retraction. Two variants of the collecting-mounting device are discussed. One is for use with standard microscope slides and one for use with 22 mm square coverslips. They simplify and speed mounting of semi-thin sections by reducing handling of the sections to a minimum. The collector-mounter greatly facilitates serialization of plastic sections which is difficult and tedious using ordinary methods. Several small instruments and details of technique that aid sectioning and mounting will also be described.

THE CONCENTRATION OF CALCIUM AND OTHER ELEMENTS AT A SUBCELLULAR LEVEL IN THE LACTATING EPITHELIUM OF RAT. Ivan L. Cameron, Rodney L. Sparks and Leonard L. Seelig, Jr., Department of Anatomy, The University of Texas Health Science Center at San Antonio, San Antonio, Texas 78284 and Department of Cell Biology, The University of Texas Health Science Center at Dallas, Dallas, Texas 75235.

Unfixed freeze-dried and uncoated sections of lactating mammary tissue from rat was analyzed for element concentration using a scanning electron microscope fitted with energy-dispersive x-ray analytical equipment. The subcellular concentration (in mmol/kg dry weight) of calcium and several other elements (Na, Mg, P, S, Cl and K) was measured in: the basal-lateral cytoplasm, the nucleus, the apical cytoplasm, and the alveolar lumen in the lactating epithelium. The element concentration data was correlated to the ultrastructural features of the microprobed areas. Ca was concentrated, 4-5 fold, in the apical cytoplasm in comparison to other parts of the cell. The lumen contents show a 10-fold increase over the apical cytoplasm. The apical cytoplasm includes the Golgi apparatus and secretory vacuoles containing dense granules or casein micelles. The latter are numerous in the lumen. Because most of the Ca in milk is known to be bound to the casein micelles, our data support the idea that Ca is sequestered in the Golgi region, and transported within the secretory vacuoles to the plasma membrane for exocytosis to the lumen. (Supported by BRSG Grant S07 RR 05654 from NIH.)

MISONIDAZOLE-INDUCED ULTRASTRUCTURAL CHANGES IN UNMYELINATED NERVE FIBERS. M.A. Casey, and R. D. Yates, Department of Anatomy, Tulane Medical School, New Orleans, Louisiana.

Misonidazole (1-(2-hydroxy-3-methoxypropyl)-2-nitroimidazole is a radiosensitizing agent which is now being tested clinically for its efficacy in enhancing the effect of radiation on solid tumors. Although the results of clinical trials are encouraging thus far, a troublesome side effect of misonidazole is a distal sensory polyneuropathy. We have initiated a study of misonidazole neuropathy in mice. Mice were given intraperitoneal injections (0.5 mg/g) of misonidazole daily for seven days. The mice were sacrificed five days after discontinuation of the drug and their sciatic nerves were examined electron microscopically. No alterations in myelinated nerve fibers were seen in this study. However, in misonidazole-treated mice, many unmyelinated nerve fibers displayed a decrease in the number of neurotubules and neurofilaments. In some fibers, the neurotubules and neurofilaments were entirely replaced by a flocculent material. Swollen unmyelinated nerve fibers were also frequently seen. These preliminary findings indicate that misonidazole can cause alterations in nerve fibers experimentally and additional studies are in progress to further characterize misonidazole neuropathy.

LOCALIZATION OF TUBULIN IN THE ELECTRON MICROSCOPE USING A TUBULIN ANTIBODY. Mike A. Clark, Dept. Cell Biology, The University of Texas Health Science Center at Dallas, 5323 Harry Hines Blvd., Dallas, Texas 75235.

The Y-1 cell line was originally isolated from a murine adrenal tumor and has retained the ability to respond to ACTH by secreting steriods. Using the light microscope and anti-tubulin antibody, we have previously demonstrated that the tubulin, prior to ACTH treatment, is in a granular form and after ACTH treatment, the cells contain many organized microtubules. Based on these previous observations, we suggested that the tubulin in the untreated cells was associated with the cholesterol crystals. We now present additional evidence in support of this hypothesis by using a new technique for localizing tubulin in the electron microscope.

Cells are grown on coverslips and fixed in 2% glutaraldehyde, 0.1M sucrose and 0.1M cacodylic acid. The cells are then washed in PBS and, in order to facilitate entry of antibody into the cells, the membranes are permeabilized in 100% acetone (-20°C) for 30 seconds. The coverslips were then placed in 0.05μg/ml of rabbit anti-tubulin antibody and 0.5% Saponin in PBS overnight. The coverslips were then washed in PBS for 1 hour and incubated in ferritin conjugated goat anti-rabbit IgG antibody overnight. Finally, the coverslips were washed for 4 hours in PBS, post-fixed in OsO_4, dehydrated and embedded in Epon.

ULTRASTRUCTURAL OBSERVATIONS ON THE HOSTPATHOGEN RELATIONSHIP BETWEEN EICHHORNIA CRASSIPES AND THE FUNGUS CERCOSPORA RODMANII. James E. Cobb, Department of Biology, Stephen F. Austin State University.

Many acres of watershed throughout the southern coastal states are infested with aquatic weeds, especially the water-hyacinth **Eichhornia crassipes** (Mart.) Solms. Control of hyacinths has been attempted by three techniques: mechanical removal, chemical control and biological control. The Hyphomycetalean fungus **Cercospora rodmanii** Conway conforms to the accepted specifications for a good biological control organism and may prove to be effective in an integrated biological control program. Research into the pathological effects of **C. rodmanii** serves to enhance our basic understanding of the overall host-pathogen relationship.

Transmission electron microscopic observations of leaf tissue of **Eichhornia crassipes** artificially inoculated with **Cercospora rodmanii** indicates that host cells are killed in advance of the fungus hyphae. This observation supports the hypothesis that damage to the host results from the production of a phytotoxin. Hyphae are distributed in the intercellular spaces of infected tissue and were observed inside dead or dying cells. There is no indication that **C. rodmanii** produces any type of specialized haustorial apparatus. The fungus reproduces by means of large, slender conidia produced on the surface of infected leaf tissue.

STRUCTURE OF THE MAMMALIAN CHROMOSOME. Arthur Cole and Ruth Chen, Physics Dept. University of Texas System Cancer Center, Houston, TX 77030.

Recent studies utilizing stereo electron microscopy, alkaline and neutral velocity sedimentation, alkaline filter elution, radiation target analysis, and molecular autoradiography, provide evidence for a detailed model of chromosome structure. The basic chromatid arrangement contains eight circular duplex DNA molecules arranged in a parallel array much like eight stretched rubber bands laid side-by-side. At 1 to 20μm intervals along each circular DNA molecule, the outgoing and returning strands are associated with a specific protein (Protein I) to form paired strands 6 nm in diameter and 30 to 100 nm long. The paired regions are overlaid with other morphologically distinct proteins in the form of 7nm (Protein II) or 22nm (Protein III) doughnut-shaped particles. Lateral associations of eight Protein III particles, from corresponding regions of the eight circular DNA molecules, form organizational rows measuring 22 X 176nm. A longitudinal condensation of the organizational rows forms a 176nm wide backbone ribbon. A 44 X 176nm centrometic structure involves a condensation of two organizational rows in a region devoid of adjacent organizational rows. Inter-row DNA strands loop outward and wind on 10nm histone core particles to form "beady string" fibers which supercoil in metaphase structures. Two distinct classes of radiating DNA loops are present in dehistonized chromatids; one forms a well bounded region extending 0.6μm from the backbone, the other forms a variably bounded region extending 4μm or more from the backbone. These and other details will be illustrated in stereo projections.

THE USE OF FERRIC-FERRICYANIDE TO LOCATE SEROTONIN-CONTAINING CELLS IN RESPIRATORY AND GASTRIC EPITHELIUM. R.D. Dey, W.A. Shannon, Jr., and S.I. Said, V.A. Medical Center, Dallas, Texas.

Identifying sufficiently large numbers of endocrine cells in thin sections for quantitative electron microscopic morphometry is more efficient if the cells can be located first in thick plastic sections. Previously, serotonin-containing cells were correlated with ferric-ferricyanide positive cells by combined fluorescence and light microscopy. In this study, ferric-ferricyanide positive cells were identified by light microscopy in

Our competitors think you should pay extra for all of these features.

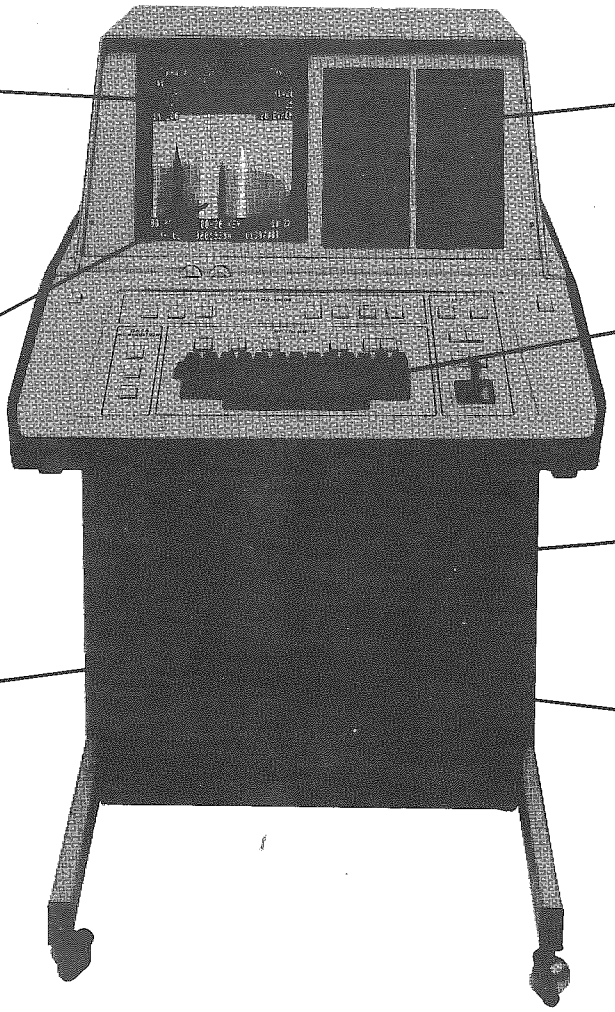

What do you think?

It's features like these that have made it possible for so many leading companies to use the EEDS II for so many different applications. For metallurgists in quality control of alloy manufacturing to failure analysis. In energy research, for solar device inspection to geological quality assurance. Other industries ranging from solid state micro-electronics to biological and general research laboratories have also found the EEDS II to be the #1 instrument for energy dispersive spectroscopy.

But think for yourself. Get the facts today. Call or write EG&G ORTEC, Materials Analysis Division, 100 Midland Road, Oak Ridge, TN 37830 (615) 482-4411.

EG&G ORTEC
Materials Analysis Division

thick plastic sections and correlated with the identical cells in thin sections. Pieces of rabbit tracheal and pyloric mucosa were fixed with glutaraldehyde and osmium, and embedded in Epon 812. Plastic sections 2μm thick were mounted on glass slides and heated for 1 hour. The plastic was removed from the sections with a mixture of propylene oxide, methanol, and potassium hydroxide for 5 minutes. (Maxwell, **J. Microscopy**, 112:253, 1977). After rinsing, the sections were stained with ferric-ferricyanide (Lillie and Burtner, **J. Histochem. Cytochem.**, 31:87, 1953) for 10 minutes. Positive cells were observed and photographed by light microscopy. Ultrastructural correlation of the ferric-ferricyanide positive cells was established 1) in thin sections of the adjacent area containing the same cell, and 2) in thin sections of reembedded ferric-ferricyanide treated sections used for light microscopy. By identifying ferric-ferricyanide positive cells with this convenient method, serotonin-containing cells can be quickly located for subsequent electron microscopy and used for morphometric determinations. (Supported by National Research Service Award No. HL-05914 from NHLBI).

VERTICAL DISTRIBUTION OF AQUATIC BACTERIA ENUMERATED WITH SCANNING ELECTRON MICROSCOPY. Thomas M. Dreier, Electron Microscopy Center, Texas A&M University, College Station, Texas.

The vertical profile of bacteria sampled from a Texas farm pond was monitored to determine quantitatively the contribution of morphologically distinct groups of bacteria to the total bacterial population. Bacteria were categorized into morphological types and enumerated using scanning electron microscopy (Dreier and Thurston, SEM, Inc. 2: 843-848, 1978). There was no significant variation in the total bacterial population as a function of depth. However, morphological types of bacteria were stratified within the water column. Rods were the dominant form in the epilimnion (a maximum of 47% at 0.8 m) while cocci were the dominant form in the thermocline (a maximum of 56% at 2.6 m). There were six dominant morphological types of bacteria: three rods (R3, R5, R9), two vibrio (V1,V7), and one cocci (C5). R3, R5, and R9 had their highest density at 0.8 m and 1.8 m. V1 had three significant density peaks, 0.8, 1.6 and 2.8m. Density maximum for V7 were observed at 0.6 m and 2.0 m. C5 had an insignificant density in the epilimnion, however it constituted from 28% to 47% of the total bacterial population in the thermocline.

ADRENERGIC INNERVATION OF THE CAROTID BIFURCATION IN THE SPONTANEOUSLY HYPERTENSIVE RAT (SHR). B.E. Engle and R. D. Yates, Department of Anatomy, Tulane Medical School, New Orleans, Louisiana.

Physiological studies have shown that the efferent sympathetic fibers to the region of the carotid bifurcation (CB) can directly effect the sensitivity of the afferent baroreceptors in the wall of the proximal portion of the internal carotid artery. These specialized receptors are sensitive to changes in arterial blood pressure, and the region of the CB is affected in individuals with essential hypertension (HT). This prompted us to investigate the distribution of sympathetic nerve fibers to the region of the CB in hypertensive animals. The spontaneously hypertensive rat develops HT with age and has been shown to be one of the best animal models for essential HT in man. Animals were sacrificed by intracardiac perfusion with 3% glutaraldehyde, and the CB was removed bilaterally. The tissue was post-fixed in osmium-tetroxide and prepared for routine electron microscopy. The area of the CB was innervated by a sparse plexus of sympathetic fibers originating from the superior cervical ganglion. The nerve fibers were unmyelinated, contained dense core vesicles, and were found deep in the adventitia in close association with fusiform shaped cells which resembled medial smooth muscle cells. These initial results seem to indicate that although the sympathetic supply to the region of the CB is altered physiologically with HT, there are apparently no corresponding morphological alterations.

ACKNOWLEDGEMENTS:This research was funded by a grant from the Tulane Chapter of Sigma Xi. Special thanks to Dr. I-li Chen and Dr. Craig Knox for their advice and support.

THYROTOXIC HEART DISEASE - REGIONAL LEFT VENTRICULAR DIFFERENCES IN THE RAT. Gerdes, A. Martin, Frederick H. Kasten and Gerald Callas, Louisiana State University Medical School, New Orleans, Louisiana, and the University of Texas Medical Branch at Galveston, Galveston, Texas.

Endocardial and epicardial tissue was compared in 6 control and 6 thyroid-treated rats. The epicardial region of control rats had 38 per cent more capillaries than the endocardial region. Control endocardial myocytes were 62 per cent larger in cross-sectional area than epicardial myocytes. Hypertrophic hearts also exhibited regional differences in capillary density as in the normal hearts but there is an overall reduction of 12 and 17.5 per cent capillary density in both regions. The average cross-sectional area of myocytes increased 34.5 per cent in the epicardium and 22.5 per cent in the endocardium. The lower capillary density of the endocardium should not be over-looked since this may be an important limiting factor in regional blood flow to the left ventricle. The reduction in capillary density associated with hypertrophic heart disease may further compound this deficit.

MICROTUBULES IN RAT SOLEUS MUSCLE. M.A. Goldstein, and J. Cartwright, Jr., Section of Cardiovascular Sciences, Department of Medicine, Baylor College of Medicine and the Methodist Hospital, Houston, Texas 77030.

The number of microtutules per square micrometer cross sectional area of soleus muscle has been determined for 28 day, 35 day, and 42 day old maturing adult sibling rats, and non-sibling mature rats, by counting microtubule profiles in electron micrographs of ultrathin sections. The values for the 28 day, 35 day, and 42 day old siblings were 0.3214, 0.1505 and 0.136 microtubules per square micrometer respectively. The mature adults averaged 0.263 microtubules per square micrometer. From our data there appears to be no significant difference between the young rats and the mature rats. However, there is a large amount of variation, from a minimum of 0.029 to a maximum of 0.403 microtubules per square micrometer in the maturing adults and from a minimum of 0.048 to a maximum of 1.999 microtubules per square micrometer in the mature adults. Even in the same animal the mean values varied (min. :0.029, max. :0.259). The mean values are similar to those from cardiac muscle. The microtubules thus appear to be a stable component of skeletal muscle. The observed variation may reflect an altered physiological state of individual cells. (Research supported by grants from American Heart Association, Muscular Dystrophy Association, and NIH (HL17269, 1K04HL00321). We acknowledge the technical help of Ms. Cherie Gorman and Mr. David Murphy.)

THE EFFECTS OF PERIPHERAL AND CENTRAL VAGOTOMY ON THE RAT AORTIC BODY ARTERIAL CHEMORECEPTORS. John T. Hansen, Department of Anatomy, The University of Texas Health Science Center at San Antonio, San Antonio, Texas 78284.

The rat aortic body arterial chemoreceptors are innervated by the vagus nerves. Like the carotid body, the aortic bodies are sensitive to changes in blood oxygen and carbon dioxide levels and initiate powerful reflexes during hypoxia and hypercapnia. Most of the nerve endings which terminate in the aortic bodies are thought to be afferent in nature, although detailed experiments have not been performed to verify this assumption. In this study, two groups of rats were anesthestized and their aortic bodies denervated by surgical vagotomy either peripheral or central to the nodose (sensory) ganglion. After one, three and seven days postoperatively, the rats were sacrificed by vascular perfusion with the appropriate aldehydes and the aortic bodies (subclavian glomera) routinely processed for electron microscopy. Virtually all of the nerve endings adjacent to the aortic body glomus cells showed evidence of axonal degeneration following peripheral vagotomy. Degenerating nerve endings exhibited swollen or condensed mitochondria, clumping of the synaptic vesicles and a flocculent cytoplasmic matrix. Nerve endings in the aortic bodies of rats with central vagotomy appeared morphologically normal. Therefore, it appears that essentially all of the nerve endings in the aortic body are afferent in nature. Because a few of these nerve endings may arise from the sympathetic ganglia, studies are presently in progress to determine what degree, if any, the aortic bodies are innervated by sympathetic efferent fibers. (Supported by a Grant-In-Aid from the American Heart Association and by funds contributed in part from the Texas Affiliate).

SUBSTRATE SELECTION:VARIATIONS IN MIGRATORY PATTERNS OF EPITHELIAL AND FIBROBLAST CELLS. Cheryl L. Hawk, Dept. Cell Biology, The University of Texas Health Science

Center at Dallas, 5323 Harry Hines Blvd., Dallas, Texas 75235.

Work done on cell motility has indicated that motile cells select gold substrates in preference to glass. Standard electron microscope grids were used as stencils to produce a pattern of gold/paladium on glass coverslips. Using a Hummer II sputter coater, 600-800 A thick, gold/paladium grid patterns were prepared. Cells were trypsinized and plated in a 100mm dish directly on the coverslips, allowed to attach for 15 minutes, after which time, the dish was flooded with media. At intervals of 4, 8, 12, 24, and 48 hours, coverslips were fixed for observation in the scanning electron microscope. Both cell types initially attach to the coverslips in a random manner, without preference for glass or metalized areas. The Y_1 epithelial cells select strongly for gold during the early time intervals, but after 12 hours, reaggregate on the glass areas. The AMT fibroblasts appear less specific in their selection pattern, prefering gold after a slightly longer time interval, but not appearing to make the same dramatic gold to glass transition.

PROBLEMS AND LIMITS IN THE ELECTRON MICROSCOPIC DIAGNOSIS OF MESOTHELIOMA. Marcella Klima, M.D. V.A. Hospital, Houston.

Despite the recognized usefulness of electron microscopy in the diagnosis of mesothelioma, in several aspects it remains problematic. Three such areas pose the basic difficulties: 1) Whether the tissue comes from a benign or malignant proliferation. 2) Whether we are dealing with a mesothelioma or a carcinoma. 3) Whether the tumor is a sarcomatous type of mesothelioma or another soft tissue tumor. In our series of 49 pleural lesions, 33 were examined ultrastructurally. No significant contribution of electron microscopy was recognized in the first group. Certain limited possibilities in differentiation were found in the third group. The most contributory role electron microscopy plays in the second group, although caution must be exercised to avoid some pitfalls. The specific ultramicroscopic diagnostic features and the misleading aspects for each group will be discussed.

THE VALUE OF ROUTINE ELECTRON MICROSCOPY IN DERMATOPATHOLOGY. Marcella Klima, M. D. Vet. Adm. Hospital, Houston, Texas.

The diagnostic use of electron microscopy in various medical subspecialities has expanded over the last decade. It has developed into a routine diagnostic method in dermatopathology, too. However, with its use the misconceptions about the unlimitted possibilities of this diagnostic approach became also obvious. Three such areas of difficulties were encountered in our practice: 1) The differentiation between certain skin diseases is not always possible (Lichen Planus, Lupus Erythematosus), 2) Lymphoid infiltrates may be overdiagnosed (Mycosis Fungoides). The origin of a skin tumor may not always be correctly recognized (Skin appendage tumors versus Basal cell carcinomas). Examples from all three categories will be presented with the suggestion that electron microscopy may not be a diagnostic solution in all instances.

ORCA BASIN: A PALEOCLIMATIC AND BIOSTRATIGRAPHIC EXAMINATION OF THE LATE PLEISTOCENE IN THE NORTHWEST GULF OF MEXICO. Arlette Schumm Levitan, Department of Oceanography, Texas A&M University, College Station, Texas.

Two twelve meter piston cores from Orca Basin, an anoxic, hypersaline, intraslope basin in the northwest Gulf of Mexico, have yielded a continuous record of the late Pleistocene. The Orca Basin sediments offer a unique opportunity to elaborate on the late Pleistocene paleontologic record of radiolarians, silicoflagellates, foraminifers, diatoms, pteropods, and calcareous nannoplankton because the microfossils are extraordinarily well preserved. Scanning electron micrographs were taken of select microfossil species. Calcareous nannofossils were used to determine the biochronology of the sediment in the cores. The significance of abundant **Emiliani huxleyi** in these cores is that the record does not extend back beyond 70,000 years. The sediment consists of a mixture of pelagic carbonates and of clay size terrigeneous detritus. The abundance of a particular cosmopolitan species group, **Gephyrocapsa oceanica** complex, relative to the total sediment was used to measure the proportion of biogenic input to detrital input. Carbonate content and coarse fraction percent (chiefly planktonic foraminifers) were used to measure changes in the sedimentary regime. Both carbonate content and coarse fraction reflect eustatic sea level fluctuations. The carbonate content of the sediment is a function of degree of dilution by land derived detritus, which in turn increases and decreases with a lowering and a rising of sea level, respectively.

THE MORPHOLOGIC SPECTRUM OF CARCINOID TUMORS, Bruce Mackay, The University of Texas System Cancer Center, Houston.

Observations from a series of over 60 carcinoid tumors will be presented. Carcinoid tumors are derived from the serotonin-forming cells that are commonest in the gastro-intestinal tract but are also found in other locations. Most carcinoid tumors have a distinctive histologic pattern in which uniform cells with central round nuclei are compactly arranged in solid aggregates; trabecular and gland-like formations are also common. A spindle cell morphology is seen in some peripheral bronchial carcinoid tumors. One bronchial carcinoid in our series showed extensive transformation to mitochondrion-rich cells. The dominant ultrastructural feature is the presence of dense-core granules and they are typically numerous and uniform in caliber. They tend to be larger in the gastro-intestinal tract tumors than in those of the lung, but there is considerable overlap. Some mid-gut carcinoids have pleomorphic granules. Microvilli are occasionally seen. Although the cell of origin of carcinoid tumors is generally considered to be of neutral crest derivation, the occasional occurence of mucin-forming carcinoid tumors, particularly in the appendix, suggests an entodermal origin.

SMOOTH MUSCLE TUMORS OF THE GASTRO-INTESTINAL TRACT, Bruce Mackay and Robert A. Weiss, the University of Texas System Cancer Center, Houston.

Mesenchymal neoplasms arising from the gastro-intestinal tract are commonly assumed to be of smooth muscle origin, but a number of the atypical and malignant examples differ in their histology from typical smooth muscle growths in other locations. This has been recognized for many years by light microscopists, but there has been no detailed attempt to study the problem at the level of the electron microscope. Our report summarises findings from an ultrastructural study of 20 malignant soft tissue tumors arising from the gastro-intestinal tract at various levels. Each was considered by light microscopy to be a leiomyosarcoma. In parallel studies, benign tumors of the stomach and intestines, and a group of smooth muscle neoplasms from other sites, have been examined. Among the 20 sarcomas, only 8 showed identifiable smooth muscle features at the ultrastructural level. They included peripheral cytoplasmic myofilaments, pinocytotic vesicles, and characteristic attachment plaques. These features were sparse or poorly defined when compared with smooth muscle tumors from other sites. The benign gastric and intestinal tumors also showed a tendency towards paucity of smooth muscle features. Among the 20 sarcomas, a spectrum of morphology could be traced from those which were of demonstrable smooth muscle origin to primitive mesenchymal tumors without evidence of specific differentiation.

ULTRASTRUCTURE OF TELIOSPORE GERMINATION IN THE RUST FUNGUS GYMNOSPORANGIUM CLAVIPES. Charles W. Mims, Department of Biology, S.F. Austin State University, Nacogdoches, Texas 75962.

Teliospores of **G. clavipes** are two celled. Each cell is uninucleate and possesses a very dense cytoplasm packed with ribosomes, mitochondria, lipid droplets and other inclusions. There is a special region in the wall of each cell at which the promycelium emerges during germination. The structure of the spore wall in this germ pore region is different from that of the remainder of the wall. During germination, the promycelium ruptures the outer portion of the spore wall although the inner layer of the spore wall is continuous with the wall of the promycelium. The nucleus eventually moves into the promycelium along with virtually all the cytoplasmic contents of the teliospore cell. The nucleus then divides meiotically, and septa are formed dividing the promycelium into four cells. Each cell of the promycelium then gives use to a slender sterigma bearing a basidiospore at its tip.

ULTRASTRUCTURE OF CULTURED HEPATOCYTES ISOLATED FROM CHOLESTEROL FED RATS. Randy L. Moses and Roger A. Davis, Departments of Anatomy and Physiology, Louisiana State University Medical Center, 1100 Florida Ave. New Orleans, LA 70119.

Ingestion of large amounts of cholesterol has been shown to cause an accumulation of cholesterol esters in the liver, resulting in altered hepatic function. In an attempt to simulate these conditions in vitro, collagenase-dissociated hepatic parenchymal cells obtained from rats fed for 60 days on a diet supplemented with 2% cholesterol in olive oil were maintained in as monolayers culture for 3 days. Cells were then fixed and embedded in situ and examined by transmission electron microscopy. The most distinctive ultrastructural feature of the cells was the accumulation of cytoplasmic lipid droplets of various sizes. In some cells lipid droplets, some of which were fusing, occupied almost the entire cytoplasmic compartment. Bile canaliculi, characterized by numerous microvilli projecting into the lumen of the canaliculus and tight junctions separating the lumen from other intercellular areas, formed between some cells. Desmosomes and punctate adherens-type junctions were also found between cells. Membranous cytoplasmic organelles included peroxysomes, lysozomes, Golgi bodies, and rough and smooth elements of the endoplasmic reticulum. The rough ER was found in stacks of lamellae and as single strands closely associated with mitochondria and lipid droplets. The smooth ER was disposed as subplasmalemmal cisternae, single strands associated with mitochondria and lipid droplets, and in areas occupied solely by smooth ER.

SPINDLE CELL SQUAMOUS CARCINOMA. J.R. Newland, M.H. Stern, M.A. Luna and B. Mackay, University of Texas System Cancer Center, Houston.

Squamous carcinomas arise from stratified squamous epithelium or through metaplastic transformation of other epithelia. The better differentiated tumors are readily identified by light microscopy, but occasionally the cells assume a spindle shape, and the tumor can then closely simulate a mesenchymal neoplasm. The primary object of this study has been to examine a group of 50 spindle cell squamous carcinomas, correlating the light microscopy with the ultrastructural findings and with the clinical information, particularly the site of origin of the tumor. 26 cases arose on the skin of the head and neck, or the lip, and 21 occurred on mucosal surfaces (tongue 5, palate 2, buccal mucosa 1, gingiva 4, tonsil 1, nasopharynx 3, larynx 5). 3 of the accessions were lymph node metastases. In addition, nodal metastatic tumor from two of the cases for which the primary tumor had been obtained was available for electron microscopy. No light microscopic evidence of squamous origin could be detected in 14 skin tumors and 8 mucosal tumors. The ultrastructural features of squamous cells, notably prominent cell junctions, desmosomes, tonofilament bundles and keratin formation, were often absent, and the tendency of the cells with assumption of a fusiform shape is towards loss of these epithelial characteristics and progressive transformation towards a mesenchymal cell. Distinction from a sarcoma consequently requires familiarity with the range of ultrastructural morphology of fibrosarcomas and malignant fibrous histiocytomas.

PRELIMINARY OBSERVATIONS ON THE VARIATIONS IN THE NUMBER OF PURKINJE CELLS IN RATS DUE TO AGE AND HYPERTENSION. M.S. Ogra, C. Knox, J. Mascorro, and R.D. Yates, Department of Anatomy, Tulane Medical School, New Orleans, Louisiana.

Electron and light microscopic studies were made on the cerebella of 3, 12, and 24 months old rats of WKY and SHR strains. Saggital sections of cerbellum previously fixed in glutaraldehyde and stained in toluidine blue, were used to count the Purkinje cells and glial cells in Purkinje cell lines measuring 350 μm in each segment counted at a time. In all, 10-14 mm cell lines were counted in each case. Preliminary results indicate that on an average the number of Purkinje cells in WKY rats decreased by 11.08% by the age of 12 months and by 14.56% at the age of 24 months. Figures for SHR rates were a decrease of 12.46% at 12 months and 26.13% by 24 months of age. There was a 25.21% decrease in the number of glial cells in WKY where as a much smaller decrease, 7.7% was observed in SHR rats. These studies are currently in progress and statistical evaluations will be considered during the presentation.

A MORPHOLOGICAL STUDY OF THE TASTE BUDS IN THE CIRCUMVALLATE PAPILLAE IN MAN BY SCANNING ELECTRON MICROSCOPY. M.L. Percy and S.O. Krolls, SEM Facilities and Department of Oral Pathology, University of Mississippi School of Dentistry Jackson, Mississippi 39216.

Exhaustive studies of the physiologic and neurologic aspects of taste have been done on man and animals, and the taste buds have been extensively studied in the rat and rabbit. However, only limited work has been done with scanning electron microscopy in man. In our project the tongues were obtained during routine autopsy procedures. The taste buds evaluated were obtained from the right and left circumvallate papillae. Each papilla was sectioned through the center and a wedge incision was made on either side. One of the wedges was prepared in the usual manner for scanning electron microscopy and mounted flat side up for viewing. The opposite wedge, a mirror image, was routinely prepared for light microscopy. In this manner the sections studied by both methods can be compared. Since taste acuity is known to decrease with age, the specimens were grouped into the following age groups: neonate, pediatric, young adults, and elderly.

The sustentacular cells were located on the exterior of the taste bud protecting the neuroepithelial cells which were centrally located, and visible through the taste pore. A population of granules of unknown function was seen in the neuroepithelial cells only. The crevices in which the serous von Ebner glands were also noted.

A CORRELATED LIGHT MICROSCOPIC, TRANSMISSION AND SCANNING ELECTRON MICROSCOPIC STUDY OF THE DEVELOPMENT OF OIL CELLS IN THE LEAVES OF MAGNOLIA GRANDIFLORA L. Michael T. Postek and Shirley C. Tucker, Department of Botany, Louisiana State University, Baton Rouge, Louisiana 70803.

In plants, oil cells are one type of cell into which oil is secreted during development. Such idioblast cells are known to exist in numerous plants and they have been used to characterize members of primitive families including the Magnoliaceae. However, there exists some controversy with regard to the ontogeny and anatomy of oil cells present in these leaves. This paper will present the developmental aspects of oil cells present in the leaves of **Magnolia grandiflora** obtained by the use of light microscopy, scanning and transmission electron microscopy.

ELECTRON MICROSCOPIC FINDINGS ON TESTICULAR BIOPSY IN NONHUMAN PRIMATE MODEL OF VARICOCELE. James A. Roberts, Ronald W. Lewis, Richard M. Harrison, Raju Thomas, and E.N. Fussell, Delta Regional Primate Research Center, Tulane University.

Five monkeys (*Macaca fascicularis*) had partial left renal vein ligation medial to the entrance of the left spermatic vein to produce a left varicocele. Three of these monkeys also had a left adrenalectomy. Five other monkeys were sham operated. Preoperative morphology was normal in 93-97% of the sperm but following restriction of the renal vein and production of palpable varicocele as many as 68% of the sperm were abnormal.

Six months following surgery the morphologic abnormalities remained in monkeys with varicocele. All monkeys then had bilateral biopsies for light and ultrastructural studies. Histologic change showed minimal peritubular fibrous and premature sloughing of spermatids of the left testicular biopsies in only some monkeys with varicocele. However, ultrastructural changes were found in all left testicles of animals with varicocele, whether with or without adrenalectomy and in none of the sham operated animals. EM Showed basement membrane deterioration, loss of Sertoli cell junctional integrity and abnormal spermatids and these changes are probably the site of damage from varicocele. These studies show early morphological changes in varicocele animals and may prove that efflux of adrenal blood does not cause the pathological changes in human varicocele.

MORPHOLOGICAL AND BIOCHEMICAL CHARACTERIZATION OF CULTURED PANCREATIC DUCTS. John R. Ruby, S. Githens, D. Holmquist, and J. Whelan, Department of Anatomy, Louisiana State University Medical Center, and Department of Biological Sciences, University of New Orleans, New Orleans, Louisiana.

Ducts were isolated from non-ductal structures by digesting pancreases with collagenese and chymotrypsin and collecting the duct fragments on sieves. The ducts were placed in a soft agarose matrix in CMRL-1066 and 10% fetal bovine serum. The cultures were maintained for up to eight weeks. Light and electron microscope observations revealed that soft agarose supported a three-dimensional architecture in

The first analytical TEM with true microcomputer control

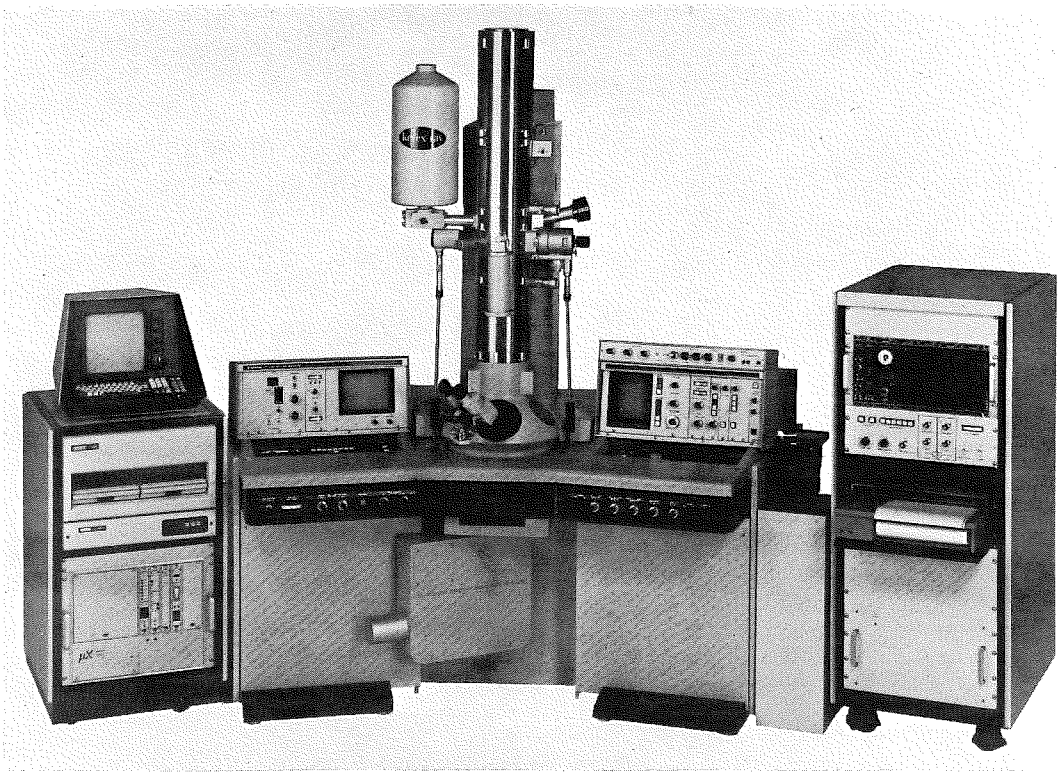

It's the H-600-1, an exceptionally powerful analytical tool featuring:

— LaB_6 Gun
— Pushbutton-selectable microscope modes: TEM (2.0 Å), SEM (20 Å), and STEM (10 Å)
— Triple condenser lens—all 7 lenses microcomputer controlled
— Ultra high (5×10^{-7} torr) vacuum system

The system is available with EDX, Energy Loss Spectroscopy, Diffraction, Beam Rocking, and Spot Scanning. The analytical modes require no specimen repositioning. And, probe sizes down to 15 Å are easily achieved for exceptional analytical capability. What's more, the H-600-1 is easy to operate. Routine setups and adjustments are done automatically by the built-in microcomputer.

For details call or write today. Hitachi Scientific Instruments Division, 411 Clyde Avenue, Mountain View, California 94043. Phone (415) 961-0461.

HITACHI
SCIENTIFIC INSTRUMENTS
NISSEI SANGYO AMERICA, LTD.

When It Comes To Scanning Electron Beams...

ETEC Has It.

A full range of top-performance products
An established reputation for quality
Innovative design ideas
Responsive service
A confirmed retrofit policy
Scheduled training seminars
A broad accessory range.

ETEC and its products are founded on a policy of concern for the customer's needs. We are confident that our scanning electron microscopes and microprobe analyzers offer you the performance you want, with the assurance of continued satisfaction.

ETEC CORPORATION

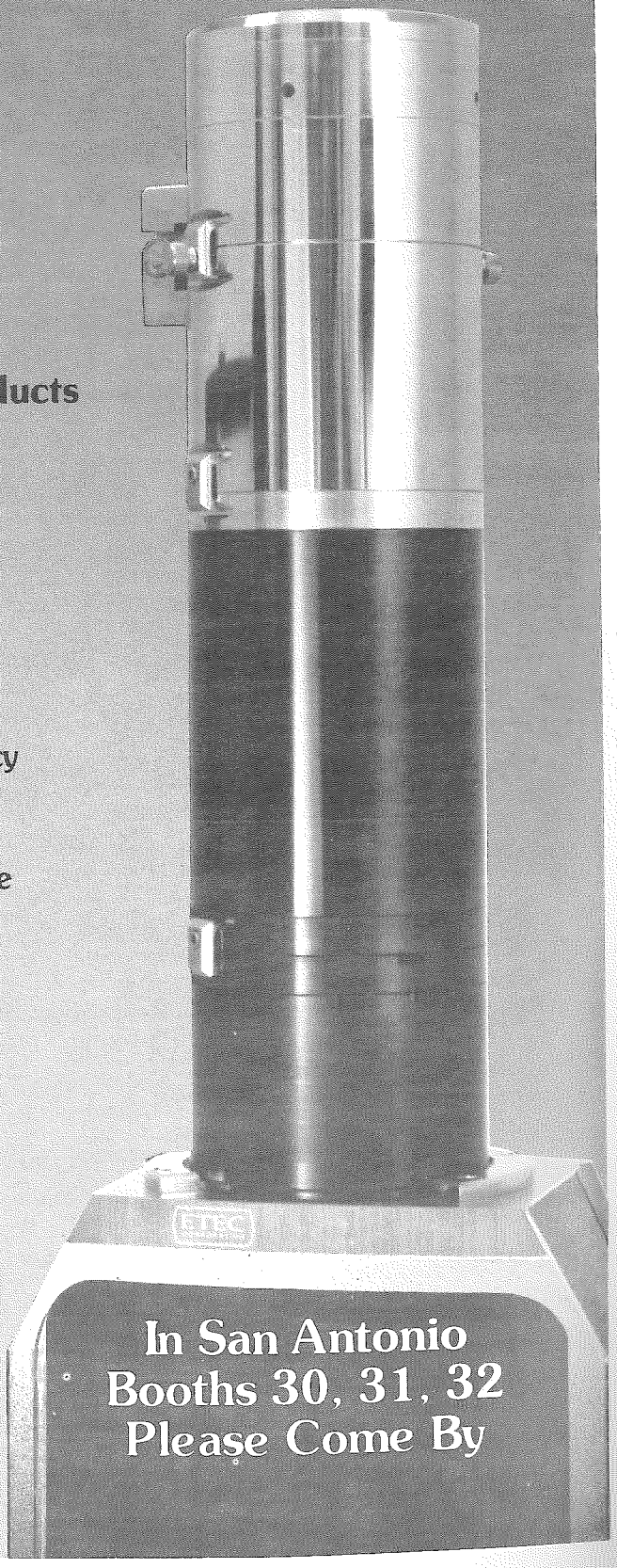

In San Antonio
Booths 30, 31, 32
Please Come By

For full product information:

ETEC Corporation
3392 Investment Blvd., Hayward, CA 94545
Tel. (415) 783-9210, TWX 910-383-0698

In Europe:

ETEC GmbH
D-7505 Ettlingen,
Einsteinstrasse 24, West Germany
(07243) 1 70 57, TLX 841-0782903

which a normal relationship between epithelium and connective tissue was maintained. After several days in culture, the duct fragments became sealed by epithelial closure of the cut ends. These ducts enlarged to various degrees, resulting in structures that ranged from cylindrical to spherical in shape. The duct walls consisted of viable epithelium and connective tissue, although the amount of connective tissue declined with age. Ultrastructurally, the most obvious change in the duct cells was the appearance of numerous bundles of filaments randomly arranged throughout the cytoplasm. Numerous dense bodies which included autophagic vacuoles, residual bodies and myelin figures were also observed. These dense bodies increased during the first two weeks but appeared to decrease during the remainder of the culture period. In the distended ducts, the normally low columnar epithelium changed to a low cuboidal or squamous type. The epithelium, however, remained contiguous. The ducts were also analyzed for their content of putative marker enzymes. Alkaline phosphatase and amylase activity declined during the culture while γ-glutamyl transpeptidase activity increased. (Supported by NCI Grant 19177).

A SCANNING ELECTRON MICROSCOPY SURVEY OF SPORE MORPHOLOGY OF THE NORTH AMERICAN SPECIES IN THE MOSS GENUS BRUCHIA. Ann E. Rushing, Department of Biology, Texas A&M University, College Station, Texas 77843.

Spore morphology has always been considered important in the identification of species within the moss genus **Bruchia** Schwaegr. Using light microscope studies, six spore morphologies have formerly been recognized in the 12 North American species. Based on scanning electron microscopy data, four spore morphologies are recognized: pitted, warty, reticulate, and spinose. Broad groupings of species are made based on spore morphology. Variation in spore size occurs in all species. Variation in spore morphology or degree of ornamentation is most prevalent in the spinose group but is also evident in the other groups. Species within a group also share some similarities of the gametophore and the sporophyte.

ULTRASTRUCTURE OF CORONARY ARTERIES IN AGING SPONTANEOUSLY HYPERTENSIVE RATS. John B. Saer, I-li Chen, Robert D. Yates, and Barbara L. Pegram*. Department of Anatomy, Tulane University School of Medicine, and *Alton Ochsner Medical Foundation, New Orleans, Louisiana.

Female normotensive Wistar-Kyoto (WKY) and spontaneously hypertensive rats (SHR) 3 months to 24 months of age were sacrificed by intracardiac perfusion with 3% glutaraldehyde in 0.1M phosphate buffer, pH 7.3. Proximal portions of the left coronary arteries were isolated, postfixed in 1% OsO_4, dehydrated in ethanols and embedded in Epon 812. Thin sections were stained with uranyl acetate and lead citrate and examined under a Siemens 101 electron microscope.

The age-related alterations in coronary arteries of SHR include an increase in Weibel-Palade bodies in endothelial cells and an invasion of smooth muscle cell (SMC) processes into the subendothelial space. Collagen and basement membrane-like material (distinguished by silver methenamine) accumulates in the media. Orcein stain suggests active synthesis of elastin by SMC. SMC develop membranous whorls, lipofuscin- and lipid-like inclusions, nuclear lobulation, cell invaginations, and numerous processes. SMC display loss of myofilaments, focal cytoplasmic necrosis and pyknotic nuclei. Debris accumulates in the extracellular space. Degenerative alterations are restricted to the medio-adventitial region at 3 months and progress toward the intima with increasing age. These results suggest that marked alterations occur in coronary arteries of aging SHR. (Aknowledgements American Heart Association-Louisiana, Inc. and E.D. Frohlich, Alton Ochsner Medical Foundation).

AHA SET OF TECHNIQUES FOR FACILITATING MORPHOLOGICAL STUDY OF VERTEBRATE MECHANORECEPTOR TERMINALS. Norman L. Salinas and Jane M. Krauhs, Department of Physiology & Biophysics, The University of Texas Medical Branch, Galveston, Texas 77550.

The advantages of embedding tissue in plastic rather than paraffin are great; however, relatively few stains have been developed for thick plastic sections and the classical methods for staining nerve endings cannot be used. We have now developed a method for staining unencapsulated mechanoreceptor endings in thick plastic sections which can be resectioned for electron microscopy. The method was developed for rat aortic arch baroreceptors, but it has been used successfully with similar tissues such as the atrium. The tissue is pinned flat in fixative to a piece of Sylgard resin and flat-embedded (pins are removed during dehydration) in a small amount of Epon. After polymerization the piece of tissue is cut out of the block, in two or more pieces if necessary, and remounted on a blank stub. The whole block is sectioned at 2μm and sections are dried onto glass slides. The stain is made by mixing 30 ml of 0.5% toluidine blue, 1% sodium borate; 20 ml of 2% p-phenylenediamine, and 5 ml of acetone. After filtering, the stain is placed in a Coplin jar with a stirring bar. Each slide is heated to 200°F, then placed in the stain for 3-5 min with stirring. Nerve endings appear dark brown against the blue connective tissue. Slides are examined for areas desirable for electron microscopy, and capsules of Epon are inverted over sections to be resectioned. The new blocks are removed from the slide by applying the proper amount of heat. Each block is trimmed to include the desired area, and thin sections are cut. Use of these methods has greatly facilitated our studies of hard-to-find sensory terminals.

THE EFFECT OF TUNICAMYCIN, AN INHIBITOR OF PROTEIN GLYCOSYLATION, ON CELL DIVISION AND SURFACE MORPHOLOGY OF SOLID AND ASCITES VARIANTS OF CHANG HEPATOMA IN VITRO. **K.E. Savage** and P.S. Baur, Div. of Cell Biol., UTMB and Shriners Burns Inst., Galveston, TX 77550.

We determined the effect tunicamycin (TM), an inhibitor of protein glycosylation, had on ascites (AS) and solid tumors (ST) **in vitro.** Using scanning electron microscopy (SEM) and cell kinetic techniques we found that the AS cell line was more sensitive to TM than the ST cell line. Cells in monolayer culture received various concentrations of TM for 24 hours. We then analyzed the cells or incubated them in fresh medium without TM for 6-192 hours. AS cells exposed continuously to 0.05 μg TM/ml medium decreased in number after 48 hours; untreated AS cells had a doubling time of 14.5 hours. Conversely, ST cells exposed continuously to 0.05 μg TM/ml medium increased population doubling time to 48 hours compared to the doubling time of 19 hours for populations of untreated cells. By SEM we found that 73% of the AS cells exposed to 0.5 μg TM/ml medium had formed blebs 30 hours after initiation of TM exposure; where as only 3-6% of the untreated AS cells had blebs. In contrast, 27% of the ST cells treated with 0.5 μg TM/ml medium had blebs 30 hours after initiation of TM exposure compared to the 2-4% in the untreated ST cells. It has been shown that blebs are more abundant on cells in G^1 than in other phases of the cell cycle. We examined TM's effect on progression of cells in the cell cycle using flow microfluorometry. Preliminary results suggest that TM blocks the AS cells in G_1 of the cell cycle. We conclude that TM can inhibit cell division in rat hepatoma cells **in vitro** by blocking them in G_1 phase of the cell cycle and the G_1 block is reflected on the cell surface morphology of the treated cells. Supported by Institutional Research Grant #1N 112A and by NIH Grant 5 R32 GM07024.

RADIOACTIVE ION MICROSCOPY. E.A. Schweikert and S.A Johnson, Center for Trace Characterization and E.L. Thurston, Electron Microscopy Center, Texas A&M University, College Station, Texas 77801.

Transmission ion microscopy is carried out with a radioactive ion beam ($^3H+$) of sufficient energy (3 MeV) to traverse thick specimens (e.g. 10μm). The emerging ions are implanted in a stack of 1.5μm thick mylar foils where their rest positions are pinpointed by autoradiography. From the pictures a tridimensional density image of the specimens can be constructed with 0.5 to 1 μm resolution. Very fragile, opaque and/or unstained specimens can be examined.

HYPOTHALAMIC MANIPULATION AND EXOCRINE PANCREAS HETEROGENEITY. W. Allen Shannon, Jr.* and Richard E. Dobbs*, Veterans Administration Medical Center and Department of Cell Biology and Physiology*, University of Texas Health Science Center at Dallas, TX 75235.

We have previously reported effects on the pancreas by hypothalamic manipulation. We report here further studies aimed particularly at exocrine cell response and interaction with the endocrine B-cell

(insulin-producing).

Weanling rats were anesthetized and placed in a stereotoxic device. Number 5 stainless steel pins were inserted through a small opening in the skull into the intervening parvicellular zone between the ventromedial and dorsomedial nuclei. The splenic pancreases were collected 10 weeks later.

Electron microscopy revealed marked insular-pancreatropic effects. The most dramatic of these appeared to be B-cell granules within the exocrine cells. Although polarized, some cells appeared to be hybrid B-cell-exocrine cells. Others contained B-cell granules isolated among zymogen granules and in what appeared to be different stages of formation, especially in the vicinity of Golgi complexes. Although hypersecretion of B-cell granules and the presence of such granules in the basal intercellular space was observed, it is unlikely that these granules entered the exocrine cell cytoplasm.

It is apparent that the lesion produced in the hypothalamus by this procedure directly resulted in major exocrine and endocrine cell alterations. It will be necessary to further analyze the indicated production of B-cell granules, i.e., insulin, by exocrine cell protein synthesis apparatus. (Supported by the Veterans Administration, N.I.H. Grant #1-ROIAM25974-01 and the North Texas Affiliate of the American Diabetes Association.)

AN ULTRASTRUCTURAL EXAMINATION AND COMPARISON OF THE DINOKARYOTIC NUCLEUS AND THE EUKARYOTIC NUCLEUS IN SELECTED ALGAE. Kathleen Shupe, Department of Biology, Texas A&M University.

The dinokaryotic nucleus has been shown to combine the ultrastructural characteristics of both the prokaryotic nucleoid and the eukaryotic nucleus. Light microscopy and scanning electron microscopy were combined to examine the ultrastructure of the dinokaryotic nucleus in the dinoflagellate, **Crypthecodinium cohnii,** the eukaryotic nucleus in the chrysophyte **Olisthodiscus luteus,** and both the dinokaryotic and the eukaryotic nucleus of the dinoflagellate **Peridinium balticum.** Nuclei were stained with methyl-green-pyronin for examination with light microscopy. Specimens for scanning electron microscopy were fixed, dehydrated, and critical point dried. Dinokaryotic nuclei stain a violet blue with methyl-green-pyronin while the eukaryotic nuclei stain a bright blue. Scanning electron microscopy revealed a dinokaryotic nucleus which was highly convoluted. The nuclear envelope is easily lysed during processing and reveals a nucleus with chromatin fibers extruding through the lysed nuclear envelope. The eukaryotic nucleus exhibits a very smooth surface. Nuclear pores could be delineated on the surface of the eukaryotic nucleus. Biochemical analysis of the structure of the chromatin from both of these nuclei help to further differentiate the dinokaryote from the eukaryote.

SMALL CELL NEUROEPITHELAL TUMORS OF THE SKIN. Elvio Silva and Bruce Mackay, The University of Texas System Cancer Center, Houston.

Studies conducted in this department have previously demonstrated that small cell tumors ultrastructurally similar to neuroblastomas of childhood can occur in adult patients. We now report clinical and pathologic studies on 11 cutaneous neoplasms that appear to fall within this category but show some distinctive features, possibly related to their location. The patients ages ranged from 56 to 86, and the majority of the tumors arose in the head and neck region. The tumors appeared to originate within the dermis and the larger tumors extended to the subcutaneous tissue, and pressed up against the epidermis ulcerating it in two instances. True epidermal involvement was not observed, indicating that these are not neoplasms of epidermal cells. By light microscopy the tumors are composed of solid masses of compactly grouped, uniformly small cells, and the rosette pattern frequently seen in pediatric neuroblastomas is not present. However, a peculiar nesting arrangement that we have not observed in small cell tumors in other locations was seen in several of the tumors. The dominant ultrastructural feature is the presence of dendritic cytoplasmic processes containing small membrane-bound granules. Microtubules are sparse, in contrast with their frequency in childhood heuroblastomas. The number of dendritic processes varies and they may be small and scanty but their presence indicates a neuroepithelial cell of origin. Regional lymph node metastases are prone to occur, and the tumors may become disseminated. Early recognization and prompt surgical excision, possibly with regional lymph node dissection, are therefore necessary.

AMELANOTIC MELANOMA. Elvio Silva and Bruce Mackay, The University of Texas System Cancer Center, Houston.

In primary tumors of melanocytes (melanomas) the characteristic feature is the presence of cytoplasmic melanin pigment. The melanin is aggregated in specific organelles, the melanosomes, and is deposited on a protein framework, the premelanosome, which has a distinctive transverse periodicity. Melanomas are aggressive tumors that metastasize readily, and with dedifferentiation the cells tend to lose their ability to form melanin. In the absence of pigment, the diagnosis of metastatic melanoma can be extremely difficult by light microscopy, and the problem is often compounded by spontaneous regression of the primary cutaneous neoplasm.

We wish to report our experience using the electron microscope to identify metastatic amelanotic melanoma. Examples from a series of over 400 cases will be shown to demonstrate the range of morphology of the individual tumor cells, and the degree to which they may mimic other neoplasms, particularly poorly differentiated carcinomas. When melanin is absent, the presence of premelanosomes may establish the diagnosis. When premelanosomes are not found, the occurrence of dense cytoplasmic bodies can be suggestive, but it is necessary to establish that they are not lysosomes: the potential of the ultrastructural Dopa reaction for this purpose will be discussed. Tubulo-reticular inclusions occur in a small proportion of metastatic melanomas and may suggest the diagnosis. Ultrastructural study is also useful in identifying the infrequent melanomas that arise in soft tissues.

LIGHT AND ELECTRON MICROSCOPICAL INVESTIGATIONS IN THE DICTYONEMATACEAE (BASIDIOLICHENS). Robert D. Slocum, Cell Research Institute and Department of Botany, University of Texas, Austin, TX 78712.

The nature of the fungus-alga association between representatives of the lichen-forming basidiomycete genus **Dictyonema** and their **Scytonema** hosts was investigated using light and electron microscopical techniques. The lichen-like basidiocarps of one species, **Dictyonema irpicinum** are shown to be established as a result of the active capture of free-living **Scytonema** trichomes by the fungal symbiont. A septate, intracellular haustorial hypha is produced by the fungus within the filamentous blue-green alga shortly after initial cell-cell contact is established. This specialized haustorial apparatus appears to enhance the survivorship of the otherwise ephemeral fungus, allowing it to maintain a long-term, stable association with the algal host.

DIRECT LIGHT AND ELECTRON MICROSCOPIC IMAGE CORRESPONDENCE FROM A SINGLE SECTION. Stewart Spiers, Jeff Bray, International Scientific Instruments, Inc.

Direct correspondence of images from a single section in both light and electron microscope modes is now possible using the ISI LEM-2000. By staining a blue section ($\sim 0.3\mu$) with both lead citrate and toluidine blue and placing it under column vacuum high quality images can be obtained in both modes by transferring the stages of the LEM-2000 from the optical axis of the light microscope to the adjacent and aparallel EM column axis. This capability has been used successfully in diagnosing renal biopsies where it is often desireable to study the sections at higher magnifications than otherwise possible with light optics with no loss in time to prepare EM sections. To aid in keeping track of vaious points of interest on the large 7mm LEM grid the stage is controlled by a microprocessor with an addressable memory capable of storing up to 100 x-y coordinates selected by the operator and recalled at random in either mode.

THE EFFECT OF FLUOROCARBON 11 (TRICHLOROMONOFLUOROMETHANE) ON THE ALVEOLI OF THE RAT LUNG. Mannie C. Steglich and J. Leon McGraw, Jr., Department of Biology, Lamar University, Beaumont, Texas 77710.

Male albino Sprague-Dawley rats were exposed to 2.5% fluorocarbon 11 for 7, 14, and 21 days. Electron microscopy, in conjunction with stereology showed several changes in lung alveolar morphology. By 7 days, the capillaries of the alveoli contained an abnormal osmiophilic

substance. After 21 days, there was a decrease in the relative volume of the multilamellar bodies of the greater alveolar cell by approximately 50%. Also, the cytoplasm of the squamous alveolar and capillary endothelial cells became amorphous and disintigrated, and their nuclei became abnormally osmiophilic.

EM STUDY OF EPIZOOTIC DIARRHEA VIRUS OF INFANT MICE, INFECTION OF INTESTINAL EPITHELIUM. J. Vollet, Ph.D., Program in Infectious Diseases & Clinical Microbiology, The University of Texas Medical School, Houston, Texas.

Rotaviruses are known to be the prime cause of infantile gastroenteritis worldwide. Due to the lack of infectivity of the human agent into appropriate animal models, the pathogenesis of viral infection was studied with the serologically related EDIM agent in newborn Balb/C mice. Following oral challenge, mice were sacrificed at various times post infection through recovery,and the intestines prepared for EM. Virus infection was seen in individual epithelial cells predominantly in the crypts of villi in the jejunum. Cisternae of the ER showed progressive dilation into sacks. These sacks became filled with lipid material and large numbers of 70 nm viral particles. The nucleus and microvilli of each infected cell appeared unaffected while mitochondria and the Golgi showed no degeneration but were displaced in location by the viral vesicles. Virus was released from the affected cells when the cytoplasm became full of vesicles inducing cell rupture releasing the virus into the lumen for fecal shedding.

A COMPARITIVE STUDY OF THE RAPHE COMPLEX IN SELECTED EUNOTIA SPECIES. Richard J. Wahrer, Dept. of Biology, Texas A&M University, College Station, Texas.

Several species of **Eunotia**, a freshwater diatom, were examined in order to elucidate its taxonomic position. The single labiate process in each valve and the terminal nodules of the raphe and their orientation could be used as criteria for classification. It was found that in the species with an undulate dorsal margin (**E. monodon** var. **constricta, E. diodon, E. pectinalis** var. **undulata**), the labiate process was excentrically oriented near the apex of the valve. In linear and paralleled margin species (**E. flexuosa, E. curvata**), the labiate process was located in the valve apex with a corresponding hyaline field.

SEM OF ZUCCHINI SEED. Mary Alice Webb and Howard J. Arnott, Department of Biology, The University of Texas at Arlington, Arlington, Texas 76019.

Cotyledon cells of zucchini seed have been studied using scanning electron microscope techniques. These techniques have been correlated with established transmission electron microscope methods to provide confirmation of many new observations. Emphasis of the study is on the structure of the dormant seed, which has been observed following anhydrous preparations for SEM and freeze-etch preparations for TEM. The dormant seed is an extremely compact structure whose features include undulating cell walls, storage protein bodies in highly organized arrays, lipid extending throughout the cell, and storage material filling intercellular spaces. Dormant seed structure is contrasted with structure observed immediately following imbibition by the seed. Cytological changes resulting from germination of the seed have also been observed using SEM techniques with emphasis on the breakdown of storage protein and fusion of protein bodies to form a large central protein vacuole.

C-TYPE PARTICLES IN THYMIC DEVELOPMENT: A CORRELATION WITH THYMIC FUNCTION. P.L. Witte, J.W. Streilein, W.A Shannon, Univ. of Texas Health Science Center, Dallas, Texas 75235.

Fetal development of the thymus gland in mice occurs during the terminal 9 days of gestation; C-type viral particles are identified ultrastructurally in epithelial reticular cells, then in thymus lymphocytes during this interval, but these particles essentially disappear at birth. A relationship between expression of C-type viruses and thymic maturation has been postulated to exist. Syrian hamsters exhibit two unusual features of thymic functional activity: (1)thymectomy as late as 4 weeks after birth can still induce a relative immunodeficient state; (2) normal, adult hamsters lack T cell functions ascribed to killer cells and suppressor cells. Expression of C type particles during fetal development of hamster thymus was studied between days 10 and day of birth (16 days). A companion study was conducted in fetal C57BL/6 mice.It was found that, as reported previously, C type particles were observed in murine thymic cells on each fetal day, reached peak expression at day 15 1/2 and virtually disappeared by day of birth. By contrast, no evidence of C-type particles was found in hamster thymic tissue, either epithelial or lymphocyte, at any time during gestation. These results verify the transient expression of C-type particles in fetal murine thymus and indicate that no comparable phenomenon is observable in hamsters. These findings imply that (1) expression of C-type virus particles during thymic differentiation is important to the full development of thymic function and that (2) Syrian hamsters may be an experiment of nature in which absence of C-type virus expression corresponds to delayed and incomplete maturation of a thymus immune system.

ULTRASTRUCTURE OF THE HYDROCARBON-PRODUCING ALGA BOTRYOCOCCUS BRAUNII (CHLOROPHYTA). Fred R. Wolf, Texas A&M University, College Station, Texas.

Colonies of **Botryococcus braunii** consist of grape-like clusters of cells embedded within an hydrocarbon matrix. Green colonies contain a mixture of long-chained hydrocarbons which may comprise up to 20% of dry weight. Certain environmental factors induce the development of the brown "resting state", of which up to 90% of the dry weight may consist of a branched triterpenoid.

Individual cells are pyriform, with the base of the cup-shaped chloroplast occupying the narrow cell posterior. The base of the chloroplast contains a pyrenoid traversed by thylakoids. The nucleus is centrally located, and often surrounded by a variety of osmiophilic bodies. The cytoplasm contains numerous mitochondria often intimately associated with certain inclusions and the inner surface of the chloroplast. Dictyosomes occur at the cell apex where they presumably paticipate in the secretion of mucilage.

Laboratory cultures subjected to nutrient stress undergo rapid senescense, during which time substantial quantities of hydrocarbons are produced by contrast to controls. Ultrastructural changes include an increase in the size and/or number of osmiophilic inclusions to the extent that the nucleus is suspended by strands of cytoplasm. The starch-engorged chloroplast and other organelles are reduced in size and restricted to the cell periphery. Aspects of wall structure and a hypothetical mode of hydrocarbon secretion will be discussed.

QUANTITATIVE ELECTRON MICROSCOPY OF CYTOPLASMIC MICROTUBULES IN 3T3 AND SV-3T3 CELLS. Danna Zimmer, Donna Turner, and B.R. Brinkley. Department of Cell Biology, Baylor College of Medicine, Houston, Texas.

Immunoflourescence studies (Brinkley et al. PNAS, USA. 73: 4981, 1975) have suggested that transformed cells contain fewer cytoplasmic microtubules than normal cells and that these are shorter and more randomly oriented. However, data from another group (Osborn & Weber. Cell. 12:561, 1977) indicates that transformed cells contain visible networks of microtubules. To further investigate this problem we have determined the volume of polymerized microtubules in 3T3 and SV-3T3 cells by electron microscopy and stereology. Analysis was carried out at approximately equivalent passages in culture. The counting methods of Reaven and Reaven (J. Cell Biol. 75:599, 1977) were used. Normal cells (n=14) show a Gaussian distribution with a mean microtubule/cytoplasmic volume ratio (M/C) of 5.0×10^{-3}. Transformed cells (n=14) show an almost bimodal distribution with a mean M/C of 3.1×10^{-3}. The downward shift of the mean M/C in transformed cells indicates a depolymerization or a change in the orientation of microtubules in these cells. Statistical analysis shows that the difference in the mean M/C is significant at 6%. The shift may also be due to the difference in shape of the cells; therefore we are increasing our sample size according to the method of Rubin and Warren (J. Cell Biol. **82**: 103, 1979) to account for the shape differences. We are also attempting to determine if this bimodal distribution may be due to variation between populations of transformed cells. Supported by a grant from the NCI CA 22610.

We Can Measure Up!

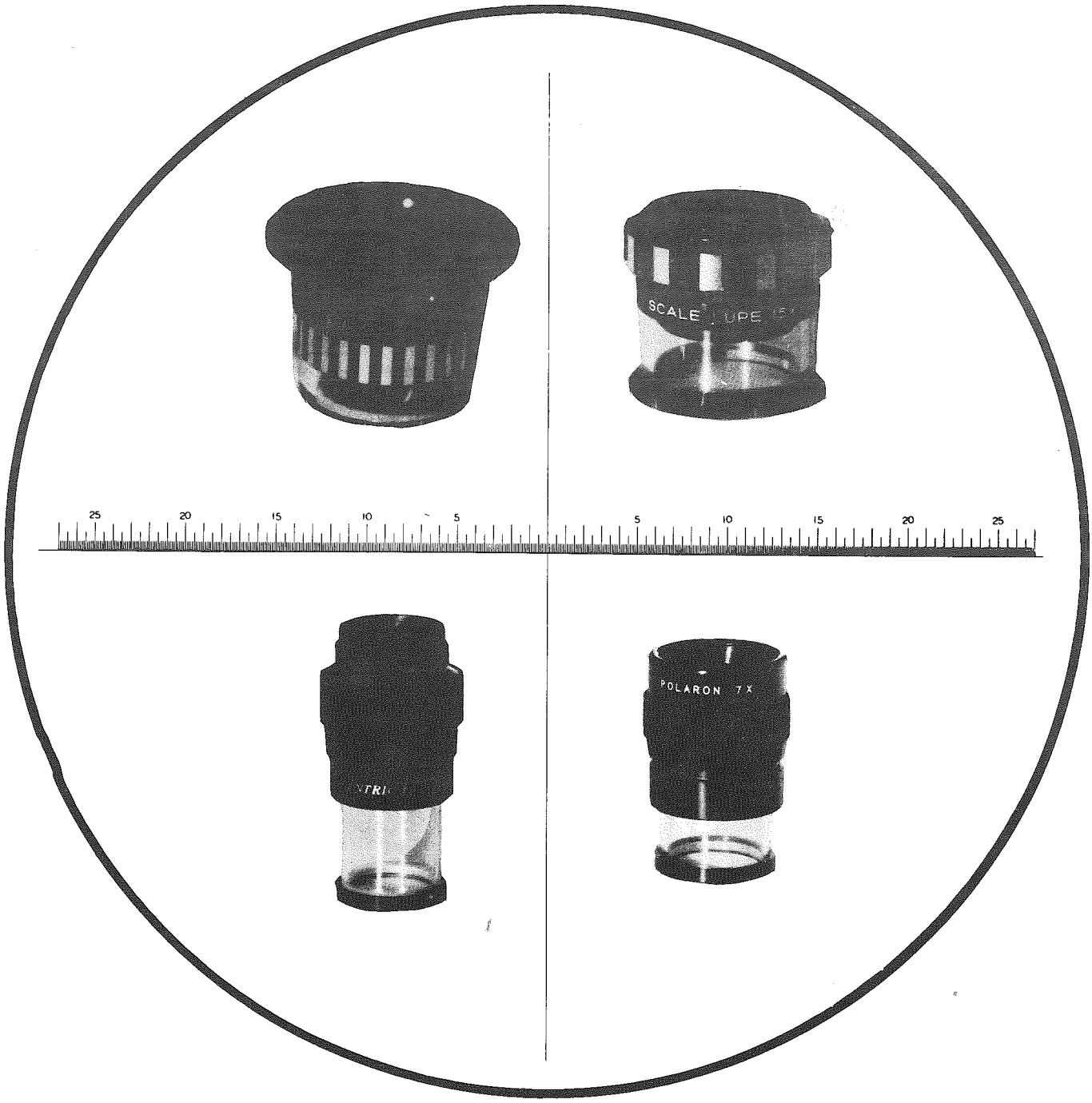

Try us for all your EM supplies and instrumentation.

Polaron Instruments Inc.
4099 Landisville Road
Doylestown, Pa. 18901
(215) 345-1782

Regional News

ARLINGTON
UNIVERSITY OF TEXAS, BIOLOGY DEPARTMENT

PUBLICATIONS

Butler, J.K., Methods for improved light microscopy microtomy. **Stain Technol.** 54: 53-69, 1979.

The Technical Note by Turnbull, T.P., A long knife maker for producing Ralph type skives. **EMSA Bull.** 9:63-65, is a partial excerpt of the paper above.

E.M. EDUCATION

The Biological Electron Microscopy Course enrolled five students, two from the Department of Psychology. Dr. Couch's E.M. students at T.C.U. exchanged visits with the U.T. Arlington E.M. students in December.

DENTON
TEXAS WOMAN'S UNIVERSITY, DEPARTMENT OF BIOLOGY

LECTURES

Dr. M. Louise Higgins attended the Central States Branch of Tissue Culture Association, Omaha, October (19-20), and the Southwest Section of the American Association for Cancer Research, Albuquerque, November (16-17), and presented papers on the "Analysis of the Mechanism of Neuroblastoma Process Transection in Culture with Pulsed UV Laser Microbeam Irradiation.

E.M. EDUCATION

Five graduate students have successfully completed the course in Electron Microscopy Techniques offered this fall. The students have become new members in the TSEM.

HOUSTON
UNIVERSITY OF TEXAS MEDICAL SCHOOL, DEPARTMENT OF NEUROBIOLOGY AND ANATOMY

GRANTS AWARDED

Richard Wiggins, Ph.D., Assisant Professor, has been awarded a Research Career Development Award from the National Institute of Neurological and Communicative Disorders and Stroke.

LECTURES AND MEETINGS ATTENDED

Nachum Dafny, Ph.D., Professor, returned in August from his sabbatical at Tel Aviv University where he studied the neurobiology of obesity and satiety. Dr. Dafny presented several lectures during his stay in Israel: On July 12 at the Aba Khoushy School of Medicine, Haifa, "Neurophysiological Evidence of Morphine Dependence and Tolerance;" July 16 at the Hadassah Medical School, Jerusalem, "The Acute and Chronic Effects of Opiates on 8 Different Brain Sites within the CNS;" July 24 at the Tel-Aviv University Sackler Medical School, Tel-Aviv, "The Interaction Between Neurotransmitters and Opiates Within the CNS;" and August 2 at the Hebrew University Faculty of Science, Jerusalem, "Is the Pineal a Gland or a Neuromodulator?"

S.J. Enna, Ph.D., Associate Professor in the Departments of Neurobiology and Anatomy and Pharmacology, was a featured speaker at the Diagnostic Immunology Conference sponsored by the Engineering Foundation held in Henniker, New Hampshire, August 6-10. His presentation was entitled "Neurotransmitter Receptor Binding Assays."

Lena Chu, Sr. Research Associate, and Marilyn Munkres, M.S., Teaching Associate, represented the department at the Electron Microscopy Society of America meeting in San Antonio, August 13-17.

Dr. Nachum Dafny attended the annual meeting of the American Society of Pharmacology and Experimental Therapeutics in PORTLAND, Oregon, August 20-23, where he presented a lecture entitled "Different Electrophysiological Signs of Tolerance and Dependence: Multiple Unit Activity in the Fore-brain." On August 22, Dr. Dafny presented a seminar entitled "Is the Pineal a Gland or a Neuromodulator?" at the Department of Anatomy of the University of Oregon Health Science Center.

Dianna Redburn, Ph.D., Associate Professor, was an invited speaker at the Satellite Meeting of the International Society for Neurochemistry in Athens, Greece, August 28-September 1. Dr. Redburn spoke on the "Biochemical Analysis of the GABA System in Retina."

S.J. Enna, Ph.D., chaired a session and presented a paper entitled "Drug and Disease-Induced Alterations in Brain Serotonin Receptors" at an international symposium on serotonin in Athens, Greece, September 11-16.

Richard Wiggins, Ph.D., Assistant Professor, attended the Texas Society for Neuroscience meetings in Dallas, October 13, and presented a paper entitled "The Cellular Basis of Brain Hypomyelination Induced by Postnatal Undernourishment."

S.J. Enna, Ph.D., presented a series of seminars the week of October 22nd. He spoke on GABA pharmacology and the neurotransmitter receptor alterations associated with neuropsychiatric disorders at Mead Johnson Pharmaceutical Co., Evansville, IN; ICI-USP Pharmaceutical Co., Wilmington, DE; and the Philadelphia Area Neuroscience Society at Jefferson Medical School in Philadelphia.

The Department of NB&A was well-represented at the recent 9th Annual Meeting of the Society for Neuroscience in Atlanta, November 2-6. Those attending and presenting their research were: Drs. Joe Wood, Professor and Chairman; Nachum Dafny, Professor; Jon DeFrance, Assoc. Professor; Zehava Gottesfeld, Assoc. Professor; Gerald Kozlowski, Assoc. Professor; Dianna Redburn, Assoc. Professor; Jo Ann McConnell, Asst. Professor; Jack Waymire, Asst. Professor; Richard Wiggins, Asst. Professor; Robert McClung, Instructor; Ron Philo, Teaching Assistant; and several research fellows and graduate students.

Attending the Annual Meeting of the American Society for Cell Biology in Toronto (November 6-8) were Michael Oberdorfer, Ph.D., Asst. Professor, and Marilyn Munkres, M.S. Dr. Oberdorfer gave a presentation entitled "Cell Death and Neuroepithelial Intercellular Spaces in the Mammalian Embryonic Eye" and Ms. Munkres presented a poster "Comparison of CR-NE Granule Content in Bovine Adrenal Medullary Tissue and Cultured Cells Using Stem Analysis."

Dr. S.J. Enna, Zehava Gottesfeld, and Dianna Redburn were invited speakers at the International Symposium on GABA and Other Inhibitory Neurotransmitters in Myrtle Beach, SC in November. Dr. Enna chaired a session on GABA receptors during which he gave a talk entitled "GABA Receptor Binding;" he also presented "Muscimol Penetration and Degradation in Mammalian Habenula." And, Dr. Redburn gave a talk entitled "GABA Receptor Binding in Bovine Retina."

Dianna Redburn, Ph.D. presented a seminar to the Biochemistry Department of the Medical University of South Carolina on November 19 entitled "Neurotransmitters in Retina."

S.J. Enna, Ph.D. presented a lecture to the Department of Pharmacology, University of Texas at San Antonio School of Medicine, on December 5 entitled "Receptor Alterations in Neuropsychiatric Disorders."

UPCOMING EVENTS

Neurochemistry and Physiology of the Visual System - Sunday, March 2, a Satellite Symposium of the 11th Annual Meeting of the American Society for Neurochemistry will be sponsored by the Department of Neurobiology and Anatomy, U.T. Medical School, and the Cullen Eye Institute of Baylor College of Medicine.

HOUSTON

BAYLOR COLLEGE OF MEDICINE
DEPARTMENT OF MEDICINE
SECTION OF CARDIOVASCULAR SCIENCES

SEMINARS

Dr. Ann Goldstein gave a seminar entitled "The Z Lattice in Cardiac Muscle" at Emory University School of Medicine in December 1979.

Mr. David Murphy presented an abstract entitled "Quantitative Studies of Ischemic Canine Myocardium" at the 5th International Symposium on Atherosclerosis in Houston in November 1979.

GENERAL NEWS

Dr. Joiner Cartwright, Jr. has joined our group as a post-doctoral fellow. He received his Ph.D. from the University of Hawaii and worked with Dr. John Arnold.

NEW EQUIPMENT

Dr. W. Barry Van Winkle has installed a new Balzers Freeze Etching system and ordered an LKB Ultratome V in his new lab. Mr. Preston Aycox has joined Dr. Van Winkle's staff as electron microscope technician.

PUBLICATIONS

Goldstein, M.A., Schroeter, J.P. and Sass, R.L.: The Z lattice in canine cardiac muscle. J. Cell Biol., 83:187-204, 1979.

Goldstein, M.A.: Ultrastructure of the ischemic myocardium. Cardiovascular Res. Center Bulletin, 18:1-33, 1979.

DEPARTMENT OF CELL BIOLOGY

PUBLICATIONS

It seems that Dr. Thomas Lin has an ever-growing list of publications in the field of immunocytochemical localizations. A paper has appeared in December **Biochemistry** and a number of them have been recently submitted for publication in **Endocrinology** and the **Journal of Cell Biology.**

Dr. Nick Mace also has a passel of papers accepted by Cancer Letters, one published and two in press. Dr. Mace has recently been doing some outstanding work in asbestos-related diseases.

NEW FACULTY and/or STAFF MEMBERS

We are pleased to welcome Dr. Brian Luck to the Department of Cell Biology, E.M. Core Facility. Dr. Luck has joined Dr. Wayne Wray's group and will be studying chromosomes and the DNA core structure.

E.M. EDUCATION

Debbie Hodges and Donna Turner will be presenting a workshop in ultra-thin sectioning at the TSEM-LSEM Joint Symposium this February. The workshop will be held in the E.M. Core Facility of the Department of Cell Biology, Room 122A.

DEPARTMENT OF MICROBIOLOGY

LECTURES

H.D. Mayor - 12/7/79 - University of Texas at El Paso: "Defective Parvoviruses and their Helpers."

PUBLICATIONS

Lalo, R.J. and Mayor, H.D.: Inhibition of the replication of parvovirus X14 by 5-Iodo-2'-deoxyuridine pre-treatment of cell cultures. J. Gen Virol. 44:577-585, 1979.

LUBBOCK

TEXAS TECH UNIVERSITY

GRANTS AWARDED

J.C. Hutson and D.M. Stocco, Sertoli Cell Function in Culture NSF $35,000.

PUBLICATIONS

Markwald, R.R., T.P. Fitzharris and D.H. Bernanke. (1979). Structural identification of complex carbohydrates. J. Histochem. Cytochem. **27**:1171-1174.

Markwald, R.R., F.M. Funderburg and D.H. Bernanke. (1979). Glycosaminoglycans: potential extracellular determinants in cardiogenesis. In **Factors Contributing to Cardiac Function.** M.F. Crass editor. Texas Reports in Biology and Medicine. Vol. 39.

Markwald, R.R. and D.H. Bernanke. (1979). Structural analysis on the effects of 6-Diazo-5-oxo-L-Norleucine on cardiac tissue morphogenesis. **Cardiac Morphogenesis and Teratology.** Thomas Pexider, editor. Perspectives in Cardiovascular Research, Raven Press, (in press).

Bolender, D.L., W.G. Seliger and R.R. Markwald (1979). A histochemical analysis of polyanionic compounds found in the extracellular matrix encountered by migrating cephalic neural crest cells. **Anat. Rec.** In press.

Bernanke, D.H. and R.R. Markwald. (1979). Effects of hyaluronic acid on cardiac cushion tissue cells in collagen matrix cultures. **Cardiac Function** M. Shetlar editor. Vol. 39. Texas Reports on Biology and Medicine.

Fitzharris, T.P., R.R. Markwald and B. Dunn. (1980). Influence of Beta aminoproprionitrile on early cardiac cushion tissue morphogenesis. **J. Mol. Cell Cardiol.** In press.

Hay, D.A. and R.R. Markwald. (1979). Localization of fucose-containing substances in developing atrioventricular cushion tissue. In **Cardiac Morphogenesis and Teratology.** Tomas Pexieder editor. Perspectives in Cardiovascular Research. Raven Press. New York. In press.

Fitzharris, T.P., R.P. Thompson and R.R. Markwald. (1979). Matrical ordering in the morphogenesis of the tunica media.

Factors Influencing Cardiovascular Function. M.F. Crass editor. Texas Reports in Biology and Medicine. Vol. 30. (In press).

Nathan, R.D., P. Houck, D.M. Stocco and R.R. Markwald. (1979). Mechanisms of pacemaker activity in embryonic cardiac muscle. In **Cardiac Morphogenesis and Teratology.** Tomas Pexieder editor. Perspectives in cardiovascular research. Raven press. New York. (In press).

Pang, P.K.T., M. Yang, C. Oguro, J.G. Phillips, J.A. Yee. Hypotensive actions of parathyroid hormone preparations in vertebrates. J. Gen. Comp. Endocrinol., in press.

Pang, P.K.T., T. Tenner, J.A. Yee, M. Yang. Specificity of the hypotensive action of parathyroid hormone in dogs and rats. Proc. Nat. Acad. Sci. (USA), in press.

Hutson, J.C., C.W. Garner and D.M. Stocco. Effects of various serum components on Sertoli cells in culture. Anat. Rec. (in press).

NEW EQUIPMENT and/or FACILITIES

Dr. Roger Markwald has recently purchased a Polaron Vacuum evaporator and freeze fracture unit for use in the department.

SAN ANTONIO
UNIVERSITY OF TEXAS HEALTH SCIENCE CENTER, DEPARTMENT OF ANATOMY

MEETINGS

Drs. Ivan Cameron, Thomas Pool, Nancy Smith and Mr. Rodney Sparks presented a series of papers on the relation between intracellular element concentration and cell reproduction at the American Society for Cell Biology meetings held in Toronto, Canada, Nov. 4-8, 1979. Following the meetings, Dr. Cameron was interviewed on Canadian National television and radio cncerning various aspects of this subject.

Dr. Vinod K. Berry attended the 12th Annual Conference of the Electron Microscope Society of India December 17-19, 1979 in Chandigarh, India. He also attended the National Symposium on Science and Technology of Vacuum, Surfaces, and Thin Films, December 21-24, 1979 in New Delhi, India.

INVITED LECTURES

Dr. Thamas B. Pool was an invited participant in the workshop: "The Potential Use of TCDD as a Tool in Molecular Biology" hosted by the National Institute for General Medical Sciences in Bethesda, Maryland, December 11-12, 1979. He spoke on the exogenous control of cell division.

RECENT PUBLICATIONS

Berry, V.K. and L.E. Murr, 1980, A morphological and ultrastructural study of the cell envelope of thermophilic and acidophilic microorganisms as compared to **Thiobacillus Ferro Oxidans**, Biotechnol, Bioengr, in press.

Cameron, Ivan L., Pool, Thomas B. and Nancy, K.R. Smith. 1979. An x-ray microanalysis survey of the concentration of elements in the cytoplasm of different mammalian cell types. J.Cell. Physiol, 101:493-502.

Herbert, D.C. 1979. Intercellular junctions is the rhesus monkey pars distalis. Anat. Rec., 195:1-6.1980 Growth patterns and hormonal profile of male rats with protein-calorie malnutrition. Anat. Rec., in press.

Sheridan, P.J. and D.C. Herbert. 1980. Nuclear uptake and retention of androgen by the pituitary gland of the hamster and the rat. Cell Tiss. Res., in press.

Rennels, E.G. and D.C. Herbert. 1980. Functional correlates of anterior pituitary cytology. In: R.O. Greep (ed.), International Review of Physiology. Reproductive Physiology. Vol. 23. University Park Press, Baltimore, MD, in press.

NEW EQUIPMENT

The SEM-XRMA facility in the Department of Anatomy has recently acquired an LKB Ultratome-V with cryokit and cryotools for ultra-thin cryosectioning. This equipment is available to all users within the U.T.H.S.C.-S.A.

EDUCATION

Dr. Nancy Smith is teaching a graduate course in electron probe x-ray microanalysis during the spring semester, 1980. An SEM course will be offered in the summer.

REGIONAL EDITORS

ERNEST F. FULLAM, INC.

Accessories for Microscopy • Scientific Consultants

P.O. Box 444 • Schenectady, New York • U.S.A. • 12301

Telephone (518) 785-5533

THE EMS-76 MINI-COATER

CATALOG
No. 1890

THE SMALLEST and LEAST EXPENSIVE COATER

- No Temperature Rise
- 20-30 Sec. Average Coating Time
- Price Includes Gold Target (Others Available)
- Etch & Carbon Coating Options Available
- Only 10½" Wide x 10" Deep
- One Year Guarantee

SNOW FLAKES

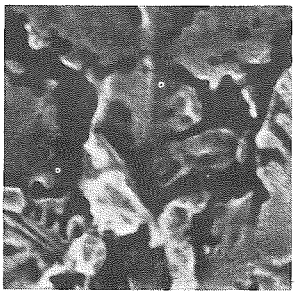

FRACTURED PARAPLAST

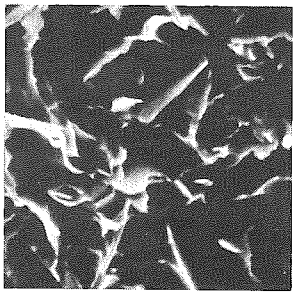

POWDERED SUGAR

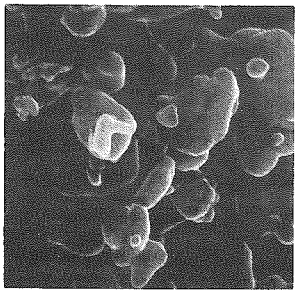

IN CANADA ORDER FROM
MICROBIOLOGICAL SUPPLIES, LTD.
41 MAPLE AVENUE, THORNHILL, ONTARIO L3T 3S9

Job Opportunities

SCANNING AND TRANSMISSION ELECTRON MICROSCOPY

A series of practical courses will be offered during June 1980:

Transmission Electron Microscopy - June 2-13
Scanning Electron Microscopy - June 16-20
Combined TEM and SEM - June 2-20

These classes are designed to introduce the participants to the theory and practical aspects of electron microscopy. Primary emphasis will be specimen preparation, operation of electron microscopes, x-ray microanalysis, and photographic and darkroom techniques.

Tuition:
$595 for TEM
$520 for SEM
$1,010 for the combined program

For more information write or call: Fred Lightfoot, George Washington University, Department of Anatomy, 2300 "I" Street, N.W., No. 406, Washington, D.C. 20037. Phone: (202) 676-2881 or 676-3511.

Position Available - EM technician: B.S. or B.A. degree, 3 years experience preferred. Salary minimum $14,000. Contact Dr. Ramon Font, Neurosurgery Sciences, Baylor College of Medicine, Houston, TX 77030. Phone: 790-4644.

Postion Available - TRW, a Fortune 100 company, is inviting applications for an exceptional technical person for the analytical section of its carbide metallurgical laboratory.

Wendt-Sonis, the carbide manufacturing division of TRW, is located in Rogers, Arkansas, which is in the picturesque Ozark Mountain and lake area of Northwest Arkansas.

The successful candidate will have a demonstrated expertise with the Scanning Electron Microscope, and the attached energy dispersive x-ray fluorescence microprobe. It would be expected that this position would lead to the analytical section supervisory post. It would be desirable if the candidate has some supervisory experience and a materials or fracture mechanics background.

We offer a competitive salary, and a full line of company-paid benefits.

Interested applicants should send their resume outlining experience and salary requirements to: Dr. J.W. Cox, TRW Wendt-Sonis, Manager of R. & D., P.O Box 9, Rogers, Arkansas 72756. We are an equal opportunity employer.

TSEM FINANCIAL REPORT
Period Ending January 1, 1980

ASSETS ON JULY 10, 1979:		
Certificate of Deposit No. 1099, Univ. Natl. Bank	$ 2,000.00	
Certificate of Deposit No. 17864, Fannin Bank	1,000.00	
Savings Account No. 10-0502435, Fannin Bank	3,115.69	
Checking Account Balance, Fannin Bank	1,493.98	
Total Assets	$ 7,609.67	$ 7,609.67
RECEIPTS:		
Dues		
Regular Membership	$ 500.00	
Student Membership	34.00	
Corporate Membership	75.00	
Transfer from Galveston Accounts	86.08	
Electron Microscopy Society of America	500.00	
Interest:		
C. of D. No. 1099	75.00	
C. of D. No. 17864	36.35	
Savings Account No. 10-0502435	85.98	
Purchase of Membership List	3.00	
Purchase of booth space for 1980 Symposium	1,600.00	
Subtotal	$ 3,007.64	(+) $ 3,007.64
DISBURSEMENTS:		
San Antonio Meeting expenses	$ 1,401.57	
1980 Symposium advance expenses	182.26	
Secretarial expenses	200.00	
Treasurer's Fidelity Bond	27.00	
Subtotal	$ 1,950.83	(−) $ 1,950.83
		$ 8,666.48
ASSETS ON JANUARY 1, 1980:		
Certificate of Deposit No. 1099, Univ. Natl. Bank	$ 2,000.00	
Certificate of Deposit No. 10-141345, Houston 1st Sav	2,000.00	
Savings Account No. 10-0502435, Fannin Bank	4,201.67	
Checking Account Balance, Fannin Bank	464.81	
Total Assets	$ 8,666.48	$ 8,666.48

Application/Nomination For Membership

I hereby apply/nominate for Regular ☐ Student ☐ Corporate ☐ membership in the Texas Society for Electron Microscopy.

Name of institution applicant or corporation nominee person _____

P. O. Address _____

_____

Information as to position, degrees, and qualifications for Membership: _____

_____

_____

_____

This nomination is accompanied by a statement of interest in and contributions to Electron Microscopy and associated fields of science.

One year's dues in the form of a check or money order should be sent with the application for Membership form. (Regular $10.00, Student $2.00, Corporate $75.00)

Signature of one Member making the nomination:

_____

Dated _____ 19 _____

This application to Membership in the Society, or this application for transfer from the grade of Student to Regular Member, signed by one Member should be sent to the Secretary to be presented at the next meeting of the Council or approval by a majority vote of the Council. Notice of approval will be mailed by the Executive Secretary.

_____

Presented to the Council at _____ meeting. Date _____

Action _____

Remarks _____

Send Application to: John Hansen
Univ. of Texas Health Science Center
Dept. of Anatomy
7703 Floyd Carl Drive
San Antonio, TX 78284

JSM-35-C
Scanning Microscope

ASSURANCE OF FUTURE VERSATILITY

- 60Å (50Å Lab6) is guaranteed up to 6 months without cleaning due to our self-maintaining electron optics.
- The eucentric goniometer is standard and facilitates the taking of stereo pairs in 30 seconds or less.
- X-ray performance is unequaled as the JSM-35 has a takeoff angle of 40 degrees, accelerating voltages from 1 to 39KV, two and four crystal spectrometers and NDX.
- More than fifty accessories are built by JEOL in order to provide future versatility.
- Expansion in areas of SIMS, particle analysis cryo, and x-ray both wave length and energy dispersive are possible for JSM-35 owners.
- Finally, the finest service and field technical assistance assures you value plus in your next SEM.

JEOL

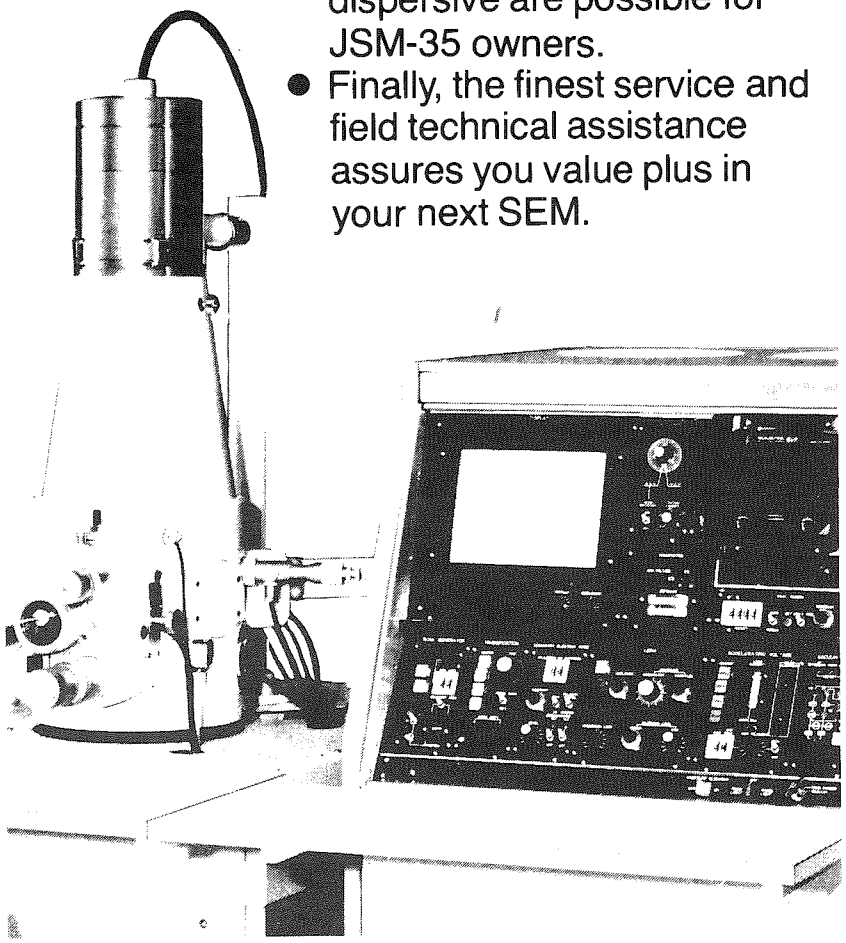

Specializing in
TEM – XRAY
SEM – AUGER

JEOL Application Laboratory, 477 Riverside Ave, Medford, Mass. 02155
617/391-7240

Quantitative microanalysis

Kevex offers more. Kevex makes it easier.

Kevex provides electron column users with the industry's most comprehensive array of software for quantitative microanalysis. Analysis with Kevex Quantex-Ray™ programs is almost sinfully easy... chiefly because we do **all** the programming. All you do is enter one or two simple keyboard commands and the rest is automatic. Only Kevex offers you so much sophistication so easily accomplished.

Here is a partial list of the capabilities of Kevex Quantex-Ray, the most emulated system in the world.

- Simultaneously acquires and processes different spectra for rapid analytical throughput.
- Automatically locates and identifies every spectrum peak.
- Accurately separates overlapping peaks, even in the presence of calibration shifts.
- Fourier processing provides optimum smoothing with no measurable peak shift or distortion.
- Automatically matches unknown spectrum to all stored spectra.
- Statistically evaluates every computed result; warning flags signal inconsistent data.
- Superimposes standard counting error on X-ray spectrum for easy statistical evaluation.
- Automatically analyzes to selected precision.
- Accepts single or multi-element standards containing up to 15 elements, which may contain overlapped peaks.
- Selects and retrieves the most appropriate standards for each analysis.
- Automatically compensates for differences in operating conditions (accelerating potential, X-ray emergence angle, beam current, etc.) between standards and unknown samples.
- Corrects for inter-element effects using Colby's Magic V.
- All programs are written in Fortran.
- Acquisition, spectrum retention and quantitation are completely automatic.

Give us the opportunity to discuss the virtues of Quantex-Ray with you. Contact:

kevex **KEVEX CORPORATION**

1101 Chess Drive Foster City, CA 94404 Phone (415) 573-5866

Secretary
Texas Society for Electron Microscopy
Department of Anatomy
Univ. Texas Health Science Center
San Antonio, Texas 78284

Non-Profit Organization
U.S. POSTAGE
PAID
Permit No. 206
San Antonio, Texas

THIRD CLASS

ADDRESS CORRECTION REQUESTED
FORM 3547 REQUESTED